

MICROBIAL INFLUENCES ON DEEP-SEA DEPOSIT FEEDERS AND DETRITAL FOOD
SOURCES

A DISSERTATION SUBMITTED TO THE GRADUATE DIVISION OF THE
UNIVERSITY OF HAWAI‘I AT MĀNOA IN PARTIAL FULFILLMENT OF THE
REQUIREMENTS FOR THE DEGREE OF

DOCTOR OF PHILOSOPHY

IN

OCEANOGRAPHY

July 2025

By

Lee C. Miller

Dissertation Committee:

Jeffrey C. Drazen, Co-Chairperson

Brian N. Popp, Co-Chairperson

Edward F. DeLong

Erica Goetze

Rebecca A. Chong

Keywords: Trophic ecology, detritus, marine microbes, deposit feeder

ACKNOWLEDGEMENTS

Thank you to my advisors Drs. Jeffrey Drazen and Brian Popp for their support, guidance, and encouragement throughout this process. Additionally, I want to thank my dissertation committee, Drs. Edward DeLong, Erica Goetze, and Rebecca Chong, for their help and advice, particularly in the realm of microbial analyses.

Thank you also to Craig Smith, David Karl, Blake Watkins, Ken Smith, Christine Huffard, Hilary Close, Sonia Romero Romero, Fuyan Li, Micheal Dowd, Jesse Black, and Gabrielle Ellis for their generosity in providing and preparing samples. Thank you to Harold Carlson, Aaron Judah, Victoria Assad, Jesse van der Grient, and Meagan Putts for their enthusiastic help in the field when collecting samples. Thank you to Natalie Wallsgrove and Andrew Burger for their invaluable assistance in the laboratory. Identification of specimens was generously provided by Rich Mooi, Andrey Gebruk, and Antonina Kremenetskaia.

The samples that contribute to this thesis were collected over seven research cruises on four vessels. Thank you to the captains, crews, and pilots of the *R/V Kilo Moana*, *R/V Western Flyer*, *R/V Atlantis*, *E/V Nautilus*, *ROV Lu'ukai*, *ROV Doc Ricketts*, *HOV Alvin*, and *ROV Heracles*.

Funding for this work was provided by the National Science Foundation, with grants awarded to Drs. Jeffrey Drazen, Brian Popp, and Craig Smith. Additional funding was provided by the Simons Foundation, the Monterey Bay Aquarium Research Institute, and the School of Ocean and Earth Science and Technology. Thank you also to the Ocean Exploration Trust for allowing me time and collections on their vessel.

My family has provided unconditional support throughout my life, and their encouragement to follow my passions wherever they lead brought me to my love of the strange invertebrates that live at the bottom of the sea. Thank you to my parents for bringing my sister and me on so many adventures, in particular those on the *S/V Chaika*, igniting my lifelong love of the ocean. I am lucky also to have been supported by amazing friends both here in Hawai'i and from afar. Finally, thank you to my partner Keeley for four years of love, laughter, and support, and for your unending willingness to listen to me talk about sea cucumbers.

ABSTRACT

Deep-sea communities are food limited, relying on detritus exported from surface waters for energy. Microbes produce, consume, and transform detrital particles, affecting their availability to deep-sea metazoans. I examined the microbial communities associated with particulate organic matter as it sinks from the euphotic zone to the abyssal plain more than four kilometers below. Compound-specific stable isotope analysis allowed me to trace both metazoan and microbial trophic processes. I found that most microbial alteration occurs in the top 500 m of the water column, the products of which support nitrifying archaeal communities. I also characterized microbial communities in sediments and in the digestive tracts of deposit-feeding echinoderms (sea cucumbers and sea urchins) to understand how microbial and metazoan food webs interact. Abyssal deposit feeders showed niche partitioning at two sites in the North Pacific, with interspecific differences in their consumption and utilization of fresh phytodetritus versus more heavily reworked small particles. More mobile species, especially holothurians capable of swimming, were able to consume fresher material, while the slower-moving species appear to rely more on microbially reworked detritus. Both small, heavily reworked particles and large, fresh particles are important to abyssal fauna, but the smaller particles are not well represented in sediment traps. The use of sediment traps to measure flux has therefore led to an underestimation of the importance of small particles to the deep benthos. Finally, I looked at changes in deposit feeder trophic ecology and gut microbiota throughout a depth gradient from shallow reefs to the abyssal plain and found that depth was the major driver of both. Deposit feeder trophic position increased from two to three (primary to secondary consumers) within the first 500 m of depth, which corresponded to the decline in particulate flux across the same depth range. Deeper-living deposit feeders are more reliant on microbial trophic intermediates than their shallow counterparts, and as depth increases the dominant gut taxa change. Detritus-based food webs in the deep ocean are influenced at multiple levels by microbial reworking, including in the often-overlooked gut microbiome.

TABLE OF CONTENTS

ACKNOWLEDGEMENTS	ii
ABSTRACT	iii
LIST OF TABLES	vii
LIST OF FIGURES	viii
CHAPTER 1. Introduction.....	1
1.1 Pelagic-benthic coupling and particle export	2
1.2 Microbial communities influencing pelagic-benthic coupling.....	3
1.3 Compound-specific stable isotope analysis: a tracer for microbial and metazoan trophic dynamics.....	5
1.4 Connecting microbial and animal food webs in the deep sea	7
1.5 Research objectives.....	8
CHAPTER 2. Transformations of particulate organic matter from the surface to the abyssal plain in the North Pacific as inferred from compound-specific stable isotope and microbial community analyses.....	10
2.1 Abstract	11
2.2 Introduction.....	11
2.3 Methods.....	15
2.3.1 Sample Collection.....	15
2.3.2 Surface particle fluxes	17
2.3.3 Amino acid compound-specific stable isotope analysis.....	18
2.3.4 Stable isotope data analysis	18
2.3.5 16S rRNA microbial community barcoding.....	19
2.3.6 Community barcoding data analysis.....	19
2.3.7 Statistical analysis.....	20
2.4. Results	20
2.4.1 Carbon flux	20
2.4.2 Compound-specific stable isotope analysis.....	21
2.4.3 Microbial community analysis	23
2.4.4 Microbial community relationships with stable isotope values.....	24
2.5 Discussion	30
2.5.1 Isotopic indications of microbial reworking of sinking POM.....	30

2.5.2 Microbial communities associated with POM at Station ALOHA	33
2.5.3 Ammonia oxidizing archaea associated with POM reworking	34
2.6 Conclusions	36
CHAPTER 3. Niche partitioning among abyssal deposit-feeding echinoderms is linked to mobility and gut microbiota.....	38
3.1 Abstract	39
3.2 Introduction.....	39
3.3 Materials and Methods.....	42
3.3.1 Sample collection	42
3.3.2 Density estimations.....	43
3.3.3 Amino acid compound-specific stable isotope analysis.....	44
3.3.4 16S rRNA microbial community barcoding.....	44
3.3.5 Stable isotope data analysis	45
3.3.6 Barcoding data analysis.....	45
3.3.7 Statistical analysis.....	45
3.4 Results	46
3.4.1 Deposit feeder communities	46
3.4.2 Compound-specific stable isotope analysis.....	47
3.4.3 Microbial community analysis	48
3.5 Discussion	56
3.5.1 Niche partitioning by particle type.....	56
3.5.2 Trophic ecology and gut microbiomes of non-swimming deposit feeders	58
3.5.3 Trophic ecology and gut microbiomes of facultatively swimming deposit feeders.....	60
3.5.4 Trophic ecology and gut microbiomes of benthopelagic deposit feeders	61
3.5.5 Potential functions of gut microbiota in abyssal deposit feeders	62
3.6 Conclusions.....	63
CHAPTER 4. Changes in gut microbiota and increases in deposit feeder trophic position with depth from shallow reefs to the abyssal plain.....	65
4.1 Abstract	66
4.2 Introduction.....	66
4.3 Methods.....	69
4.3.1 Sample collection	69
4.3.2 POC flux.....	70

4.3.3 Compound-specific stable isotope analysis.....	70
4.3.4 16S microbial community barcoding	71
4.3.5 Stable isotope data analysis	71
4.3.6 Statistical analysis.....	71
4.4 Results	75
4.4.1 Trophic changes with depth.....	75
4.4.2 Gut microbiota changes with depth.....	76
4.5 Discussion	82
4.5.1 Deposit feeder trophic position increases with depth.....	82
4.5.2 Identity and potential function of gut-associated microbiota.....	83
4.5.3 Potential archaeal contributions to deposit feeder diets	85
CHAPTER 5. Conclusions.....	87
5.1 Chapter 2: Transformations of particulate organic matter from the surface to the abyssal plain in the North Pacific as inferred from compound-specific stable isotope and microbial community analyses	88
5.2 Chapter 3: Niche partitioning among abyssal deposit-feeding echinoderms is linked to mobility and gut microbiota	90
5.3 Chapter 4: Gut microbiota associated with increases in deposit feeder trophic position with depth from shallow reefs to the abyssal plain	91
5.4 Synthesis and future directions	92
APPENDIX A.....	95
APPENDIX B	97
REFERENCES	98

LIST OF TABLES

Table 2.1 Particle sample information.....	17
Table 3.1. Abyssal deposit feeder sample information.....	49
Table 4.1. Deposit feeder and sediment sample information	73

LIST OF FIGURES

Figure 2.1. Total carbon flux at Stations M and ALOHA.....	25
Figure 2.2. $\delta^{15}\text{N}_{\text{SAA}}$ values, estimated trophic positions, and ΣV values of particles	26
Figure 2.3. Particle mixing model based on $\delta^{15}\text{N}$ values of threonine and alanine	27
Figure 2.4. Identity of microbial communities associated with particles.	28
Figure 2.5. Particle microbial community Principal Coordinate Analysis (PCoA).....	29
Figure 2.6. Proportion of ASVs in filtered particle samples assigned to the Nitrosopumilaceae family and the corresponding $\delta^{15}\text{N}_{\text{SAA}}$ values for those samples.....	29
Figure 3.1. $\delta^{15}\text{N}_{\text{SAA}}$ values, estimated trophic positions, and ΣV values of abyssal deposit feeders and sediments.....	50
Figure 3.2. Trophic position difference between sediments and gut contents and between gut contents and deposit feeder tissue.....	51
Figure 3.3. Contribution of different particle types to deposit feeder diets	52
Figure 3.4. Identity of microbial communities in sediments and gut contents.....	53
Figure 3.5. Sediment and gut contents microbial PCoA.....	54
Figure 3.6. Microbial community alpha diversity in gut contents and sediments	54
Figure 3.7. ASVs significantly enriched in digestive tracts versus sediments.....	55
Figure 4.1. Sample locations and depths.....	77
Figure 4.2. $\delta^{15}\text{N}_{\text{SAA}}$ values, estimated trophic positions, and ΣV values of deposit feeders, gut contents, and sediments across depth.....	78
Figure 4.3. Probabilistic Principal Component Analysis (PCA) based on $\delta^{13}\text{C}$ values of essential amino acids	79
Figure 4.4. Identity of microbial communities associated with gut contents and sediments.....	81
Figure 4.5. Sediment and gut contents microbial PCoA.....	81
Figure 4.6. Depth trends of microbial taxa in gut contents and sediments	82

CHAPTER 1. Introduction

1.1 Pelagic-benthic coupling and particle export

The deep ocean is a food-limited environment, characterized by a lack of sufficient light for *in situ* photosynthesis. All deep-sea benthic and pelagic organisms depend on detritus sinking from surface waters, with the exception of isolated chemosynthetic habitats (Gibson et al. 2002; Smith et al. 2008a). Surface production and energy is transported to the deep sea primarily as particulate organic matter (POM), along with dissolved organic matter (DOM) (Alldredge 2000) and organic material actively transported by vertically migrating zooplankton and nekton (Steinberg and Landry 2017; Saba et al. 2021). Deposit feeders, which are the focus of Chapters 3 and 4 of this thesis, primarily consume POM, forming the base of deep benthic food webs (Roberts et al. 2000; FitzGeorge-Balfour et al. 2010). POM quantity and quality generally decrease with depth, driving benthic community biomass, abundance, size structure, diversity, and more (Smith et al. 1997, 2008b; Johnson et al. 2007; Sweetman and Witte 2008; Billett et al. 2010; Huffard et al. 2016).

The POM that fuels these so-called “brown” food webs (in contrast to photosynthetic “green” food webs) is a diverse assortment of phytodetritus (Rice et al. 1986; Beaulieu 2002; Richardson and Jackson 2007), fecal pellets (Hofmann et al. 1981; Turner 2015), animal carcasses (Lebrato et al. 2013; Smith et al. 2014), and more. As these various types of POM sink out of the euphotic zone, they undergo complex transformations, including both remineralization and production, by microbial and metazoan communities in the water column (Wakeham et al. 1984; Alldredge 1998; Mestre et al. 2018). The breakdown and reworking of POM results in only 0.5-2% of net primary production reaching abyssal depths (Wakeham et al. 1984; Buesseler et al. 2007). Decreasing lability with depth, meanwhile, means that the small proportion of POM that reaches the deep sea is composed of refractory compounds that are more difficult for animals to break down and digest (Herndl and Reinthaler 2013). Within the category of POM, flux magnitude and composition is influenced by particle size, density, and composition (De La Rocha and Passow 2007). Larger and denser particles reach the seafloor much faster and retain their lability, providing higher quality food to benthic communities (Durkin et al. 2021). These include animal carcasses and fecal pellets, which often arrive in irregular pulses following surface phytoplankton blooms (Smith et al. 2014; Doherty et al. 2021).

The methodologies we use to capture and study POM influence our understanding of the importance of various particle types. Moored and drifting sediment traps, which collect gravitational flux, have been a valuable tool for quantifying POM flux for decades (Buesseler et al. 2000; Honjo et al. 2008). However, they have significant biases, including under-sampling horizontally advected and slowly-sinking particles (Buesseler 1991). Zooplankton that actively enter traps to feed on the captured material can lead to overestimations of flux (Buesseler et al. 2000). In contrast, particles can be filtered *in situ* from the water column, which allows for the targeted collection of certain size fractions, including the smaller fractions that are largely missed by sediment traps (Buesseler et al. 2000; Bishop et al. 2012). However, *in situ* filtration captures neutrally buoyant particles as well, making it an inaccurate measurement of POM flux. In combination with other methods of quantifying flux, such as ^{234}Th disequilibrium (Buesseler et al. 2006), examining sediment trap material and filtered particles together provides a more complete picture of the POM fueling deep-sea food webs.

1.2 Microbial communities influencing pelagic-benthic coupling

As detritus sinks from the surface to the deep benthos, it is colonized and consumed by dynamic communities of microbes, including bacteria, archaea, fungi, and protists (Grossart et al. 2003; Salazar et al. 2016; Boisdansky et al. 2017). Particle-associated communities undergo complex successional dynamics, with the importance of adaptations to hydrostatic pressure increasing with depth (Bartlett 1999; Datta et al. 2016; Pelve et al. 2017; Stephens et al. 2024). Due to the different composition and sinking speeds of smaller versus larger particles, microbial community composition differs substantially by particle size (Abramson et al. 2010), and also between free-living and particle-attached communities (Rieck et al. 2015; Ma et al. 2024). These communities heterotrophically break down organic material, decreasing the lability and quantity of POM with depth (Herndl and Reinthaler 2013). Additionally, many free-living and particle-attached bacteria and archaea regenerate organic material through chemolithoautotrophy, including sulfur compound oxidation (Swan et al. 2011) and nitrification (Karl et al. 1984). Nitrification is common in oligotrophic water columns and is generally a two-step process split between ammonia oxidizing archaea, which oxidize NH_3 to NO_2^- , and nitrifying bacteria that

oxidize NO_2^- to NO_3^- (Mincer et al. 2007; Ward 2008; Martens-Habbena et al. 2009; Church et al. 2010).

Microbial communities in sediments further transform POM once it reaches the seafloor. As in the water column, this includes both heterotrophy (Corinaldesi 2015; Hoffmann et al. 2017; Hoshino et al. 2020) and chemolithoautotrophy, including nitrification (Begmatov et al. 2021; Hollingsworth et al. 2021; Zhao et al. 2023). Sediment microbial communities show niche partitioning, with certain taxa increasing in abundance in response to pulses of certain types of detritus (Hoffmann et al. 2017). As with water column microbes, sediment microbes have the potential to both increase and decrease the lability and availability of detrital material for higher trophic levels. Deep-sea deposit feeders (DFs) consume not just phytodetritus and other organic material originating in surface waters, but also often show evidence of utilizing significant bacteria-derived biomass (Neto et al. 2006; Drazen et al. 2008; Rodkina et al. 2023). It can be difficult, however, to determine to what extent bacterial contributions to detrital material occur during euphotic zone production, particle export through the water column, or once POM reaches the seafloor.

An additional but often overlooked source of microbial community transformations of detritus is within the digestive tracts of animals, particularly detritivores including suspension and deposit feeders. Microbes residing in the digestive tracts of animals are derived from their diet, as well as often forming distinct communities that benefit from the specific gut environment (Benson et al. 2010; Sullam et al. 2012). Gut microbiome composition is dependent on environmental factors and animal species, as well as individual variation in immunity and diet (Benson et al. 2010; Stagaman et al. 2017; Huang et al. 2020; Li et al. 2023). In the deep sea, most gut microbiome studies have occurred in fishes and at chemosynthetic habitats (e.g. Yang et al. 2015; Aronson et al. 2016), leading to a lack of knowledge of the identity and functions of gut microbiota in detritus-based environments (Osman and Weinnig 2022). The few studies that have examined microbiomes in deep detritivores have found gut communities distinct from those in the sediment, with the potential to aid in the breakdown of phytodetritus otherwise unavailable to animals (Amaro et al. 2009, 2012; Peoples et al. 2024). In Chapters 3 and 4 of this dissertation, I examine the gut microbiota of deposit-feeding echinoderms in the deep sea, connecting benthic microbial and animal food webs.

1.3 Compound-specific stable isotope analysis: a tracer for microbial and metazoan trophic dynamics

The various sizes and types of sinking POM differ in their importance for deep pelagic and benthic communities. The utilization of different types of detritus can be quantified using natural abundance carbon and isotope composition, whose isotope ratios ($\delta^{13}\text{C}$ and $\delta^{15}\text{N}$) are affected by both the origin and trophic dynamics of organic material. Different photosynthesizers, such as terrestrial C3 and C4 plants, microplankton, and seagrasses, fractionate carbon to different degrees (Larsen et al. 2009). $\delta^{15}\text{N}$ values of phytoplankton also vary spatially and temporally, based on the nitrogen sources available and interspecific differences in fractionation associated with assimilation (Rolff 2000). However, trophic transformations by bacteria, fungi, protists, and animals all lead to ^{15}N enrichment, making it difficult to determine the $\delta^{15}\text{N}$ value of material at the base of a food using higher trophic level material such as animal tissue (McMahon et al. 2015; Steffan et al. 2015; Ohkouchi et al. 2017). While less trophic fractionation occurs for carbon (Zanden and Rasmussen 2001), there is often overlap in bulk $\delta^{13}\text{C}$ values among photosynthetic endmembers.

Because $\delta^{13}\text{C}$ and $\delta^{15}\text{N}$ values are affected by primary production of organic material as well as subsequent microbial and metazoan reworking, disentangling these processes can be difficult when the isotopic composition of material at the base of a food web is not known, as is often the case in the deep sea (Hannides et al. 2013; Gloeckler et al. 2018). Instead of determining $\delta^{13}\text{C}$ and $\delta^{15}\text{N}$ values in bulk material, quantifying their values in individual amino acids gives more insight into the complex trophic dynamics affecting POM and organisms in the deep sea. Compound-specific stable isotope analysis of amino acids (AA-CSIA) allows for more detailed understandings of trophic dynamics, particularly in environments with multiple potential sources of organic material.

Essential amino acids (EAAs) cannot be synthesized by metazoan consumers and must instead be obtained through their diets. Thus, the $\delta^{13}\text{C}$ values of EAAs (generally isoleucine, leucine, lysine, phenylalanine, threonine, and valine) create a “fingerprint” that allows different types of organic matter to be traced through a food web with minimal effects of trophic steps (Larsen et al. 2009, 2013; McMahon et al. 2016). Amino acids can also be characterized as source or trophic amino acids, distinguished by ^{15}N fractionation during trophic steps. Trophic

amino acids undergo metabolic transamination that causes ^{15}N enrichment by up to 10‰ with each metazoan trophic step (McClelland and Montoya 2002; Ohkouchi et al. 2017). Source amino acids, on the other hand, do not have their C-N bonds broken during metazoan metabolism, so their $\delta^{15}\text{N}$ values increase very little throughout animal food webs (Chikaraishi et al. 2007, 2009; Ohkouchi et al. 2017). $\delta^{15}\text{N}$ values of source amino acids ($\delta^{15}\text{N}_{\text{SAA}}$) can distinguish different organic matter sources, such as phytoplankton versus heterotrophic bacteria, with their values remaining consistent throughout trophic levels (Hannides et al. 2009, 2013). $\delta^{15}\text{N}_{\text{SAA}}$ values are higher in smaller particles, likely due to their slower settling times which allow for more microbial heterotrophic reworking and associated isotope fractionation of source amino acids (Hannides et al. 2013; Ohkouchi et al. 2017; Gloeckler et al. 2018). Comparisons of $\delta^{15}\text{N}_{\text{SAA}}$ values in particles to those of zooplankton and nekton reveals that these small, slowly-sinking particles make up in the base of mesopelagic and bathypelagic food webs, with smaller particles becoming increasingly important with depth and in lower POM flux ocean regions (Gloeckler et al. 2018; Romero-Romero et al. 2020).

Additionally, we can compare the $\delta^{15}\text{N}$ values of trophic and source amino acids, typically using glutamic acid as the trophic and phenylalanine as the source amino acid, to estimate the trophic position of organic material without needing to know the $\delta^{15}\text{N}$ value of the material at the base of the food web (McClelland and Montoya 2002; Chikaraishi et al. 2009). This is valuable when studying deep-sea food webs, which may utilize a wide range of detrital food sources with differing $\delta^{15}\text{N}$ values (Hannides et al. 2013). $\delta^{15}\text{N}$ values of individual amino acids can also be used to calculate two indices, degradation index (DI) and ΣV , that provide further insight into microbial reworking of organic material. DI uses the selective preservation of different AAs based on their abundances in refractory materials such as cell walls to characterize the degree of degradation in organic material (Dauwe et al. 1999; McCarthy et al. 2007). The ΣV parameter is used as a proxy for total heterotrophic reworking, based on the increasing deviation of individual amino acid $\delta^{15}\text{N}$ values from the average $\delta^{15}\text{N}$ amino acid value as heterotrophic resynthesis leads to increasingly distinct $\delta^{15}\text{N}$ values among amino acids (McCarthy et al. 2007). Combining AA-CSIA analyses, including $\delta^{13}\text{C}$ EAA fingerprinting, $\delta^{15}\text{N}$ SAA values, trophic position estimates, DI, and ΣV , gives significant insight into food web dynamics in otherwise poorly understood ecosystems such as the deep benthos.

1.4 Connecting microbial and animal food webs in the deep sea

Microbial and metazoan food webs exist at different spatial scales and are often studied using disparate methodologies. However, they overlap and influence one another in many ways. Many primary producers, particularly in the oligotrophic open ocean, are microbial, supporting surface food webs as well as deep-sea metazoans via the export of detritus (Thiel et al. 1989; Nomaki et al. 2021). Additionally, microbes consume DOM, making it available to higher trophic levels via the “microbial loop” (Azam 1998; Herndl and Reinthaler 2013). Microbial communities also have close symbioses with individual animal species and organisms, including parasitism, commensalism, and mutualism (Osman and Weinnig 2022). In the deep sea, reducing habitats such as hydrothermal vents, cold seeps, and whale falls have been the focus of most symbiosis studies. In these ecosystems, chemosynthetic microbial communities support abundant assemblages of animals that in turn provide a stable habitat maintaining access to electron donors and acceptors (Dubilier et al. 2008; Dick 2019). Mutualistic relationships between animals and microbes often take advantage of this tradeoff, with the diverse metabolic pathways within microbes allowing access to energy sources otherwise unavailable to animals, while animals’ complex multicellular body structures provide habitats and environmental engineering (Boucher et al. 1982; Chaston and Goodrich-Blair 2010).

Gut microbiomes, a major location of animal-microbe symbioses, are the focus of Chapters 3 and 4 of this thesis. Many terrestrial herbivores and detritivores have well-known symbioses with gut microbiota that help them break down and consume recalcitrant material such as cellulose and lignin (Huang et al. 2022). Animals in the deep sea, particularly those that consume detritus exported from surface waters, similarly must be able to utilize low-quality food such as phytodetritus or fecal pellets that have undergone extensive remineralization and repackaging (Ruhl and Smith 2004). Based on the few animals whose gut microbiomes have been quantified, specialized gut communities with metabolisms capable of breaking down material and supplementing nutrients do occur in the deep sea (He et al. 2018; Peoples et al. 2024). However, the overall impact of these associations on deep-sea food web structure has rarely been considered.

As an example of microbial influences on deep-sea metazoan food webs, I focus on the relationships between deposit-feeding echinoderms and their gut microbiota. Echinoids and in particular holothurians are dominant megafauna in terms of biomass and abundance on much of

the deep seafloor (Hessler and Jumars 1974; Kaufmann and Smith 1997; Huffard et al. 2016; Amaro et al. 2019; Kuhnz et al. 2020). They consume low-quality detritus that forms the base of benthic food webs, with niche partitioning based on movement speeds, tentacle morphology, and more allowing diverse communities to exist on abyssal plains (Jumars et al. 1990; Miller et al. 2000; Iken et al. 2001). In particular, faster-moving echinoderms encounter and consume fresh pulses of phytodetritus first, leaving slower-moving species reliant on poorer quality material (Lauerman et al. 1997; Pierrat et al. 2022) These interspecific differences in feeding strategies allow me to compare the use of gut microbiota between species that consume different types of POM. Additionally, their relatively large size allowed me to separate their digestive tracts from their bodies, and in some cases provided enough gut material for AA-CSIA.

AA-CSIA has revealed that some abyssal deposit feeders are secondary consumers of detritus at the high flux Station M (Romero-Romero et al. 2021). $\delta^{13}\text{C}$ EAA signatures, DI values, and ΣV values in gut contents were distinct from those in sediments, leading us to hypothesize that gut microbiota act as the primary consumers, with deposit feeders feeding on microbial byproducts and/or microbial biomass itself. I continue this work by examining deposit feeders from additional sites, including the oligotrophic Station ALOHA as well as throughout a full depth gradient from shallow reefs to abyssal plain, to determine whether utilizing gut microbiota as trophic intermediates is a widespread adaptation for deposit feeders. deposit feeder communities are often diverse, even in areas with low POC flux, likely due to niche partitioning on the basis of particle size and quality (Hessler and Jumars 1974).

1.5 Research objectives

Throughout my three data chapters, I examine the microbial communities associated with detrital material that makes up the base of deep-sea food webs, as well as those associated directly with deposit feeders via gut symbioses. This dissertation examines how microbes affect the limited food source available to deep-sea detritivores. Chapter 2 focuses first on the POM that forms the base of deep benthic food webs, characterizing the microbial communities associated with sinking detritus and using nitrogen AA-CSIA to quantify microbial and metazoan transformations. This chapter extends AA-CSIA to abyssal depths for the first time, using it to distinguish multiple types of POM and demonstrate that common methods of capturing particles

differ in their capture of each POM type. The primary objective of Chapters 3 and 4 is to characterize deposit-feeding echinoderms and their gut microbiota as an example of a microbe-metazoan symbiosis in a deep-sea detrital food web, with the goal of determining how the symbiotic use of microbes differs based on the quantity and quality of POM. Chapter 3 compares two abyssal sites with an order of magnitude difference in abyssal flux, while Chapter 4 uses depth as a proxy for flux, comparing the trophic ecology and gut microbiome composition of deposit feeders across a 4700 m depth gradient around the Hawaiian Islands. This is, to my knowledge, the largest depth gradient across which gut microbiota have been compared within a single study, which allows me to come to large-scale conclusions about trends in the trophic position and gut microbiomes of deposit feeders with depth.

CHAPTER 2. Transformations of particulate organic matter from the surface to the abyssal plain in the North Pacific as inferred from compound-specific stable isotope and microbial community analyses

Lee C. Miller, Hilary G. Close, Kalina C. Grabb, Christine L. Huffard, Fuyan Li, David M. Karl, Kenneth L. Smith, Jr., Edward F. DeLong, Claudia R. Benitez-Nelson, Jeffrey C. Drazen, Brian N. Popp

2.1 Abstract

Particulate organic matter (POM) produced in surface waters undergoes extensive reworking and breakdown by microbial and metazoan communities as it sinks to the abyssal seafloor and serves as the base of benthic and pelagic food webs. Here, we examined how various size classes of POM in the oligotrophic North Pacific Subtropical Gyre (Station ALOHA) and in the eutrophic California Current System (Station M) undergo microbial alteration throughout the water column. Compound-specific stable isotope analysis showed that sampling method strongly impacts the type of POM quantified as export to the deep sea. Moored abyssal sediment traps captured material that matched the isotopic composition of surface POM, indicating they collected large, fast-sinking particles, in contrast to the more heavily reworked particles collected with *in situ* filtration at the same depths. Extending $\delta^{15}\text{N}$ analyses of amino acids to bathypelagic and abyssopelagic depths for the first time, we confirmed that most particle remineralization and reworking occurs within the upper ~400 m of the water column regardless of initial surface productivity. At Station ALOHA, we further used 16S rRNA barcoding to characterize the microbial communities associated with the POM. We found that chemolithoautotrophic ammonia-oxidizing archaea are abundant in the upper water column at Station ALOHA and that their abundance corresponded to regions of high heterotrophic reworking as indicated by amino acid isotope analysis.

2.2 Introduction

Particulate organic matter (POM) formed in surface waters sinks through the water column, decreasing in quantity and quality such that only a fraction, typically 0.5-2% of primary production, ultimately reaches abyssal depths (Buesseler et al. 2007; Grabowski et al. 2019). Throughout the pelagic and benthic deep sea, POM forms the base of food webs, supporting a diverse array of microbes, protozoans, and metazoans. As such, sinking POM is a critical component of matter and energy transport from the surface to the deep sea, along with smaller contributions from dissolved organic matter (DOM) (Allredge 2000), larger pieces of detritus such as carrion (Lebrato et al. 2013), and vertically migrating zooplankton and micronekton (Steinberg and Landry 2017; Saba et al. 2021). The chemical energy supplied to deep sea

environments is controlled, in part, by surface production, with more POM reaching the seafloor in areas with higher primary production (De La Rocha and Passow 2007; Mestre et al. 2018) and during seasonal, often spring or summer, pulses (Beaulieu 2002; Gooday and Hughes 2002; Karl et al. 2012). The quantity and timing of POM export in turn drive benthic community structure and dynamics (Smith et al. 2002a; Sweetman and Witte 2008; Smith et al. 2018).

The quantity and quality of POM that supports deep-sea communities is influenced by several factors. In addition to the magnitude and composition of overlying surface production (Beaulieu 2002; Lutz et al. 2007; Marsay et al. 2015; de Melo Viríssimo et al. 2022), particle flux varies by size, density, and composition (De La Rocha and Passow 2007). Sinking particles are disaggregated and remineralized by microbial and metazoan communities (Wakeham et al. 1984), with larger and denser aggregates sinking faster and reaching the seafloor having undergone less reworking (Alldredge 1998; Mestre et al. 2018). Different sizes of particles also host distinct microbial communities (Duret et al. 2019), which vary by season (Poff et al. 2021) and across depth (Pelve et al. 2017). This variety in particle composition complicates our understanding of what types of organic flux contribute most to export and food supply for deep-sea communities.

POM flux across space and time has often been quantified using surface-tethered, bottom-moored, and neutrally buoyant sediment traps, driving our understanding of the flux (Buesseler et al. 2000; Honjo et al. 2008) and chemistry (Wakeham et al. 1984) of sinking particles throughout the ocean. However, sediment traps have long been known to both over- and under-sample certain types of POM, including horizontally advected material and small, slowly-sinking particles (Buesseler 1991), and can be biased by the activity of zooplankton swimmers (Buesseler et al. 2000). Stable isotope analysis of organic carbon and nitrogen has shown that small, slowly-sinking and suspended particles, which tend to be under-sampled by sediment traps, can be an important food source for lower mesopelagic and upper bathypelagic zooplankton and micronekton (Hannides et al. 2013; Gloeckler et al. 2018; Romero-Romero et al. 2020). Work using sediment traps to characterize particle flux may therefore underestimate the importance of certain types of POM flux for deep-sea communities, but the extent to which this is true for abyssal ecosystems requires study of particles and trap material from abyssopelagic depths. In this study, we compare amino acid $\delta^{15}\text{N}$ values of sediment trap

material to POM filtered and size-fractionated from the water column to quantify a range of particle types potentially used by deep-sea organisms.

Chemical transformations of particulate flux are driven, in part, by particle-associated microbial communities. The organic material in particles is colonized and remineralized by free-living, epiphytic, and animal-associated bacteria and archaea, some of which form complex and dynamic communities on the surface of particles (Pelve et al. 2017; Boeuf et al. 2019). The high concentrations of organic molecules in particles relative to the surrounding water make them microbial hotspots, and POM can be thought of as island habitats distinct from the background, nutrient-poor water (Herndl and Reinthaler 2013). Particles are first colonized by an initial community of bacteria associated with euphotic eukaryotes; however, they are subsequently replaced by a diverse communities capable of degrading a variety of substrates (Datta et al. 2016; Pelve et al. 2017). Additionally, as particles sink through the water column, microbes adapted to increasing pressure and decreasing temperature may become more competitive (Yayanos 1995; Martín-Cuadrado et al. 2007; Karl and Church 2017). Particle size influences the communities that form; large, fast-sinking particles export surface-derived taxa, while smaller particles form more deep-adapted communities (Ma et al. 2024).

Sinking, and especially suspended particles, across multiple sites show increases in $\delta^{15}\text{N}$ values throughout the top 500 m of the water column due to microbial activity, which shows a preference for remineralization of chemical bonds with lower $\delta^{15}\text{N}$ values (Saino and Hattori 1980; Altabet et al. 1991). Compound-specific stable isotope analysis of individual amino acids (AA-CSIA) is a technique that has allowed novel insights into the transformations and utilization of different types of organic material by various organisms and food webs. Amino acids can be classified as “source” or “trophic,” with trophic amino acids (e.g., glutamic acid, alanine) being isotopically fractionated during heterotrophic metabolism and undergoing enrichment in ^{15}N with each trophic step (McClelland and Montoya 2002; Popp et al. 2007). By contrast, the nitrogen in source amino acids (e.g., phenylalanine, lysine) is isotopically fractionated only by primary production and microbial heterotrophy, so the $\delta^{15}\text{N}$ values of source amino acids remain largely unaltered by metazoans. By comparing the $\delta^{15}\text{N}$ values of trophic and source amino acids, the trophic positions associated within metazoans and POM can be estimated without independent measurement of the $\delta^{15}\text{N}$ value of the material at the base of the food web (Chikaraishi et al. 2007, 2009; Popp et al. 2007). Additionally, the $\delta^{15}\text{N}$ values of source amino acids will vary

based on the composition of particles as well as their transformations by microbial communities, allowing us to distinguish particles of different size classes and trace their changes as they sink throughout the water column (Hannides et al. 2013; Gloeckler et al. 2018; Romero-Romero et al. 2020; Wojtal et al. 2023). Certain amino acids, such as threonine and alanine, when normalized to the $\delta^{15}\text{N}$ value of phenylalanine, form distinct clusters of $\delta^{15}\text{N}$ data that can be used in mixing models to distinguish types of POM such as fecal pellets (Doherty et al. 2021; Wojtal et al. 2023). These analyses have expanded our understanding of upper ocean export processes but have not previously been extended through the water column to the abyssal seafloor.

Free-living and particle-attached microbial communities are responsible for significant transformations of sinking organic material, as evidenced by increasing $\delta^{15}\text{N}$ values with depth (Altabet et al. 1991; Smith et al. 2002b), particularly of source amino acids (Gloeckler et al. 2018; Wojtal et al. 2023), but the specific taxa responsible for these changes have not been identified. Here, we examine microbial community composition in the context of stable isotope transformations in size-fractionated particles at Station ALOHA, an oligotrophic site in the North Pacific Subtropical Gyre (NPSG). In general, microbial communities in the NPSG are highly depth-stratified with minimal temporal variability and community composition driven by light and nutrient concentrations (DeLong et al. 2006; Mende et al. 2017, 2019). In NPSG surface waters, bacterial communities include large numbers of Cyanobacteria, particularly *Prochlorococcus* spp. (DeLong et al. 2006; Mende et al. 2019; Reintjes et al. 2019). Below the euphotic zone, there is a sharp change in microbial community composition towards heterotrophic taxa, although Cyanobacteria DNA from presumably dead or inactive individuals is observed throughout the water column to abyssal depths (Mende et al. 2017, 2019). Additionally, dark chemolithoautotrophy creates newly fixed organic material in the mesopelagic zone (Karl et al. 1984; Ingalls et al. 2006). In oligotrophic NPSG sites such as Station ALOHA, ammonia-oxidizing archaea and bacteria perform nitrification and regenerate nitrate in the upper water column (Dore and Karl 1996; Ingalls et al. 2006). With increasing depth, microbes tend to have genomes indicative of increasingly particle-attached rather than free-living lifestyles (DeLong et al. 2006; Zhao et al. 2020). In general, particle-attached and free-living communities follow different patterns in community composition, depth distribution, and diversity, meaning that sampling method can have a large influence on results (Mestre et al. 2018; Boeuf et al. 2019b; Mende et al. 2019; Comstock et al. 2024).

This study seeks to further our understanding of POM export, with a focus on the composition, colonization, and changes of associated microbial communities as material sinks from the euphotic zone to abyssal waters. We compare these processes using amino acid compound-specific stable isotope analysis to quantify trophic changes and POM remineralization at Station ALOHA and at the more eutrophic and seasonally variable Station M, located in the California Current Ecosystem. At both sites, abyssal communities depend on POM exported from the euphotic zone. Here, we seek to better understand how microbial and metazoan transformations of the sinking material differ between the two contrasting productivity regimes. At Station ALOHA, we also use DNA barcoding to identify the bacterial and archaeal communities that potentially drive these changes. By characterizing how POM is transformed by microbial communities throughout the full water column, including the less understood bathypelagic and abyssopelagic, we contribute to an understanding of the different types of detritus that fuel deep-sea food webs.

2.3 Methods

2.3.1 Sample Collection

Sinking and suspended particles were collected from two abyssal sites in the Northeast Pacific, Station ALOHA and Station M. Station ALOHA (22°45'N, 158°W) is located within the NPSG, an oligotrophic site with a distinct summer export flux mediated by diazotrophs (Karl and Lukas 1996; Karl et al. 2021). By contrast, Station M (34°50'N, 123°00'W) is located within the California Current Ecosystem and experiences high productivity and pronounced seasonality (Smith and Druffel 1998; Smith et al. 2018). Collections at Station ALOHA occurred in February 2014, August 2014, July 2019, January 2020, and July 2020, while collections at Station M occurred in April and October 2019 (Table 1).

At both sites, we deployed sediment traps at 50 and 600 meters above the bottom (mab) at depths of approximately 3400 and 3950 m at Station M and 4100 and 4650 m at Station ALOHA (Table 1). These depths have been chosen to mimic historical sampling where 50 mab represents the near seafloor flux but with the possibility of sediment resuspension, while 600 mab represents a depth above the benthic boundary layer and thus is most likely free from resuspended sediments (Smith et al. 2013). Traps contained 5% formaldehyde in filtered

seawater to prevent additional microbial activity on captured material. McLane Parflux sediment traps (Mark 78H with 0.65m² collection area) were deployed at Station ALOHA from March 2019 to February 2020 with an average (but varying) sample frequency of 14 days. Trap sampling at Station M occurred with 16-day sampling frequency over the period of this study. Unfortunately, the traps became clogged by a pulse of detritus in early April 2019 just prior to reservicing. During the subsequent deployment a failure in the trap mooring string caused a prerelease and loss of the existing samples. As such, no samples were collected concurrent with the October 2019 cruise and *in situ* particle collections.

In addition to the sediment traps, we collected particles using *in situ* filtration by McLane pumps in 2019 and 2020. The pumps were equipped with mini-MULVS filter holders (Bishop et al. 2012) with three tiers of filters (140 mm diameter) to fractionate particles into three size classes: large (>53 μm , acid-cleaned Nitex mesh filters), small (1-53 or 0.7-53 μm , precombusted QMA quartz or GF/F glass microfiber filters), and submicron (0.3-1 μm , precombusted GF75 glass microfiber filters). This method is intended to exclude motile metazoans but capture all other non-motile material in the water column (Bishop et al. 2012). Depending on depth, 371-6708 L of seawater were filtered. Upon recovery, large particles were washed off of the Nitex filters using 0.2 μm -filtered seawater and captured on 25 mm diameter QMA or GF/F filters. At Station ALOHA, 25 mm punches were taken from GF75 and QMA filters for DNA, ²³⁴Th and bulk carbon and nitrogen content and isotope analysis. All filters were then frozen at -80°C. Data from filtered particles collected in 2014 and analyzed for compound-specific stable isotope analysis are shown for Station ALOHA samples from 25 – 1200 m. These samples were collected and analyzed using similar methods, and were previously reported in Gloeckler et al. (2018).

Table 2.1 Sample types, analyses, and collection locations and dates.

Sample type and location	Analyses	Depth range	Collection dates
Station ALOHA			
Size-fractionated particles	AA-CSIA, ²³⁴ Th disequilibrium	25 – 1200 m	February, August 2014 (Gloeckler et al. 2018)
	AA-CSIA	1500 – 4650 m	July 2019; July, January 2020
	16S rRNA barcoding	25 – 4650 m	July 2020
Abyssal sediment traps	AA-CSIA, carbon flux	4100, 4650 m	March 2019 – January 2020
	16S rRNA barcoding	4000 m	July 2014, 2015, and 2016 (Li et al. 2023)
Station M			
Size-fractionated particles	AA-CSIA, ²³⁴ Th disequilibrium	25 – 3950 m	April/May 2019, October 2019
Abyssal sediment traps	AA-CSIA, carbon flux	3400, 3950 m	March 2018 – April 2019

2.3.2 Surface particle fluxes

Total ²³⁴Th measurements were collected as described in Umhau et al. (2019). Briefly, 2L water samples were collected from the upper 400 m of the water column using Niskin bottles, spiked with ²³⁰Th as a yield tracer at a pH ~1, allowed to equilibrate, and a mixture of KMnO₄. KMnO₄ and MnCl₂ added to co-precipitate Th with MnO₂ after increasing the pH to ~8. Precipitates were filtered onto 25 mm QMA filters, air dried and measured with a low level RISO beta within two weeks of sample collection. Measurements were also taken on 25 mm punches of size-fractionated particles filtered as described above. Samples were recounted 6 months later for background measurement and total Th recoveries were chemically digested and measured using ICP-MS (Pike et al. 2005). Resulting ²³⁴Th activities were used in a steady state ²³⁴Th model to determine export fluxes that were converted to sinking PC fluxes using the C/Th ratio measured on size fractionated particles (Umhau et al. 2019).

Additional estimates of euphotic zone C flux at Station M were determined using the satellite-derived export flux algorithm developed by Kahru et al. (2020). At Station ALOHA, free floating particle interceptor traps deployed at 150 m for 3 days and poisoned with 5% formalin as part of the Hawaii Ocean Time-series observations were also used to measure POM flux.

2.3.3 Amino acid compound-specific stable isotope analysis

QMA and GF75 filters were freeze dried, and AA-CSIA was performed as described in Hannides et al. (2009). Briefly, samples were hydrolyzed with 6 N HCl and purified with a cation exchange column. They were then esterified using a 4:1 isopropanol:acetyl chloride mix and derivatized with a 3:1 methylene chloride:trifluoroacetyl anhydride mix. The resulting trifluoroacetyl and isopropyl ester derivatives were purified with chloroform extraction and acetylated a second time to ensure complete derivatization and stored at -20°C until analysis. Individual amino acid $\delta^{15}\text{N}$ values were measured using a Thermo Scientific Delta V Plus IRMS interfaced to a trace gas chromatograph fitted with a 60 m BPx5 capillary column through a GC-C III combustion furnace (980°C), reduction furnace (680°C), and liquid nitrogen cold trap. Internal reference materials norleucine and aminoadipic acid, with known isotopic compositions, were co-injected with each sample. Every three sample injections, a full suite of 14 amino acid reference compounds, in which the $\delta^{15}\text{N}$ values were known through analysis of pure compounds using an elemental analyzer interfaced with an IRMS (Hannides et al. 2020) and intercalibrated with colleagues at three University laboratories, was injected for quality assurance. $\delta^{15}\text{N}$ values were normalized using a linear regression between the measured $\delta^{15}\text{N}$ values and known $\delta^{15}\text{N}$ values from the reference suite for each amino acid. The uncertainty for each amino acid value was calculated as the standard deviation of three injections, where sufficient material allowed.

2.3.4 Stable isotope data analysis

$\delta^{15}\text{N}$ values of source amino acids ($\delta^{15}\text{N}_{\text{SAA}}$) were calculated as the average $\delta^{15}\text{N}$ values of phenylalanine and lysine. While other source amino acids are often included, due to the low amounts of amino acids in our deepest samples only lysine and phenylalanine were consistently detected in high enough amounts across all samples. Trophic position (TP) was calculated as in Chikaraishi et al. (2009): $\text{TP} = (\delta^{15}\text{N}_{\text{Glx}} - \delta^{15}\text{N}_{\text{Phe}} - 3.4)/7.6 + 1$, where $\delta^{15}\text{N}_{\text{Glx}}$ and $\delta^{15}\text{N}_{\text{Phe}}$ are the $\delta^{15}\text{N}$ values of glutamic acid (Glx, including the contribution of glutamine) and phenylalanine (Phe) in the sample. $3.4 \pm 1\%$ is the difference between $\delta^{15}\text{N}_{\text{Glx}}$ and $\delta^{15}\text{N}_{\text{Phe}}$ in primary producers (β), and $7.6 \pm 1\%$ is the trophic discrimination factor (TDF_{AA}). The uncertainty in the TP values was calculated as the propagated error (Ohkouchi et al. 2017).

We used the ΣV parameter as a proxy for heterotrophic resynthesis of amino acids, defined as the average deviation of $\delta^{15}\text{N}$ values of trophic AAs from their mean value. ΣV values

incorporate bacterial heterotrophy in addition to the eukaryotic trophic steps reflected in trophic position estimates (McCarthy et al. 2007). ΣV was calculated as $\Sigma V = 1/n \Sigma \text{Abs}(\chi_i)$, where n is the total number of AAs used for the calculation and χ_i is the deviation of the $\delta^{15}\text{N}$ value of amino acid i from the mean $\delta^{15}\text{N}$ value of the n amino acids [$\delta^{15}\text{N}_i - (\Sigma \delta^{15}\text{N}_i)/n$]. We used the amino acids alanine, valine, isoleucine, proline, aspartic acid, and glutamic acid to calculate ΣV .

We used MixSIAR (Stock et al. 2018) to create a Bayesian mixing model based on the endmembers of Doherty et al. (2021), utilizing $\delta^{15}\text{N}$ values of threonine and alanine normalized to the $\delta^{15}\text{N}$ values of phenylalanine as in Wojtal et al. (2023). These endmembers include zooplankton collected from the upper 200 m in multiple ocean regions, fecal pellets generated by captured zooplankton, cultured prokaryotic and eukaryotic phytoplankton, and high molecular weight DOM and POM filtered from the upper 1000 m of the water column near the coast of Kona, Hawai‘i (McCarthy et al. 2013; Yamaguchi and McCarthy 2018; Doherty et al. 2021). For our purposes, we combined the zooplankton and fecal pellets into one “zooplankton-influenced” endmember.

2.3.5 16S rRNA microbial community barcoding

Environmental DNA was isolated from size-fractionated particle samples using a DNeasy PowerWater Kit. The hypervariable V4-V5 region of the 16S rRNA gene was amplified via PCR using the primers 515f (GTGYCAGCMGCCGCGGTAA) and 808rB (GGACTACNVGGGTWTCTAAT). Each PCR reaction contained 2.5 μL environmental DNA (5-370 ng/ μL), 5 μL forward and 5 μL reverse primer (1 μM), and 12.5 μL 2x Platinum™ Hot Start PCR Master Mix (Invitrogen, catalog #13000014). PCR amplification was as follows: 95°C for 3 minutes; 30 cycles of 95°C for 30 seconds, 55°C for 30 seconds, and 72°C for 30 seconds; 72°C for 5 minutes, and hold at 4°C. The resulting PCR products were sequenced using an Illumina MiSeq platform at the Advances Studies in Genomics, Proteomics, and Bioinformatics at the University of Hawai‘i at Mānoa. Station ALOHA 4000 m sediment trap 16S rRNA data were collected and reported previously in Li et al. (2023).

2.3.6 Community barcoding data analysis

16S rRNA sequences were analyzed using DADA2 version 1.28.0 (Callahan et al. 2016), implemented in R version 4.3.0. Briefly, quality scores were calculated based on error rates, and

reads were filtered according to the following parameters: maximum of 2 expected errors and minimum length of 240 bases for forward reads and 160 bases for reverse reads. The reads were then dereplicated, and consensus quality scores were constructed and used in a denoising algorithm to infer error rates and distinguish sequencing errors from true sequence variations. The resulting amplicon sequence variants (ASVs) had chimeras removed and were assigned taxonomy using the Silva 138.1 prokaryotic SSU taxonomic training data (McLaren and Callahan 2021).

2.3.7 Statistical analysis

Statistical analyses were performed in R version 4.3.0 using the package *vegan* (Oksanen et al. 2024). We used analysis of variance (ANOVA) to determine whether stable isotope parameters ($\delta^{15}\text{N}$ values and trophic position) varied by particle type (water column submicron, small, and large particles and those captured in sediment traps) and depth. To distinguish samples based on microbial community composition, we used a Principal Coordinate Analysis (PCoA) based on a Bray-Cutis dissimilarity matrix calculated at the ASV level. We used permutational analysis of variance (PERMANOVA) to investigate whether microbial community composition differed by particle type and depth. To relate the isotopic and microbial community data, we performed a probabilistic Principal Component Analysis (PCA) based on $\delta^{15}\text{N}$ values of five source amino acids (phenylalanine, lysine, serine, tyrosine, and glycine) then fit the relative abundance of each ASV as vectors onto the ordination as a linear trend surface using the R package *envfit* (Oksanen et al. 2024). ASVs with $P < 0.05$ were considered to have their abundance significantly correlated with changes in $\delta^{15}\text{N}_{\text{SAA}}$ values.

2.4. Results

2.4.1 Carbon flux

Total PC flux, as measured with sediment traps and satellite-derived estimates, was an order of magnitude higher at Station M than at Station ALOHA at both 150 m and 600 mab (Fig. 2.1). The 150 m water depth was chosen to fall below the mixed layer during all seasons at both sites based on temperature profiles, and 600 mab was chosen as an abyssal measurement that

would not be influenced by benthic boundary layer effects. While PC flux measured using $^{234}\text{Th}:^{238}\text{U}$ disequilibria at 150 m was near or below the detection limit ($< 300 \text{ dpm m}^{-2} \text{ d}^{-1}$) during both sampling periods at Station M, satellite-derived estimates show a late summer increase in PC export that occurred shortly after our pump sampling (Fig. 2.1a). While we do not have abyssal flux measurements concurrent with pump sampling at Station M, sediment trap fluxes from the previous year and the 10-year average show that surface export is reflected in summertime abyssal flux increases (Fig. 2.1c). At Station ALOHA, ^{234}Th -derived PC flux at 150 m was 17.25 ± 11.66 and $9.99 \pm 2.30 \text{ mg C m}^{-2} \text{ d}^{-1}$ in summer 2019 and 2020, respectively, while in winter 2020 it was below the detection limit (Fig. 2.1b). We compared ^{234}Th derived PC fluxes with PC fluxes measured from drifting sediment traps at 150 m at Station ALOHA as part of the Hawai'i Ocean Time-series, which showed similar summer export pulses occurred during our pump sampling in 2014 and 2019 (Fig. 2b). Particle flux pulses were also seen during both years in abyssal sediment traps (Fig. 2.1d). While we do not have shallow or deep trap estimates of flux during 2020 at Station ALOHA, the ten-year averages reveal that 2014 and 2019 followed typical flux patterns (Fig. 2.1b, d).

2.4.2 Compound-specific stable isotope analysis

Some samples, particularly those from abyssal depths, did not have sufficient material to analyze in triplicate. For these, we assumed a conservative $\pm 1\text{‰}$ error for $\delta^{15}\text{N}_{\text{SAA}}$ values as in Doherty et al. (2021) and Wojtal et al. (2023). At both sites, average $\delta^{15}\text{N}$ values of the source amino acids lysine and phenylalanine ($\delta^{15}\text{N}_{\text{SAA}}$) differed between particle size fractions (two-way ANOVA; Station M, $F = 6.98$, $P = 0.0042$; Station ALOHA, $F = 12.92$, $P < 0.001$) and over depth (two-way ANOVA; Station M, $F = 4.32$, $P = 0.0074$; Station ALOHA, $F = 7.37$, $P < 0.001$), although there was not an interaction between particle size and depth (two-way ANOVA, $P > 0.05$). For this analysis, depths were binned into 25, 50, 75, 100, 150, 200, 250, and 400 m, with all deeper samples grouped together, as the top 400 m is where the greatest change occurred (Fig. 2.2a, d). $\delta^{15}\text{N}_{\text{SAA}}$ values in filtered particles generally increased with depth within the upper 400 m, with the largest increases occurring in the submicron and small size fractions at Station ALOHA (Fig. 2.2g). Throughout the water column, the largest particles ($>53 \mu\text{m}$) had lower $\delta^{15}\text{N}_{\text{SAA}}$ values than the submicron and small size fractions (Fig. 2.2a). This trend was consistent throughout the water column at Station ALOHA despite the time lag of samples <1200 m collected in 2014 and

samples >1500 m collected in 2019 and 2020. The material captured in sediment traps moored at 600 and 50 mab had lower $\delta^{15}\text{N}_{\text{SAA}}$ values than any of the size fractions of particles filtered at the same depth. Instead, sediment traps at both sites captured material with similar $\delta^{15}\text{N}_{\text{SAA}}$ values to filtered particles at the surface (Fig. 2.2g). For both sediment trap and filtered POM and within each size class, the POM from 50 mab had higher values than that from 600 mab (Fig. 2.2a, d). There were no significant seasonal differences in $\delta^{15}\text{N}_{\text{SAA}}$ values at either site (Student's t-test, $P > 0.05$).

At both sites, the estimated trophic position varied between particle size (two-way ANOVA; Station M, $F = 5.26$, $P = 0.012$; Station ALOHA, $F = 5.27$, $P = 0.0015$) but was not significantly influenced by depth (two-way ANOVA, $F = 0.638$, $P > 0.05$). Trophic levels reached maximum values of around 2 within the euphotic zone and then stayed consistent throughout the water column within a size class, with some notable exceptions (Fig. 2.2b, e). At Station M, the large particles had a trophic level of 2.26 ± 0.09 at 100 m, which decreased to 0.99 at 1500 m (Fig. 2.2b). The trophic levels of sediment trap material from Station M were higher than those of any of the filtered particles, ranging from 2.05 ± 0.05 to 3.18 ± 0.09 , except the large particles at 50 and 600 mab in Fall 2019 (Fig. 2.2b). Similarly, at Station ALOHA the highest trophic levels were found in bathypelagic large and small particles from July 2020 and sediment trap material from all seasons, although these trophic levels were not as high as those at Station M, with the highest values being 2.25 ± 0.05 in the sediment trap 50 mab in July 2019 and 2.56 in large particles at 1500 m in July 2020 (Fig. 2.2e). As with $\delta^{15}\text{N}_{\text{SAA}}$ values, no seasonal differences in trophic level were observed (Student's t-test, $P > 0.05$) and values remained generally consistent below 500 m despite the six-year time difference in sample collection (Fig. 2.2d, g, Table 2.1).

The ΣV parameter, an estimate of heterotrophic amino acid resynthesis, followed similar patterns to the $\delta^{15}\text{N}_{\text{SAA}}$ values, increasing in the euphotic zone and then remaining similar within each particle size fraction (Fig. 2.2c, f). Additionally, sediment trap material had lower ΣV values than filtered particles at depth except for small particles at Station M (Fig. 2.2c). No seasonal differences in ΣV were found at either site (t-test, $P > 0.05$), and while values at Station ALOHA changed with depth, particularly in the large size fraction (Fig. 2.2f), there were no overall differences in the samples collected in 2014 versus 2019 and 2020.

A Bayesian mixing model based on that of Doherty et al. (2021) revealed that the particles had varying proportions of microbially degraded organic matter, phytoplankton/phytodetritus, and zooplankton carcasses/fecal pellets. Overall, the large particles had the highest proportions (up to 52.5%) of zooplankton-derived material, while submicron and small particles near the surface had the most phytoplankton/phytodetritus components (up to 47.7%) (Fig. 2.3). Both filtered particles and sediment trap material had high proportions of microbially degraded organic matter, between 36.5 and 77.9% (Fig. 2.3). At Station ALOHA, particle types differed in their proportion of phytoplankton/phytodetritus (one-way ANOVA, $F = 6.76$, $P < 0.001$) and zooplankton-derived material (one-way ANOVA, $F = 9.21$, $P < 0.001$), but not microbially degraded material (one-way ANOVA, $P > 0.05$). At Station M, particle types differed only in proportion of microbially degraded material (one-way ANOVA, $F = 9.21$, $P = 0.0028$).

2.4.3 Microbial community analysis

Among 18 samples of filtered POM, 16S rRNA sequencing yielded 1,738,683 reads, with 718 to 187,180 reads per sample. After filtering and trimming 1,440,267 reads were left. The paired reads were merged, and 50.3% were removed as chimeras. This resulted in 8,333 ASVs from 18 samples being used for the following analyses. Alpha diversity was similar among most samples, with low outliers being the 0.3-1 μm particles at 1500 and 4100 m, using both the Shannon and Simpson indices (Supplemental data). a

The phyla Cyanobacteria, Proteobacteria, and Thaumarchaeota were the most abundant among all the samples, with Cyanobacteria dominating euphotic 0.3-1 μm and 1-53 μm samples and Thaumarchaeota being most prominent in 0.3-1 μm mesopelagic and 1-53 μm abyssopelagic particles (Fig 4a-c). Most Thaumarchaeota were members of the Nitrosopumiliaceae family, while at the genus level most Cyanobacteria ASVs belonged to *Prochlorococcus* spp. Proteobacteria were abundant throughout the water column, making up at least 25% of ASVs in almost all samples (Fig. 2.4a-c). Community composition in moored sediment trap samples, collected in 2014-2016 and presented previously in Li et al. (2023), differed from the filtered samples, with similar contributions of Proteobacteria, but a much larger proportion of Epsilonproteobacteria (Fig. 2.4d). Microbial community composition was influenced by depth

(PERMAOVA, $F = 2.69$, $P = 0.002$), but not by particle size (PERMANOVA, $F = 1.22$, $P > 0.05$) (Fig. 2.5).

2.4.4 Microbial community relationships with stable isotope values

We created a probabilistic PCA of the samples based on $\delta^{15}\text{N}$ values of the source amino acids glycine, serine, phenylalanine, tyrosine, and lysine, which loosely grouped the samples by particle size (Fig. S1). The probabilistic PCA allowed us to include all five amino acids despite missing values for some amino acids in some samples (Table S1). Of the 8,333 unique ASVs detected among all particle samples, 58 were significantly correlated with isotopic principal components when their abundance was considered as environmental vectors (multiple regression, $P < 0.05$). 49 of the 58 significant ASVs were within the archaeal Nitrosopumilaceae family (Table S1). When all amino acids, including both trophic and source AAs, were used to create the probabilistic PCA, 143 ASVs were significantly correlated as environmental vectors. None were Nitrosopumiliaceae (Fig. S1). Instead, 122 were Cyanobacteria.

We further used general linear models to determine the relationship between the abundance of the family and isotopic values. We found that $\delta^{15}\text{N}_{\text{SAA}}$ values had a positive correlation with Nitrosopumiliaceae abundance in the euphotic and mesopelagic zones (Linear Regression, $F = 17.23$, $P = 0.006$), but not when abyssopelagic samples were included (Linear Regression, $F = 0.64$, $P > 0.05$). To determine whether this correlation was only due to changes with depth, we tested the correlation of both family and isotopic values with depth. The abundance of Nitrosopumiliaceae was positively correlated with depth in the euphotic and mesopelagic zones (Linear Regression, $F = 7.64$, $P = 0.020$) but not when abyssal samples were included (Linear Regression, $F = 0.93$, $P > 0.05$) (Fig. 2.6). In contrast, $\delta^{15}\text{N}_{\text{SAA}}$ values were positively correlated with depth across the whole water column (Linear Regression, $F = 4.99$, $P = 0.047$).

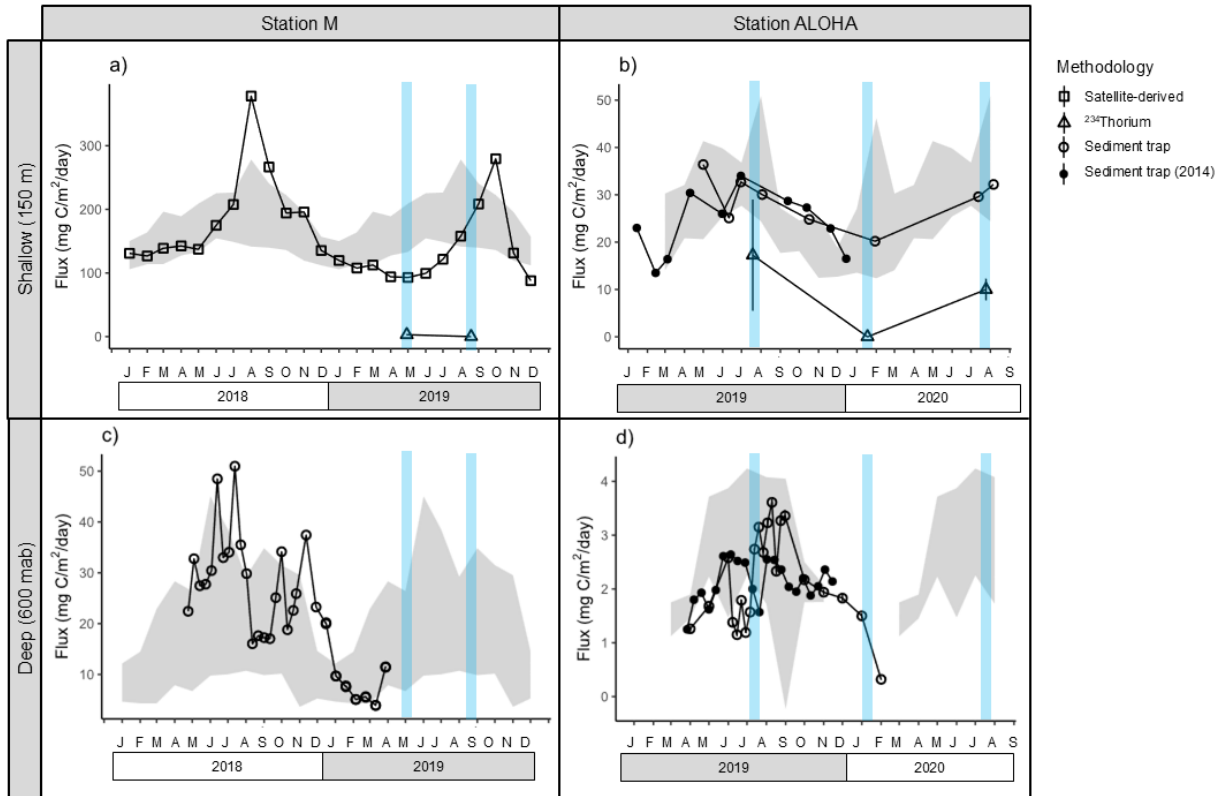


Figure 2.1. Total C flux at **a, b**) 150 m and **c, d**) 600 mab, as measured using satellite-derived estimates (squares), ²³⁴Th disequilibrium (triangles), and sediment traps (circles; drifting traps at 150 m and moored traps at 600 mab). At Station ALOHA, trap data from 2014 (filled circles) are overlaid on the 2019 data. Gray shaded regions show the 10-year average ± standard deviation (2010-2019) for **a**) satellite-derived estimates, **b**) drifting sediment traps, and **c, d**) moored sediment traps. Blue bars indicate filtered particle sampling periods during 2019 and 2020.

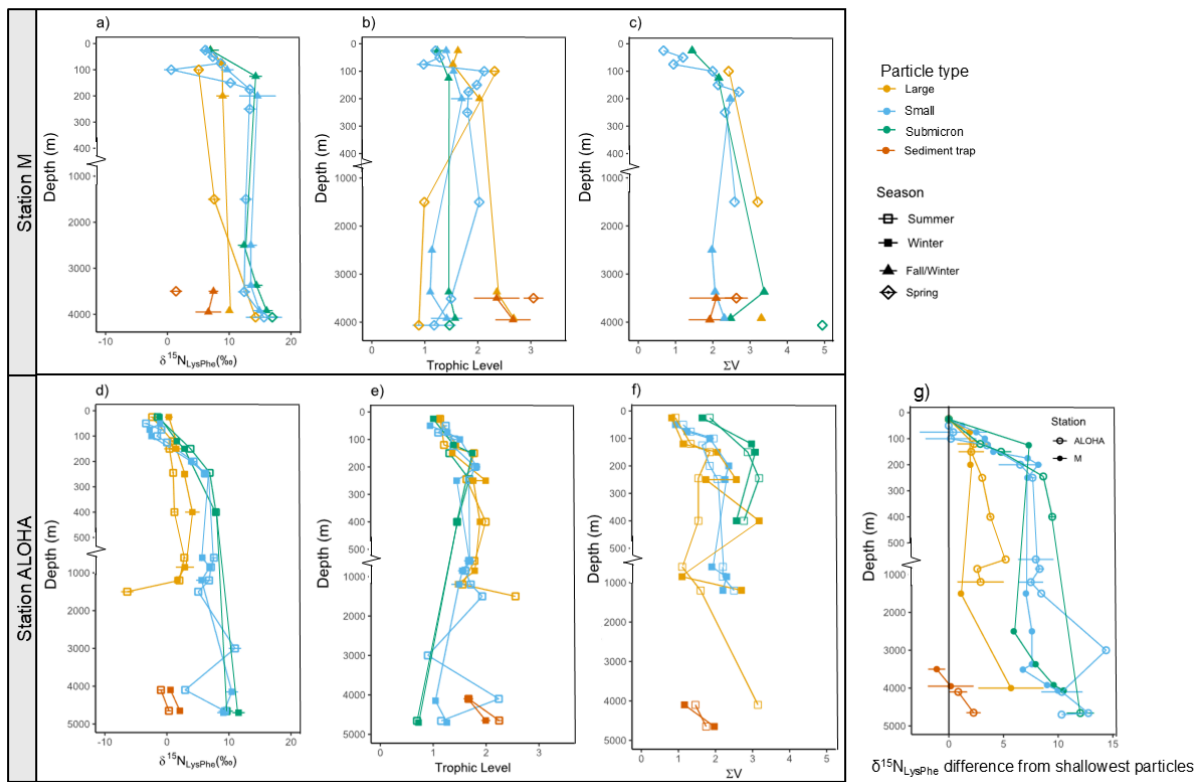


Figure 2.2. **a, d)** $\delta^{15}\text{N}_{\text{SAA}}$ values, **b, e)** estimated trophic levels, and **c, f)** ΣV parameter of filtered particles and sediment trap material from **a-c)** Station M and **e-f)** Station ALOHA. **g)** $\delta^{15}\text{N}_{\text{SAA}}$ values standardized to the values at 25 m within each size class, site, averaged between the seasons. Error bars show **a, d)** the average analytical error of lysine and phenylalanine, **b, e)** propagated error, and **g)** standard deviation, where available. Note the scale changes on the y axes.

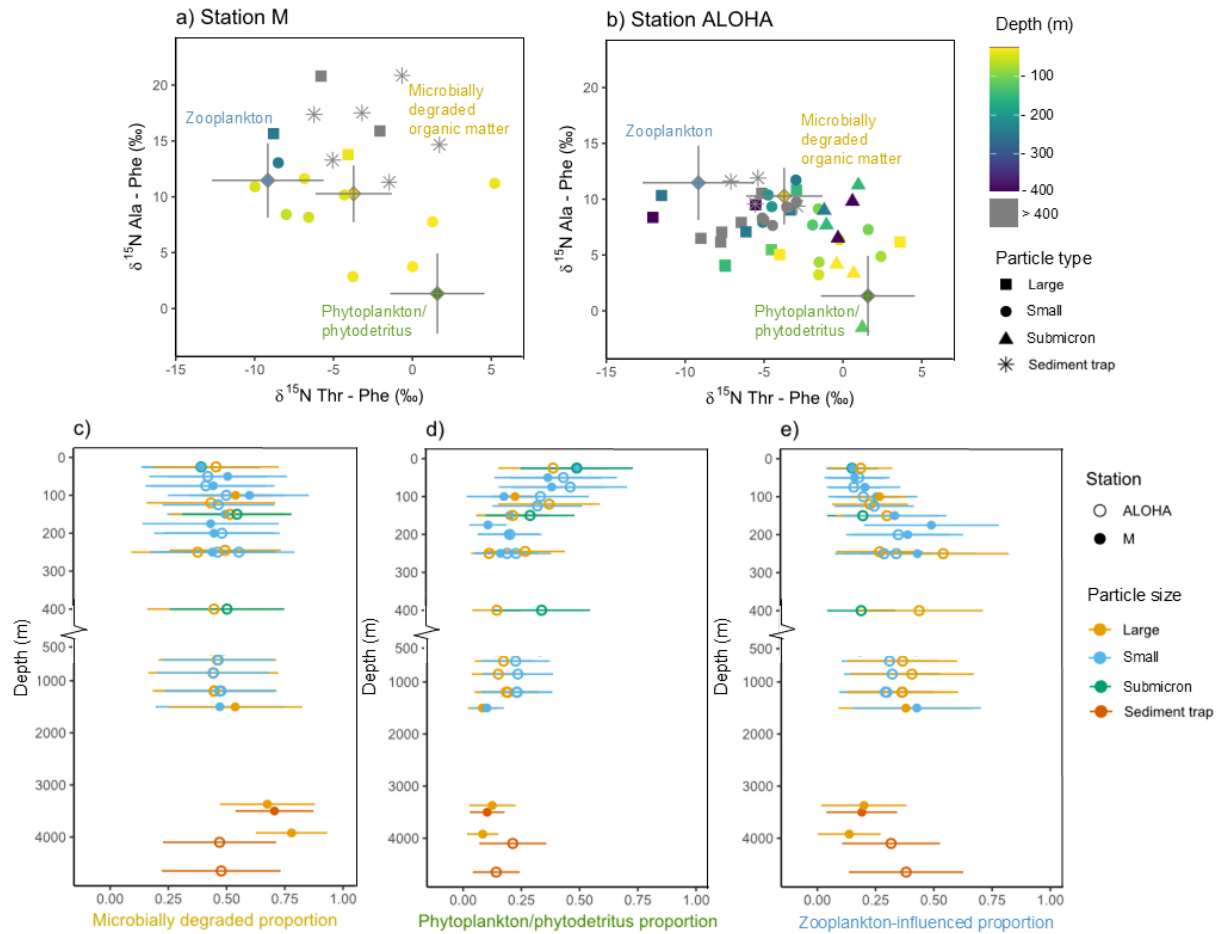


Figure 2.3. $\delta^{15}\text{N}$ values of threonine and alanine, normalized with phenylalanine as in Doherty et al. (2021). The mean and standard deviation of each endmember from Doherty et al. (zooplankton plus zooplankton fecal pellets, microbially degraded organic matter, and phytoplankton/phytodetritus) are overlaid on our particle data at **a)** Station M and **b)** Station ALOHA. **c-e)** The results of a Bayesian mixing model using the endmembers of Doherty et al., with error bars showing standard deviation.

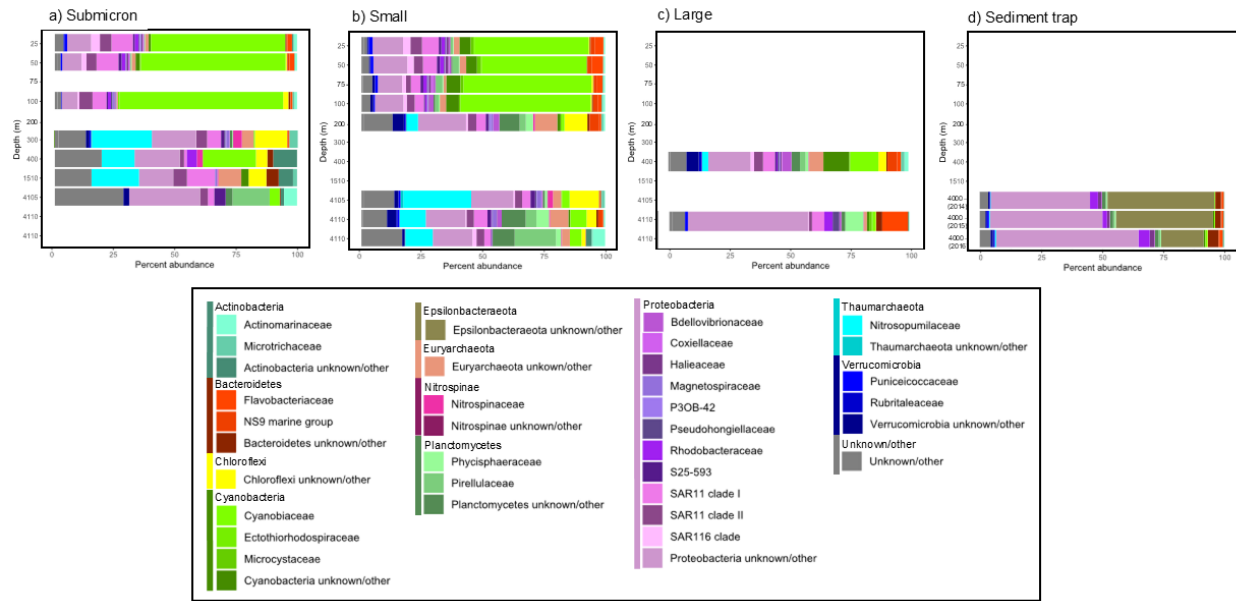


Figure 2.4. Taxonomic assignments of ASVs at Station ALOHA as a percentage of sequences from sediment traps and particles size fractionated to **a)** submicron 0.3-1 μm , **b)** small 1-53 μm , and **c)** large >53 μm . **d)** Material captured in abyssopelagic sediment traps in July 2014, 2015, and 2016, from Li et al. (2023). Taxonomic assignments shown are the 25 most abundant families and 10 most abundant phyla among all samples.

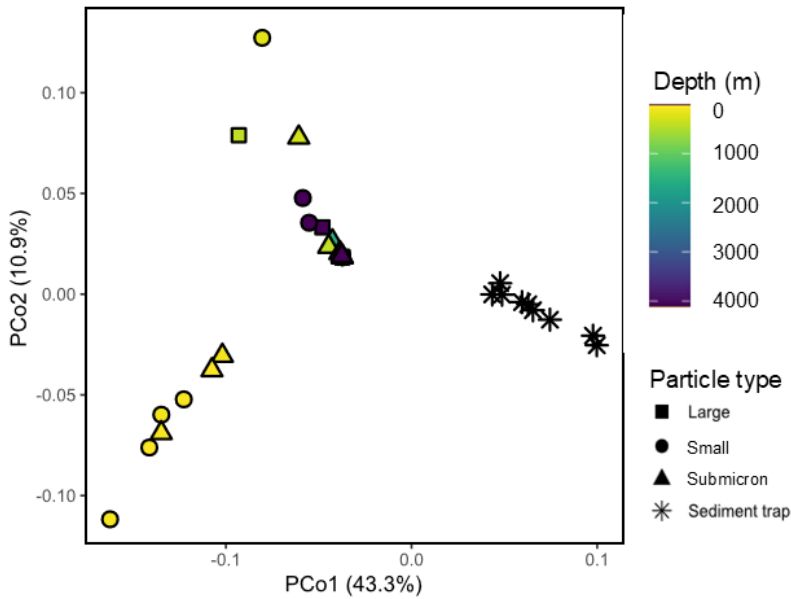


Figure 2.5. Principal Coordinate Analysis (PCoA) based on Bray-Curtis dissimilarity matrix of ASV abundances, showing differences in microbial community composition. Points are colored by depth and shapes indicate particle size.

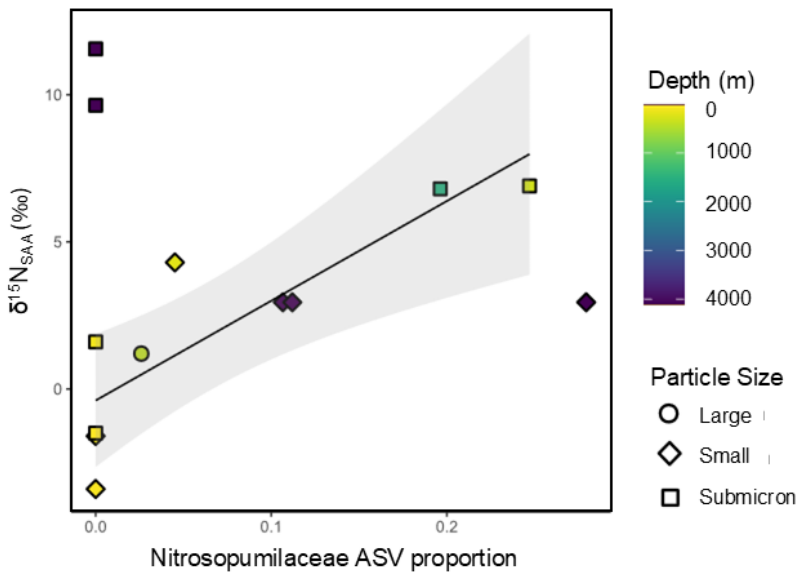


Figure 2.6. Proportion of ASVs in filtered particle samples assigned to the Nitrosopumilaceae family and the corresponding $\delta^{15}\text{N}_{\text{SAA}}$ values for those samples. Points are colored by depth and shapes indicate particle size. Linear regression is shown taking into account only the points from <1500 m, $y = 33.89x - 0.39$.

2.5 Discussion

Sinking POM flux is a key mechanism of carbon export and provides energy to deep-sea food webs. Transformations of particles below the euphotic zone, however, have been poorly characterized. We quantified particle transformations and associated microbial communities throughout the water column, from the surface to the abyssal plain. We compared POM captured in moored sediment traps, a sampling methodology that has frequently been used to quantify flux, with size-fractionated particles filtered *in situ* at two sites in the North Pacific with contrasting productivity. Sediment traps disproportionately captured material that isotopically resembled surface particles, suggesting they primarily capture large and/or fast-sinking flux. Additionally, we combined compound-specific stable isotope analysis with 16S rRNA barcoding and found that the abundance of ammonia-oxidizing archaea in the lower euphotic and upper mesopelagic at Station ALOHA was associated with increasing $\delta^{15}\text{N}$ values of source amino acids, linking microbial recycling of organic material to areas of the upper water column with high amounts of remineralization.

2.5.1 Isotopic indications of microbial reworking of sinking POM

Sediment trap, thorium disequilibrium, and satellite-derived estimates of flux at Station M and Station ALOHA supported our understanding of the differences between the two sites, with an order of magnitude more carbon reaching the abyssopelagic at Station M (Fig. 2.1). While both sites showed seasonality in export magnitude, the differences between low and high flux seasons were greater at Station M (Fig. 2.1). The large seasonal differences at Station M were reflected in the isotopic composition of sediment trap material, with higher $\delta^{15}\text{N}_{\text{SAA}}$ values in the fall, the higher flux season (Fig. 2.2a). Higher $\delta^{15}\text{N}_{\text{SAA}}$ values may be indicative of more microbial remineralization (Hannides et al. 2013), as well as changes in the dominant primary producers or utilization of surface nitrate (Casciotti et al. 2008; Décima and Landry 2020). We did not find consistent seasonal differences in the size-fractionated particles at Station M, nor in any of the similarly sampled time points at Station ALOHA (Fig. 2.2). This suggests that while the magnitude of flux is seasonally variable at both sites, the processes of POM production and remineralization remain consistent throughout the year.

We found an overall trend of increasing $\delta^{15}\text{N}_{\text{SAA}}$ values with depth, although the increase was primarily confined to the top 250 m of the water column (Fig. 2.2). Increases in $\delta^{15}\text{N}$ values of source amino acids indicate microbial, but not metazoan, reworking of organic material due to heterotrophic breaking of C-N bonds and, in some cases, *de novo* synthesis by chemotrophic microbes (Hannides et al. 2013; Ohkouchi et al. 2017). At Station ALOHA, samples from depths 1200 m and above were collected in 2014, while samples from 1500 m and below were collected in 2019 and 2020. Despite this time gap, the $\delta^{15}\text{N}_{\text{SAA}}$ values, trophic positions, and ΣV values remained generally consistent within each size fraction (Fig. 2.2d-f). This consistency suggests that although $\delta^{15}\text{N}_{\text{SAA}}$ values in surface water samples can exhibit seasonal variability, these values converge at depth with minimal variation between 1200 m and abyssal depths (Hannides et al. 2009). Notably, smaller size fractions exhibited larger increases in $\delta^{15}\text{N}_{\text{SAA}}$ values, likely due to slower sinking speeds, which allow for greater reworking (Guidi et al. 2008).

Submicron and small particles underwent greater increases in $\delta^{15}\text{N}_{\text{SAA}}$ values at Station ALOHA than at Station M, suggesting less efficient export and more microbial reworking at the oligotrophic site (Fig. 2.2g; Henson et al. 2012). A mixing model based on Doherty et al. (2021) indicated that microbially reworked organic matter is a major component of POM at both sites, but the extent of microbial degradation is greater at Station ALOHA (Fig. 2.3d). The larger surface export fluxes at Station M seem to be largely captured in the deep moored sediment traps, while the smaller surface fluxes at Station ALOHA undergo more remineralization as indicated by larger relative increases in $\delta^{15}\text{N}_{\text{SAA}}$ values (Fig. 2.2g). At both sites, the greatest changes in $\delta^{15}\text{N}_{\text{SAA}}$ values and trophic position occurred within the upper ~400 m, with smaller subsequent changes throughout the rest of the water column (Fig. 2.2), suggesting that the lower euphotic and upper mesopelagic zones are where the majority of POM remineralization takes places. Similarly large changes in $\delta^{15}\text{N}_{\text{SAA}}$ values with depth in the upper ~400 m have also been observed in the central equatorial Pacific and in the northeast Pacific (Romero-Romero et al. 2020; Wojtal et al. 2023).

At both sites, sampling method (*in situ* filtration versus moored sediment traps) had a strong influence on the characteristics of POM captured as reflected in stable isotope values. The material captured in sediment traps near the seafloor had lower $\delta^{15}\text{N}_{\text{SAA}}$ values and higher trophic levels than particles filtered *in situ* from comparable depths during similar times (Fig. 2.2). Instead, sediment trap material had isotopic values more closely matching filtered particles

from surface waters, or in the case of Station M, large particles in the mesopelagic zone (Fig. 2.2a, d). Moored sediment traps are known to under-sample small, slowly-sinking particles (Buesseler et al. 2000; Honjo et al. 2008). Our data support these findings, as large filtered particles with similar $\delta^{15}\text{N}_{\text{SAA}}$ values to the sediment trap material likely sank much faster than the smaller size fractions (Guidi et al. 2008). The combination of low $\delta^{15}\text{N}_{\text{SAA}}$ values and high trophic levels (up to 3 at Station M) also indicates that the material captured in sediment traps may be mostly metazoan-derived, such as from zooplankton fecal pellets, consistent with previous reports (Boeuf et al. 2019). On the other hand, results of a mixing model based on $\delta^{15}\text{N}$ values of threonine and alanine indicated that the sediment trap material was largely composed of microbially degraded POM, especially at Station M; however this may be because sediment trap values fall outside the range of any of the three endmembers (Fig. 2.3a). Doherty et al. (2021) measured epipelagic zooplankton and their freshly produced fecal pellets, while fecal pellets originating in surface waters but captured in abyssal sediment traps would have time to undergo degradation by both gut-derived and water column bacteria. Additional fecal pellets produced by zooplankton below the euphotic zone may also contribute to the material captured in sediment traps.

Taken together, our different isotopic analyses suggest somewhat contradictory results as to the type of material we captured in sediment traps: low $\delta^{15}\text{N}_{\text{SAA}}$ values suggest sediment trap material matched large and fast-sinking particles similar to surface particles, trophic positions of 2-3 indicate metazoan-derived material, the threonine/alanine mixing model suggests microbially degraded material, while relatively low ΣV values indicate minimal microbial reworking (Fig. 2.2, 2.3). These AA-CSIA analyses were developed mainly in shallow water systems and may not account for some of the unique microbial pathways that occur in the deep sea. In particular, the “microbially degraded” endmember we used in the alanine/threonine mixing model was based on only four measurements of DOM at a maximum depth of 915 m (Doherty et al. 2021). This method of distinguishing types of organic material could have improved utility and applicability by incorporating additional DOM samples from greater depths, different ocean regions, and taking into account the wide variety of microbial metabolic pathways and their impact on $\delta^{15}\text{N}$ values of amino acids (Ohkouchi et al. 2017).

Regardless, the isotopic differences between the deep moored sediment trap material and filtered particles suggest that sediment traps, one of the primary methods of quantifying and

identifying the export flux that supplies food to abyssal communities, do not capture a more heavily degraded proportion of the POM in the abyssopelagic that could be used as an additional food source by benthic abyssal ecosystems. Differences in the $\delta^{15}\text{N}_{\text{SAA}}$ values of sediment trap materials and *in situ* filtered particles have important implications for interpreting the POM that sustains deep-sea communities. Romero-Romero et al. (2021) reported the average $\delta^{15}\text{N}_{\text{SAA}}$ values (lysine and phenylalanine) in the gut (11.5‰, range 7.5 to 15.0‰) and body tissues (10.7‰, range 8.1 to 13.9‰) of deposit feeder at Station M. These values are higher than those observed in sediment trap materials and overlap with the $\delta^{15}\text{N}_{\text{SAA}}$ values of *in situ* particles. This suggests that POM collected in sediment traps – and possibly the flux measured in deep traps – may not accurately represent the exported POM that supports deep-sea deposit feeder communities, at least at Station M.

2.5.2 Microbial communities associated with POM at Station ALOHA

The ASVs associated with large (>53 μm) particles are likely dominated by particle-attached taxa, while the submicron (0.3-1 μm) reads are likely associated with free-living microbes and the small (1-53 μm) size fraction likely represents a mix of both communities (Suzuki et al. 2017). The microbial communities associated with different particle sizes were similar in surface waters, but increasingly differed with depth, suggesting the development of distinct communities as POM sinks from surface waters (Fig. 2.4, 2.5). At the surface, all sizes of particles are relatively fresh and labile (as in Wakeham et al. 1984), leading to the formation of similar communities dominated by photoautotrophic Cyanobacteria, but the different sinking speeds and labilities associated with large and small particles below the euphotic zone likely selected for the increasingly distinct communities (Comstock et al. 2024).

Unlike the isotopic parameters, microbial communities changed continuously throughout the water column, with composition influenced primarily by depth (Fig. 2.5). The euphotic zone particles (less than 200 m in depth) clustered together and were dominated by Cyanobacteria, with communities at 200-400 m forming their own looser cluster that overlapped with the deep filtered particles (Fig. 2.5). This sharp transition in community composition below the euphotic zone has been observed previously at Station ALOHA and elsewhere (DeLong et al. 2006; Bryant et al. 2016; Mende et al. 2017). The submicron, small, and large filtered particles in the abyssopelagic hosted unique communities (Fig. 2.4). This could result from the different sinking

speeds of particles, with the larger particles (>53 μm filtered and sediment trap captured) facilitating the rapid export of surface taxa while the slower-sinking small and submicron particles have more time to be colonized by piezophilic deep-sea specialists (Ma et al. 2024). Alternatively, the higher $\delta^{15}\text{N}_{\text{SAA}}$ values of smaller particles at Station ALOHA (Fig. 2.2d) indicate they have been partially hydrolyzed, therefore containing less labile organic material and possibly selecting for specialist communities able to metabolize different molecules. The direction of the relationship between microbial community composition and particle quality and composition is not clear, and most likely the two influence one another. By combining AA-CSIA and microbial community barcoding, we are able to determine which microbial communities are most associated with POM breakdown. One of the most consistent results throughout all depths and particle sizes was the presence of Proteobacteria, including SAR11, known to be a prominent heterotroph at Station ALOHA (Bryant et al. 2016).

Poff et al. (2021) and Li et al. (2023) sequenced and identified microbial communities in sediment traps deployed at 4000 m at Station ALOHA from 2014 to 2016. The trap-captured communities were distinct from those associated with particles we filtered from the same depths (Fig. 2.5). Sediment traps contained many of the same broad taxonomic groups as those identified here in the filtered particles, but in different proportions. Notably, Thaumarchaeota and Planctomycetes comprised a much smaller proportion of reads than in our abyssal samples. Furthermore, their deep moored sediment traps were dominated by the genera *Arcobacter* and *Colwellia* in the phyla Epsilonbacteraeota and Proteobacteria, respectively, neither of which comprised a significant proportion of the reads in our filtered samples (Fig. 2.4). In combination with our finding that abyssal sediment trap material has much lower $\delta^{15}\text{N}_{\text{SAA}}$ values than filtered particles, these microbial community differences reinforce the finding that the fast-sinking particles captured in sediment traps undergo different microbial reworking by different communities than the small particles we filtered from the water column.

2.5.3 Ammonia oxidizing archaea associated with POM reworking

While members of archaeal family Nitrosopumilaceae only made up 6% of ASVs across all samples, they were responsible for 84% of the ASVs significantly correlated with $\delta^{15}\text{N}_{\text{SAA}}$ principal components (Fig. S1), and their abundance had a significant positive relationship with $\delta^{15}\text{N}_{\text{SAA}}$ values in the upper water column at Station ALOHA (Fig. 2.6). Ammonia oxidizing

archaea (AOA) such as Nitrosopumilaceae are abundant free-living archaea throughout the euphotic and mesopelagic tropical Pacific where they play a crucial role in the first step of nitrification by oxidizing ammonia to nitrite (Karner et al. 2001; Church et al. 2010; Beman et al. 2012). Comstock et al. (2024) also found abundant Nitrosopumiliaceae reads in the lower euphotic and upper mesopelagic at the similarly oligotrophic Bermuda Atlantic Time Series, around the same depths at which $\delta^{15}\text{N}_{\text{SAA}}$ values increased in $< 6 \mu\text{m}$ particles. While their presence as indicated by 16S rRNA abundance does not guarantee the Nitrosopumilaceae we observed at Station ALOHA are actively performing ammonia oxidation, other work in similar parts of the ocean found that the abundances of the *amoA* ammonia oxidation gene were similar to AOA 16S rRNA abundance, suggesting that nearly all AOA are likely contributing to nitrification, which is relatively high in the upper ocean at Station ALOHA (Dore and Karl 1996; Dore et al. 1998; Mincer et al. 2007; Beman et al. 2008, 2012; Church et al. 2010).

It is unlikely that Nitrosopumilaceae directly drive the increase in $\delta^{15}\text{N}_{\text{SAA}}$ values in filtered particles at Station ALOHA, as their production of new organic matter from ammonia oxidation probably does not lead to source amino acids with higher $\delta^{15}\text{N}$ values than those synthesized by heterotrophic breakdown of organic matter (Ohkouchi et al. 2017; Yamaguchi et al. 2017), although to our knowledge no studies have directly measured the $\delta^{15}\text{N}$ values of AOA amino acids. Additionally, while barcoding showed that they are prominent members of the free-living community in the midwater (Fig. 2.4) they are unlikely to dominate the biomass to the extent that they contribute overwhelmingly to the increase in $\delta^{15}\text{N}_{\text{SAA}}$ values. Instead, we propose that the relationship we found between Nitrosopumilaceae abundance and $\delta^{15}\text{N}_{\text{SAA}}$ values is indicative of a zone of increased heterotrophic breakdown, where the resulting products support archaeal chemoautotrophy. The high amounts of microbial breakdown of POM at Station ALOHA, which on its own decreases the quantity and quality arriving at the seafloor, may also lead to large amounts of organic matter recycling in the upper water column through archaeal and bacterial nitrification of the products of heterotrophic breakdown such as ammonia. The relationship between Nitrosopumilaceae abundance and $\delta^{15}\text{N}_{\text{SAA}}$ values was not significant if abyssopelagic particles were included (Fig. 2.6). While we did find Nitrosopumilaceae in abyssal samples (Fig. 2.4), pelagic ammonia oxidation has not been documented at those depths at Station ALOHA (Ward 2008). While AOA activity is not a primary driver of POM breakdown in the water column, their significant association with increasing $\delta^{15}\text{N}_{\text{SAA}}$ values in the lower

euphotic and upper mesopelagic zones suggests that their presence at Station ALOHA is driven by some of the same factors that lead to the low quality of POM export that reaches abyssal communities.

The non-Nitrosopumilaceae ASVs that had significant correlations with $\delta^{15}\text{N}_{\text{SAA}}$ principal components belonged to the SAR11 clade and the phyla Euryarchaeota, Nitrospinae, and Verrucomicrobia (Fig. S1c, d). Nitrospinae includes nitrite oxidizing bacteria (Mincer et al. 2007; Jameson et al. 2023), which contribute to surface and midwater nitrification although at lower rates than AOA, particularly in nutrient-poor environments like the NPSG, due to AOA's higher affinity for ammonium (Martens-Habbena et al. 2009). The presence of significant ASVs assigned to SAR11 indicates that they are not only prevalent throughout the water column, but also play a role in increasing $\delta^{15}\text{N}_{\text{SAA}}$ values via heterotrophic reworking.

2.6 Conclusions

A combination of amino acid compound-specific $\delta^{15}\text{N}$ values and 16S rRNA community barcoding revealed that different sizes of POM host distinct microbial communities, which correspond with differences in lability and amount of heterotrophic reworking as they sink from euphotic to abyssopelagic depths. At both the eutrophic Station M and the oligotrophic Station ALOHA, sediment traps captured large, fast-sinking particles more similar to surface particles than particles filtered *in situ* at the same depths, suggesting that sediment traps miss a significant proportion of the POM in the abyssopelagic that could be used as a food source by abyssal organisms. As the first study to use AA-CSIA to examine particle transformations throughout the entire water column, we found that $\delta^{15}\text{N}_{\text{SAA}}$ values underwent large changes primarily between 200 and 400 m as POM exited the euphotic zone, and then remained similar within each size class down to abyssal depths. Microbial community composition changed throughout the water column even at high taxonomic levels but the communities in the lower euphotic and upper mesopelagic were associated with the greatest amount of heterotrophic transformation of sinking POM, as evidenced by changes in $\delta^{15}\text{N}_{\text{SAA}}$ values. Additionally, the abundance of the ammonia oxidizing archaea Nitrosopumilaceae at Station ALOHA had a significant relationship with changes in $\delta^{15}\text{N}_{\text{SAA}}$ values, suggesting that high rates of heterotrophic POM breakdown in the

lower euphotic and upper mesopelagic supports midwater autotrophic nitrification and POM recycling at oligotrophic abyssal sites.

**CHAPTER 3. Niche partitioning among abyssal deposit-feeding echinoderms
is linked to mobility and gut microbiota**

Lee C. Miller, Sonia Romero-Romero, Brian N. Popp, Jeffrey C. Drazen

3.1 Abstract

Deposit-feeding echinoderms are dominant megafauna on abyssal plains, where they consume organic detrital material at the base of the benthic food web. However, the strategies they use to survive on irregular pulses of poor-quality detritus remain poorly understood in many regions. Using compound-specific stable isotope analysis of amino acids, we found that deposit-feeding holothurians and echinoids in the oligotrophic North Pacific Subtropical Gyre are secondary rather than primary consumers of detritus, consistent with earlier findings from the productive California Current Ecosystem suggesting they consume gut microbial biomass or its products. At both sites, gut microbiomes were dominated by Actinobacteria, Proteobacteria, and Planctomycetes, and in some species, by the ammonia-oxidizing archaea Nitrosopumilales. Many of the more mobile deposit feeders, including swimming holothurians, also contained high proportions of Cyanobacteria in their guts during high-flux seasons, demonstrating that fast-moving taxa can consume fresher phytodetritus than slower-moving and non-swimming species. Using a mixing model based on $\delta^{15}\text{N}$ values of source amino acids we found that deposit feeders capable of swimming consume a higher proportion of larger and fresher particles than obligate benthic species, directly linking swimming behavior to feeding selectivity. Differences in the gut microbiota of deposit feeders on abyssal plain ecosystems, characterized by both high- and low-flux regimes, corresponds to niche partitioning based on detritus of differing nutritional qualities.

3.2 Introduction

Deep-sea benthic food webs are dependent on organic matter exported from surface waters, which often arrives as irregular pulses of phytodetritus (Rice et al. 1986; Smith et al. 1996), animal carcasses (Lebrato et al. 2013), and fecal pellets (Steinberg and Landry 2017). Deposit-feeding echinoderms, particularly holothurians, dominate the megafaunal biomass and abundance on abyssal plains (seafloor between 3000-6000 m depth; Lauerman et al. 1996; Ruhl 2007). They are responsible for extensive reworking of phytodetritus and other types of surface-derived flux (Kaufmann and Smith 1997; Ginger et al. 2001), and have traditionally been considered primary consumers of detritus (Ginger et al. 2001). However, recent work using compound-specific stable isotope analysis has revealed that abyssal deposit feeders (DFs) at

Station M in the California Current Ecosystem are secondary consumers two trophic levels above the sedimentary organic matter they consume, with gut microbiota potentially acting as intermediate primary consumers (Romero-Romero et al. 2021). This finding suggests that both enteric and environmental microbial communities may play an important role at the base of abyssal food webs.

Holothurian and echinoid DFs show niche partitioning based on adaptations such as movement speed (Iken et al. 2001), tentacle morphology (Pierrat et al. 2022), and particle selectivity (Miller et al. 2000; FitzGeorge-Balfour et al. 2010). After seasonal pulses of phytodetritus, highly mobile taxa are able to quickly consume the fresh material while slower-moving species are adapted to survive on the less labile material left over (Iken et al. 2001). Moreover, the abundance of abyssal DFs is directly related to rates of surface primary production (Gooday 2002; Ruhl and Smith 2004; Smith et al. 2008a; b). Elpidiid populations (Holothuroidea: Elasipodida: Elpidiidae) are particularly responsive to changes in detrital flux, following “boom and bust” cycles with orders of magnitude changes in abundance following increases in surface production at Station M and the Porcupine Abyssal Plain (Kaufmann and Smith 1997; Uthicke et al. 2009; Billett et al. 2010; Huffard et al. 2016). Additionally, many deep-sea holothurians, particularly in the order Elasipodida and the family Synallactidae, have morphological adaptations that allow them to swim above the seafloor and cover large distances while expending little energy (Miller and Pawson 1990; Chimienti et al. 2019; Gebruk and Kremenetskaia 2024). Facultative swimmers are observed occasionally taking off from the seafloor and swimming for short distances, while benthopelagic species spend the majority of their time drifting or swimming in the water column (Chimienti et al. 2019; Gebruk and Kremenetskaia 2024). It has been hypothesized that they use their swimming ability to find food patches and consume fresher material (Chimienti et al. 2019; Gebruk and Kremenetskaia 2024), but to date there has been no direct evidence.

Another adaptation that may allow deep DFs to survive on low-quality food is their association with enteric microbial communities. Bacteria occur in high abundances on the tentacles and within digestive tracts of abyssal holothurians (Roberts et al. 1991; Amaro et al. 2012, 2019) and shallow echinoids (Schwob et al. 2020; Rodríguez-Barreras et al. 2021, 2023). Fatty acid profile analysis and essential amino acid $\delta^{13}\text{C}$ values revealed that in addition to phytodetritus, bacteria-derived material makes up a large portion of some holothurians' diets

(Drazen et al. 2008; Kharlamenko et al. 2018; Romero-Romero et al. 2021; Rodkina et al. 2023), particularly at oligotrophic sites (Amaro et al. 2019). These bacteria-derived fatty acids may come from microbial reworking on sinking detritus or in sediments (Durden et al. 2020), but consistent RNA concentrations along digestive tracts and elevated bacterial activity relative to sediments suggest that a resident microbiome exists within abyssal holothurians, capable of breaking down ingested organic material that the host may be unable to digest (Roberts et al. 2001; Witbaard et al. 2001). Additionally, Amaro et al. (2012) found that gut-associated bacterial communities differed significantly in composition from those in surrounding sediments, with many taxa found only in digestive tracts. DFs and grazers often contain gut microbiota specialized to their trophic niche (Rodríguez-Barreras et al. 2021), but defining the nature of animal-microbe associations in the deep sea is difficult due to the limitations of sampling and the general difficulty of conducting feeding experiments. Gut microbiomes of holothurians in the deep sea have been studied only in a few locations (Deming et al. 1981; Amaro et al. 2012), and never in echinoids living below the euphotic zone.

Biomarkers have been extensively used for understanding the trophic ecology of DFs. In particular, fatty acids and other lipids have been used to quantify the dependence of DFs on phytodetritus versus bacteria and other organic sources (Drazen et al. 2008; Amaro et al. 2019; Rodkina et al. 2023). Compound-specific stable isotope analysis of individual amino acids (AA-CSIA) allows for estimations of trophic position and assignments of food sources to consumers. Amino acids are classified as “source” or “trophic,” with trophic amino acids undergoing fractionation and increasing in $\delta^{15}\text{N}$ values with each trophic step during heterotrophic metabolism. Source amino acids, on the other hand, increase in $\delta^{15}\text{N}$ value primarily during microbial reworking and remain mostly unaltered by metazoan metabolism. An accurate estimate of trophic position can thus be gained by comparing $\delta^{15}\text{N}$ values of source and trophic amino acids without a need for independent measurements of the $\delta^{15}\text{N}$ values of material at the base of the food web (Chikaraishi et al. 2007, 2009; Popp et al. 2007). Additionally, the $\delta^{15}\text{N}$ values of source amino acids ($\delta^{15}\text{N}_{\text{SAA}}$) can be used to match animals with their potential food sources, including different size of particulate organic matter (POM) (Hannides et al. 2013; Romero-Romero et al. 2020).

Here, we examine the roles that gut-associated microbiota play in the trophic ecology of abyssal DFs. We contrast animals at Station M, where large pulses of phytodetritus and

gelatinous zooplankton carcasses provide relatively labile food to high densities of DFs (Smith and Druffel 1998; Smith et al. 2008b, 2014), with animals from Station ALOHA, situated in the oligotrophic North Pacific Subtropic Gyre (Karl and Lukas 1996; Karl et al. 2021). We also compare the trophic ecology of swimming holothurians and exclusively benthic holothurians and echinoids to test whether swimming behavior is a method of niche partitioning on the abyssal plain. We combine AA-CSIA with 16S rRNA microbial community barcoding to tie the trophic ecology and mobility of deposit-feeding taxa to their gut microbiota.

3.3 Materials and Methods

3.3.1 Sample collection

Animals and sediment cores were collected from the abyssal plain at Station M (34°50'N, 123°00'W) using the HOV *Alvin* in April-May 2019 (i.e. spring) and ROV *Doc Ricketts* and October 2019 (i.e. fall). At Station ALOHA (22°45'N, 158°W) animals and sediment cores were collected with the ROV *Lu'ukai* in July 2019 and 2020 (i.e. summer), and January 2020 (i.e. winter). At Station M, we collected the echinoid *Echinocrepis rostrata* (fall n = 2, spring n = 2) and the holothurians *Oneirophanta mutabilis* (fall n = 2, spring n = 2), *Peniagone* sp. (fall n = 2, spring n = 2), and *Scotoplanes globosa* (spring n = 2; Table 2.1). At Station ALOHA, we collected an unknown echinoid possibly within the genus *Pilematechinus* (herein referred to as *Pilematechinus* aff.; summer n = 6, winter n = 1) and holothurians *Eynpniastes eximia* (summer n = 1) and *Psychropotes* spp. (summer n = 2, winter n = 1), as well as individuals within the cryptic genus *Benthodytes* (summer n = 3) and cryptic family Elpidiidae (summer n = 3), which included individuals belonging to the cryptic genera *Amperima* and *Peniagone* that we were not able to identify to species level (Table 2.1). All specimens of *Peniagone* sp., *Benthodytes* spp., and *E. eximia* were recovered with empty digestive tracts. Gut evacuation is common when swimming holothurians, such as these species, take off from the seafloor (Miller and Pawson 1990; Gebruk and Kremenetskaia 2024).

DFs were dissected on board to isolate gut contents for AA-CSIA and rRNA barcoding, and tissue samples for AA-CSIA. Holothurians were dissected with a longitudinal cut along the ventral side and echinoids were dissected with a circular cut along the top of the test. Digestive tracts were carefully removed from the animals and opened using ethanol-sterilized tools. We

used scissors to cut the digestive tracts open and scooped out the contents with a spatula, avoiding including pieces of the gut wall. Samples of gut contents were taken near the mouth for “foregut,” near the anus for “hindgut,” and around the middle of the tract for “midgut.” For animals with too little material, all gut contents were combined into one sample. Gut contents and tissue samples were stored at -80°C until analysis. 7 cm diameter sediment cores were sliced to collect the top 0.5 cm, placed in petri dishes, and frozen at -80°C .

To characterize the isotopic composition of POM, we collected size-fractionated particles at both sites using *in situ* filtration by McLane pumps at 50 meters above the bottom (mab), at depths of approximately 3950 m at Station M and 4650 m at Station ALOHA. The pumps were equipped with mini-MULVS filter holders with three tiers of filters (140 mm diameter) to fractionate particles into three size classes as described in Bishop et al. (2012): large ($>53\ \mu\text{m}$, acid-cleaned Nitex mesh filters), small ($1-53$ or $0.7-53\ \mu\text{m}$, precombusted QMA quartz or GF/F glass microfiber filters), and sub-micron ($0.3-1\ \mu\text{m}$, precombusted GF75 glass microfiber filters). Approximately 3000-6000 L were filtered for each sample. Upon retrieval, large particles were washed off the Nitex filters using $0.2\ \mu\text{m}$ filtered seawater and captured on 25 mm diameter QMA filters and all filters were frozen at -80°C .

Additionally, we deployed moored sediment traps (McLane Parflux Mark 78H with $0.65\ \text{m}^2$ collection area) at 50 mab at both sites, containing 5% buffered formalin in filtered seawater. Traps were deployed at Station M from December 2018 to March 2019 with a sample frequency of 16 days, and at Station ALOHA from March 2019 to February 2020 with an average sample frequency of 14 days. Unfortunately, the traps at Station M were clogged by a pulse of detritus in early April 2019 just prior to reservicing and the trap mooring string failed during the subsequent deployment causing a prerelease and loss of samples. No sediment trap samples are thus available from Station M concurrent with our Fall 2019 collections.

3.3.2 Density estimations

At Station M, DF densities were determined from a single ROV video transect on 10/19/2019, covering $2287\ \text{m}^2$, previously reported in Kuhnz et al. (2020). At Station ALOHA, we combined four seafloor ROV video transects, conducted on 7/20/2019, 7/21/2019, 8/1/2020, and 8/2/2020, covering a total area of $23,020\ \text{m}^2$. Field of view was estimated for each transect using lasers 15 cm apart (average of 6.5 m across all transects) and multiplied by the distance to

calculate area covered for each transect. Based on the number of observations of each taxa, the density was calculated as individuals/km² for each transect. We report the average \pm standard deviation among the four transects.

3.3.3 Amino acid compound-specific stable isotope analysis

AA-CSIA was performed on freeze dried samples of animal tissue, gut contents, sediments, size-fractionated particles, and sediment trap material as described in Hannides et al. (2013) and Chapter 2 of this thesis. Derivatized amino acid $\delta^{15}\text{N}$ values were analyzed using a Thermo Scientific Delta V Plus IRMS interfaced to a trace gas chromatograph fitted with a 60 m BPx5 capillary column through a GC-C III combustion furnace (980°C), reduction furnace (680°C), and liquid nitrogen cold trap. Each sample was co-injected with internal reference amino acids norleucine and aminoadipic acid, which have known $\delta^{15}\text{N}$ values. For quality assurance, between every three sample injections we injected a full amino acid reference suite of 16 compounds with known $\delta^{15}\text{N}$ values. $\delta^{15}\text{N}$ values of sample amino acids were normalized using a linear regression between the measured and known values from the reference suite. The uncertainty for each amino acid $\delta^{15}\text{N}$ value was calculated as the standard deviation of three injections, where there was sufficient material available. The overall average uncertainty among all samples was 0.46‰.

3.3.4 16S rRNA microbial community barcoding

We isolated environmental DNA from animal gut contents and surface sediments using a DNeasy PowerSoil Kit. We amplified the hypervariable V4-V5 region of the 16S rRNA gene via PCR using the primers 515f (GTGYCAGCMGCCGCGGTAA) and 808rB (GGACTACNVGGGTWTCTAAT). Each PCR reaction contained 2.5 μL environmental DNA (0.5 – 350 ng/ μL), 5 μL forward and 5 μL reverse primer (1 μM), and 12.5 μL 2x Platinum™ Hot Start PCR Master Mix (Invitrogen, catalog #13000014). The PCR amplification protocol was as follows: 95°C for 3 minutes; 30 cycles of 95°C for 30 seconds, 55°C for 30 seconds, and 72°C for 30 seconds; 72°C for 5 minutes, and hold at 4°C. The resulting PCR products were sequenced using an Illumina MiSeq platform at the Advances Studies in Genomics, Proteomics, and Bioinformatics at the University of Hawai‘i at Mānoa.

3.3.5 Stable isotope data analysis

The average $\delta^{15}\text{N}$ value of phenylalanine and lysine was used as the $\delta^{15}\text{N}$ values of source amino acids ($\delta^{15}\text{N}_{\text{SAA}}$). Trophic position ($\text{TP}_{\text{Glx-Phe}}$) was calculated as in Chikaraishi et al. (2009): $\text{TP} = (\delta^{15}\text{N}_{\text{Glx}} - \delta^{15}\text{N}_{\text{Phe}} - 3.4)/7.6 + 1$, where $\delta^{15}\text{N}_{\text{Glx}}$ and $\delta^{15}\text{N}_{\text{Phe}}$ are the $\delta^{15}\text{N}$ values of glutamic acid (Glx, including the contribution of glutamine) and phenylalanine (Phe) in the sample. $3.4 \pm 1 \text{ ‰}$ is the difference between $\delta^{15}\text{N}_{\text{Glx}}$ and $\delta^{15}\text{N}_{\text{Phe}}$ in primary producers (β), and $7.6 \pm 1 \text{ ‰}$ is the trophic discrimination factor (TDF_{AA}). The uncertainty in the TP values was calculated as the propagated error (Ohkouchi et al. 2017).

The ΣV parameter is a proxy for heterotrophic resynthesis of amino acids, determined from the average deviation of $\delta^{15}\text{N}$ values of trophic AAs from their mean value. We calculated ΣV as in McCarthy et al. (2007): $\Sigma\text{V} = 1/n \sum \text{Abs}(\chi_i)$, where n is the total number of AAs used for the calculation and χ_i is the deviation of the $\delta^{15}\text{N}$ value of amino acid i from the mean $\delta^{15}\text{N}$ value of the n amino acids [$\delta^{15}\text{N}_i - (\sum \delta^{15}\text{N}_i / n)$]. We used the amino acids alanine, valine, proline, aspartic acid, and glutamic acid to calculate ΣV .

3.3.6 Barcoding data analysis

16S rRNA sequences were analyzed using DADA2 version 1.28.0 (Callahan et al. 2016), implemented in R version 4.3.0. Briefly, quality scores were calculated based on error rates and reads were filtered to a maximum of 2 expected errors and minimum length of 240 bases for forward reads and 160 bases for reverse reads. The reads were dereplicated and consensus quality scores were constructed and used in a denoising algorithm to infer error rates and distinguish sequencing errors from true sequence variations. The resulting amplicon sequence variants (ASVs), which represent unique microbial variants, had chimeras removed and were assigned taxonomy using the Silva 138.1 prokaryotic 16S rRNA taxonomic training data (McLaren and Callahan 2021). Alpha diversity was estimated using the estimate richness function from the phyloseq R package (McMurdie and Holmes 2013).

3.3.7 Statistical analysis

Statistical analyses were performed in R version 4.3.0 using the package vegan (Oksanen et al. 2024). We used t-tests to compare trophic positions and ΣV values between the two sites and between seasons. A two-component linear mixing model was created based on the $\delta^{15}\text{N}$

values of the source amino acids phenylalanine and lysine in potential sources of detritus: 1-53 μm filtered particles (“small presumably recalcitrant particles”) and material captured in moored sediment traps (“large presumably labile particles”), both captured at 50 mab. We used as endmembers (types of detritus consumed as food sources) for each animal particles collected during the same season and at the same site as each animal, with the exception of fall at Station M where we used spring sediment trap material as no traps were collected in the fall. The sediment trap material is composed largely of fresh, fast-sinking large particles that resemble surface particles, while the small filtered particles have higher $\delta^{15}\text{N}_{\text{SAA}}$ values reflective of greater microbial reworking (Chapter 2, this thesis). The $\delta^{15}\text{N}_{\text{SAA}}$ values of all animals fell between the two endmembers.

For microbial community composition, we created a Principal Coordinate Analysis (PCoA) based on a Bray-Curtis dissimilarity matrix of ASV abundance at the order level and compared DF species and gut regions with a permutational multivariate analysis of variance (PERMANOVA). Additionally, we compared the Shannon diversity, Simpson diversity, and Chao1 ASV richness of microbial communities between sample types with an analysis of variance (ANOVA). We also used ANOVA to compare the proportional abundance of certain microbial taxa in the digestive tracts of different animal species. For all analyses, $P < 0.05$ was considered significant. Data are presented as the mean \pm standard deviation.

3.4 Results

3.4.1 Deposit feeder communities

At Station M, *Peniagone* sp. were by far the most abundant DF taxon in fall 2019, with 106,252 individuals/ km^2 , followed by *S. globosa* (5247 individuals/ km^2), *E. rostrata* (3498 individuals/ km^2), and *O. mutabilis* (1747 individuals/ km^2). At Station ALOHA, the most abundant DFs seen during summer video transects were *E. eximia* at 402 ± 526 and *Pilematechinus* aff. at 425 ± 557 individuals/ km^2 . Only one *Elpidiidae* sp. (22 ± 43 individuals/ km^2) and one *Psychropotes* sp. (66 ± 131 individuals/ km^2) were observed during all four transects, and no *Benthodytes* spp. individuals were seen (collections occurred between transects). Additionally, our *E. eximia* density is likely an underestimation, as that species is frequently observed swimming or drifting in the water column higher than the average altitude of

1.5 m during our transects (Ohta 1985; Miller and Pawson 1990). No video transects were done in the spring at Station M or in the winter at Station ALOHA, but densities are unlikely to vary substantially within a 6 month time span (Kuhnz et al. 2020).

Deposit-feeding holothurians at both sites were classified as non-swimmers (*O. mutabilis* and *S. globosa*), facultative swimmers (*Bentho-dytes* spp. and *Psychropotes* spp.), or benthopelagic (*E. eximia*, *Elpidiidae* spp., and *Peniagone* sp.) based on the classifications of Miller and Pawson (1990) and Gebruk and Kremenetskaia (2024). All echinoids were considered non-swimmers.

3.4.2 Compound-specific stable isotope analysis

The trophic position of individual DF tissue ranged between 2.5 ± 0.1 (*O. mutabilis*; TP \pm propagation error) and 3.3 ± 0.1 (*O. mutabilis*) at Station M and 2.4 ± 0.1 (*Psychropotes* spp.) and 4.1 ± 0.1 (*E. eximia*) at Station ALOHA (Fig. 3.1e, f). The trophic position of gut contents relative to sediments ($\Delta TP_{\text{Gut-Sediment}}$) was approximately one at Station M: *E. rostrata* 0.70 in fall and 0.7 ± 0.6 in spring, *O. mutabilis* 1.1 ± 0.1 in fall and 1.6 ± 0.8 in spring, and *S. globosa* 0.8 ± 0.9 in spring (Fig. 3.2a). Unfortunately, the low amino acid content of sediment samples at Station ALOHA prevented us from conducting a similar analysis. Among all species, trophic position overall was higher in tissue than in gut contents (paired t test, $t = -3.70$, $P = 0.0035$), with a i.e., $\Delta TP_{\text{Tissue-Gut}}$ of around one trophic step, although there was high intraspecific variation: *E. rostrata* 1.1 in fall and 1.2 ± 0.8 in spring, *O. mutabilis* 0.6 ± 0.6 in fall and 0.8 ± 0.8 in spring, *S. globosa* 0.9 ± 1.0 in spring, and *Pilematechinus* aff. 1.2 in summer (Fig. 3.2b). The exception was a single *Psychropotes* sp. individual, which had gut contents 0.8 trophic steps higher than its tissue (Fig. 3.2b). Trophic position did not differ by swimming ability (ANOVA, $P > 0.05$).

At both sites, $\delta^{15}\text{N}_{\text{SAA}}$ values of animal tissue and gut contents fell within the range of values of POM collected near the seafloor. The material captured in sediment traps had lower $\delta^{15}\text{N}_{\text{SAA}}$ values than filtered particles in the 0.3-1 μm (submicron) and 1-53 μm (small) size fractions, which were also higher than those of the animals (Fig. 3.1a, b). Based on our two-factor mixing model, we found no difference between sites in overall proportion of small, recalcitrant particle versus large, labile POM material utilization, with $40.3 \pm 22.5\%$ and $40.0 \pm 23.5\%$ utilization of large, labile material at Stations ALOHA and M, respectively (t-test, $P >$

0.05; Fig. 3.3). However, large, labile material utilization was higher during the fall than during the spring at Station M (t-test, $t = 4.16$, $P < 0.001$), while no seasonal differences were observed at Station ALOHA (t-test, $P > 0.05$). Benthopelagic animals had a significantly larger contribution of large, labile material in their diet ($56.7 \pm 17.5\%$), followed by facultative swimmers ($44.6 \pm 21.4\%$) and non-swimmers ($33.6 \pm 22.2\%$; ANOVA, $F = 4.43$, $P = 0.016$).

ΣV , a proxy for heterotrophic resynthesis, was higher in DF gut contents than in tissue (paired t test, $t = 2.34$, $P < 0.05$). ΣV was also higher in DF tissue at Station ALOHA than at Station M (t test, $t = 2.69$, $P < 0.05$). ΣV values in gut contents did not, however, differ between sites (t test, $P > 0.05$).

3.4.3 Microbial community analysis

After cleaning and filtering, 16S rRNA sequencing yielded 946,549 reads in 64 samples. Microbial community composition in gut contents differed by site (PERMANOVA, $F = 9.31$, $P < 0.001$), and by DF taxon (PERMANOVA, $F = 2.68$, $P < 0.001$) (Fig. 3.4, 3.5). At Station ALOHA, sediment microbial communities differed from those in gut contents (PERMANOVA, $F = 4.23$, $P < 0.05$), but not by season (PERMANOVA, $P > 0.050$). At Station M, community composition differed between guts and sediments (PERMANOVA, $F = 2.63$, $P < 0.05$) and by season (PERMANOVA, $F = 2.63$, $P < 0.001$). Within taxa, the gut region (foregut, midgut, or hindgut) did not influence community composition (PERMANOVA, $P > 0.05$). Swimming ability also did not affect gut microbial composition (PERMANOVA, $P > 0.05$).

Shannon diversity was lower in gut contents than in sediment (t test, $t = -2.60$, $P = 0.044$), as was Simpson diversity (t test, $t = -2.79$, $P = 0.010$), but Chao1 richness did not differ between gut contents and sediment (t test, $P > 0.05$; Fig. 3.6). None of the three diversity measures differed between DF species (ANOVA, $P > 0.05$).

Based on DESeq2 differential abundance analysis (pairwise by DF species, $P < 0.05$), 8195 ASVs were significantly enriched in DF digestive tracts relative to sediments, while 5133 ASVs were significantly enriched in sediments relative to digestive tracts (Fig. 3.7). Gut-enriched ASVs were diverse, with prominent contributions from the phyla Acidobacteria, Actinobacteria, Planctomycetes, and Proteobacteria. Sediment-enriched communities were similar in taxonomic composition, but with larger proportions of Thaumarcheota and smaller proportions of Actinobacteria than the gut-enriched communities (Fig. 3.7).

Table 3.1. Isotopic and ecological information of DF species collected at each site and season. Swimming ability was assigned based on Miller and Pawson (1990) and Rogacheva et al. (2012). Trophic position and contribution of large particles are the average \pm standard deviation within each season.

Station	Taxon	n (isotope analysis)	n (16S rRNA analysis)	Trophic position	Contribution of large particles (%) to diet	Swimming ability	Density (individuals km ⁻²)
ALOHA	Family Elpidiidae	3 (summer)	2 (summer) 1 (winter)	3.1 \pm 0.1	54.3 \pm 10.9	Benthopelagic	22 \pm 43
	Family Pelagothuriidae <i>Enypniastes eximia</i>	1 (summer)	0 (summer)	4.1	58.1	Benthopelagic	402 \pm 526
	Family Psychropotidae <i>Benthodytes</i> spp. <i>Psychropotes</i> spp.	3 (summer)	0 (summer)	3.3 \pm 0.1	30.6 \pm 17.4	Facultative	N/A
		2 (summer)	1 (summer)	2.8	52.3 \pm 22.5	Facultative	66 \pm 131
		1 (winter)	2 (winter)	3.4	63.7		
	Family Urechinidae <i>Pilematechinus</i> aff.	6 (summer) 1 (winter)	6 (summer) 1 (winter)	3.1 \pm 0.3 3.3	24.1 \pm 24.3 47.7	Non-swimmer	425 \pm 557
M	Family Deimatidae <i>Oneirophanta mutabilis</i>	2 (spring)	2 (spring)	3.3 \pm 0.0	14.8 \pm 12.3	Non-swimmer	1749
		2 (fall)	3 (fall)	2.8 \pm 0.4	43.1 \pm 18.0		
	Family Elpidiidae <i>Peniagone</i> sp.	2 (spring)	2 (spring)	3.1 \pm 0.1	37.0 \pm 1.7	Benthopelagic	106,253
		2 (fall)	0 (fall)	3.1 \pm 0.3	79.2 \pm 9.8		
	<i>Scotoplanes globosa</i>	2 (spring)	1 (spring)	2.6 \pm 0.1	32.2 \pm 11.4	Non-swimmer	5247
	Family Pourtalesiidae <i>Echinocrepis rostrata</i>	2 (spring)	2 (spring)	2.8 \pm 0.3	27.3 \pm 7.6	Non-swimmer	3498
2 (fall)		3 (fall)	3.0 \pm 0.1	65.5 \pm 22.6			

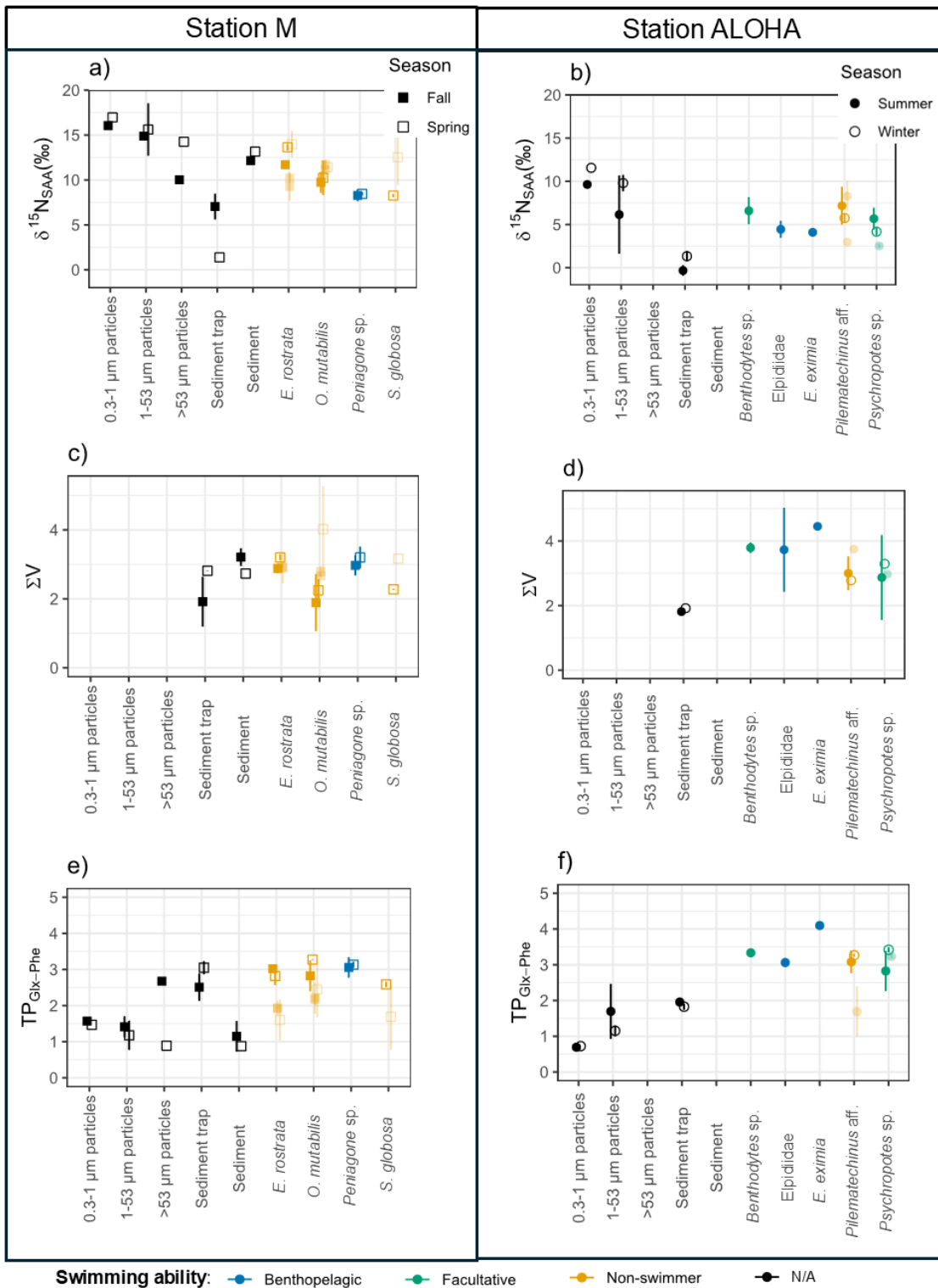


Figure 3.1. a, b) $\delta^{15}\text{N}$ source amino acid values of animal tissue (indicative of the lability of organic material at the base of the food web), gut contents (lighter points), and various

particulate organic matter sources near the seafloor. **c, d**) ΣV parameter (proxy for microbial heterotrophic reworking). **e, f**) Estimated trophic positions ($TP_{Glx-Phe}$). Points are averages within a season and error bars represent standard deviations. Colors indicate the swimming ability of the deposit feeder species.

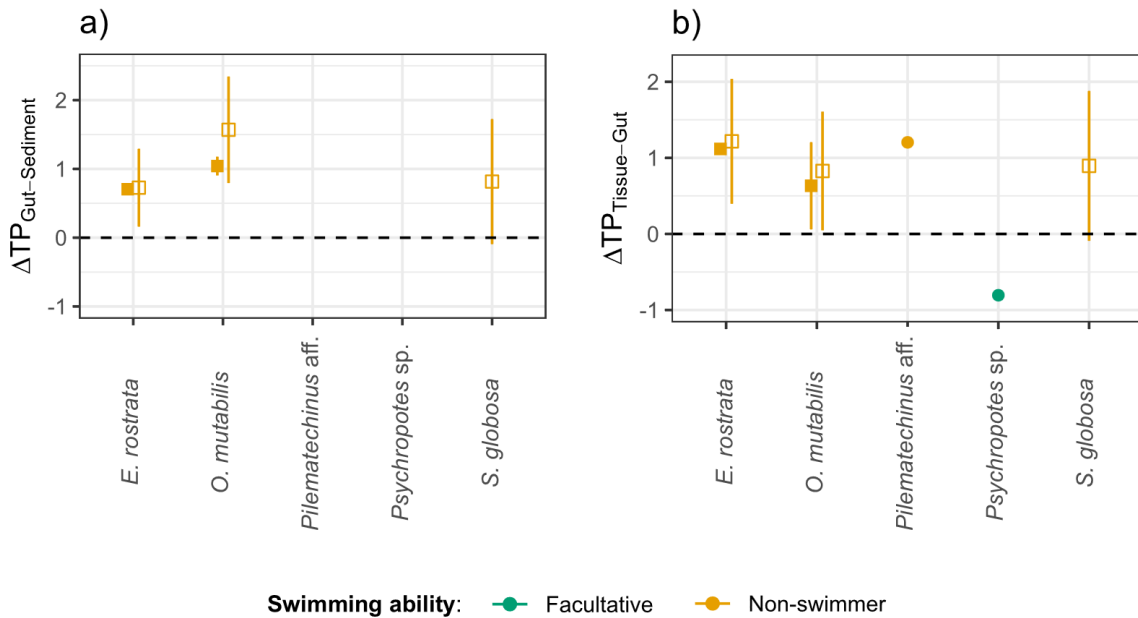


Figure 3.2. The difference in trophic positions between **a**) DFs gut contents and sediment and **b**) tissue and gut contents, averaged within a season (mean \pm SD; open symbols: spring; closed symbols: fall and summer) at each site (squares, Station M; circles, Station ALOHA). Points are averages within a season and error bars represent standard deviations. Colors indicate the swimming ability of the deposit feeder species.

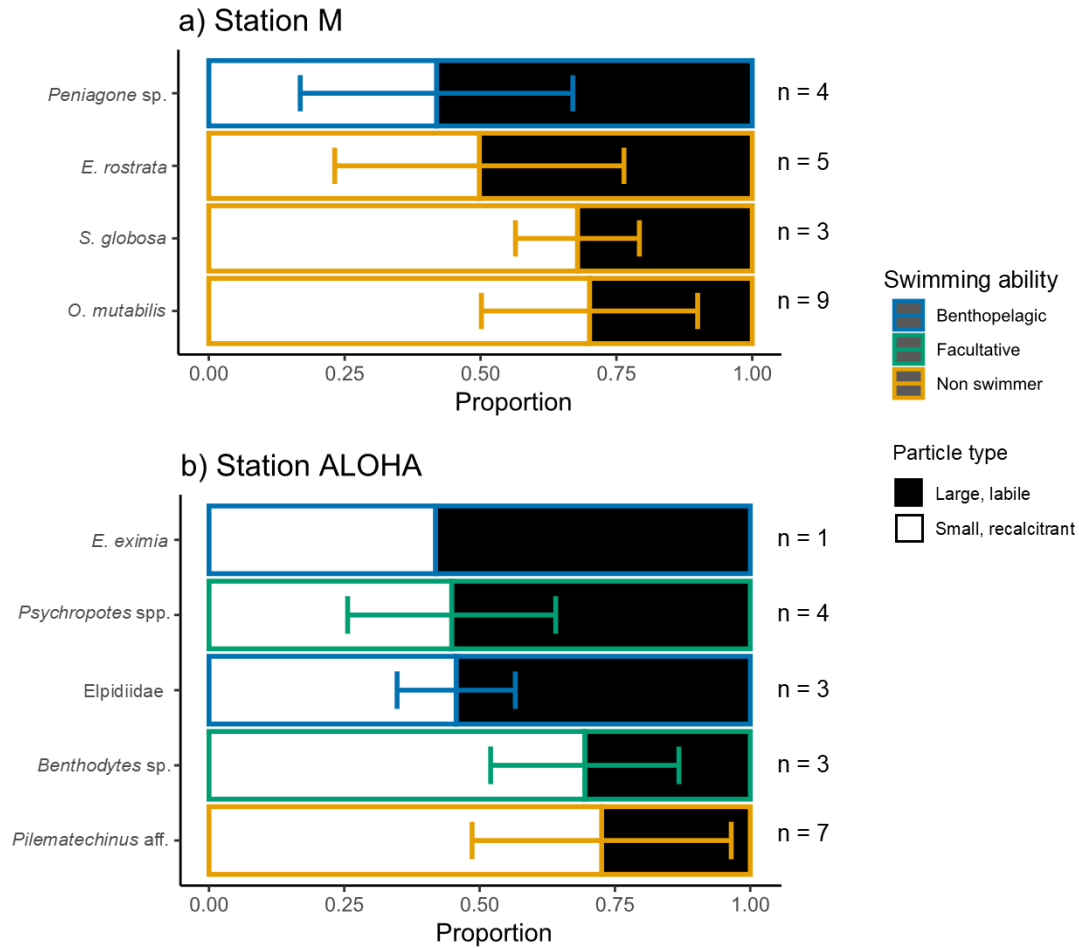


Figure 3.3. Results of a two-factor mixing model based on $\delta^{15}\text{N}_{\text{SAA}}$ values of particles captured in sediment traps (“large, labile”) and 1-53 μm particles filtered from the water column (“small, recalcitrant”), 50 mab. Error bars show standard deviation. Colors indicate the swimming ability of the deposit feeder species.

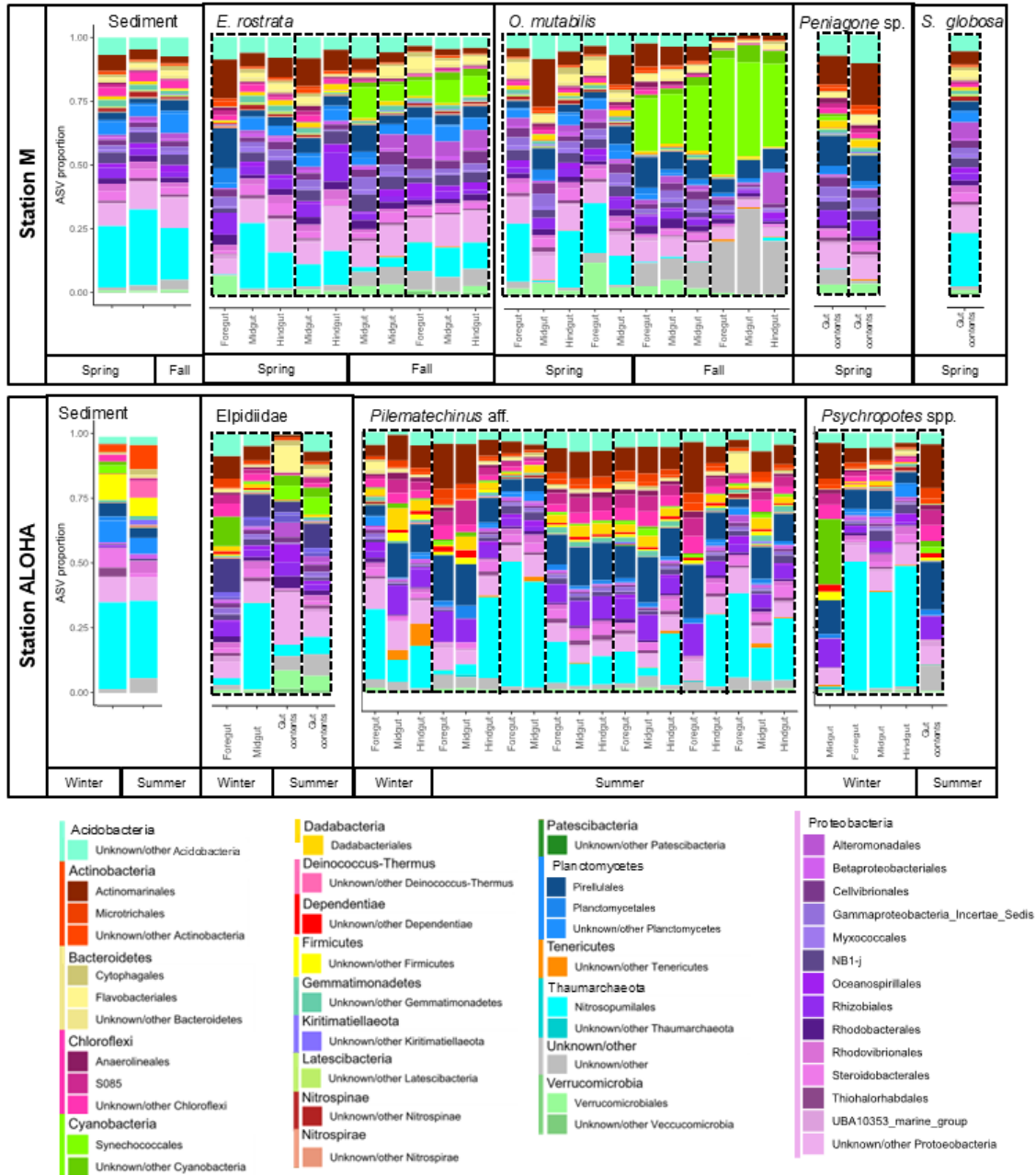


Figure 3.4. Microbial community composition in sediments and gut contents, shown as proportion of ASVs assigned to each of the top 25 most abundant orders. For animals where multiple parts of the gut were analyzed, dotted lines outline a single individual. Top row are Station M animals and bottom row are Station ALOHA animals.

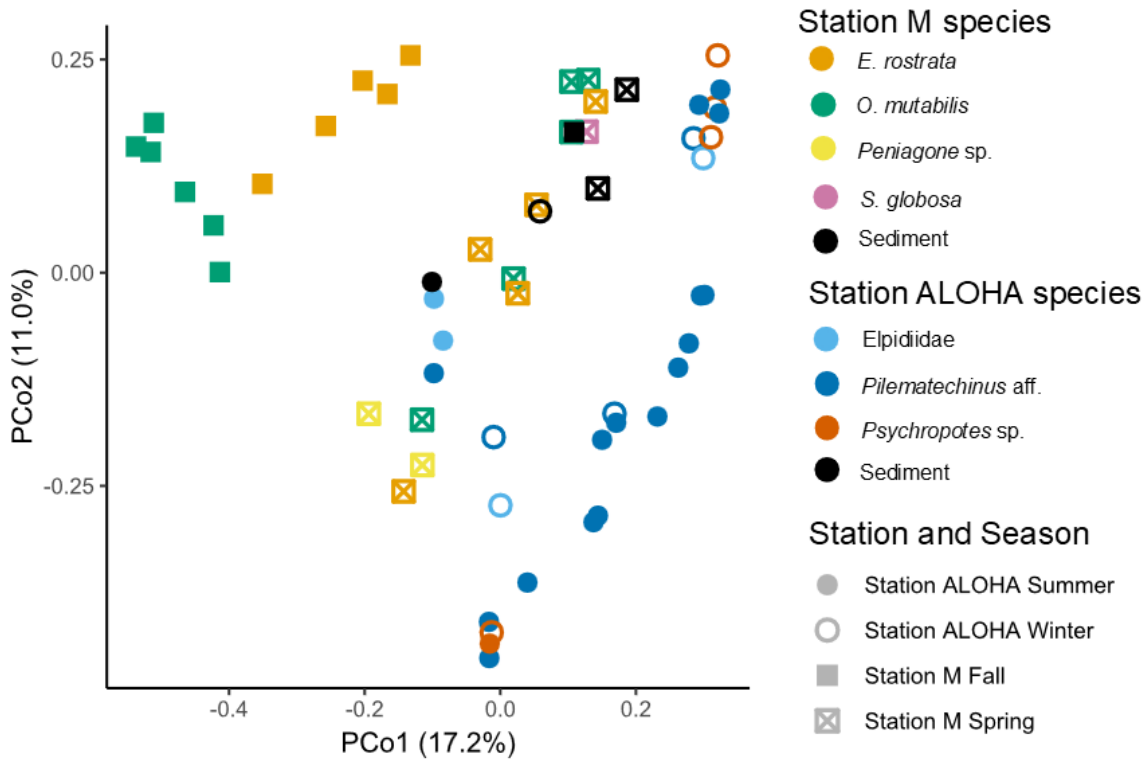


Figure 3.5. Principal coordinate analysis (PCoA) of microbial community composition in surface sediments and guts of DFs using a Bray-Curtis dissimilarity matrix based on ASV abundance.

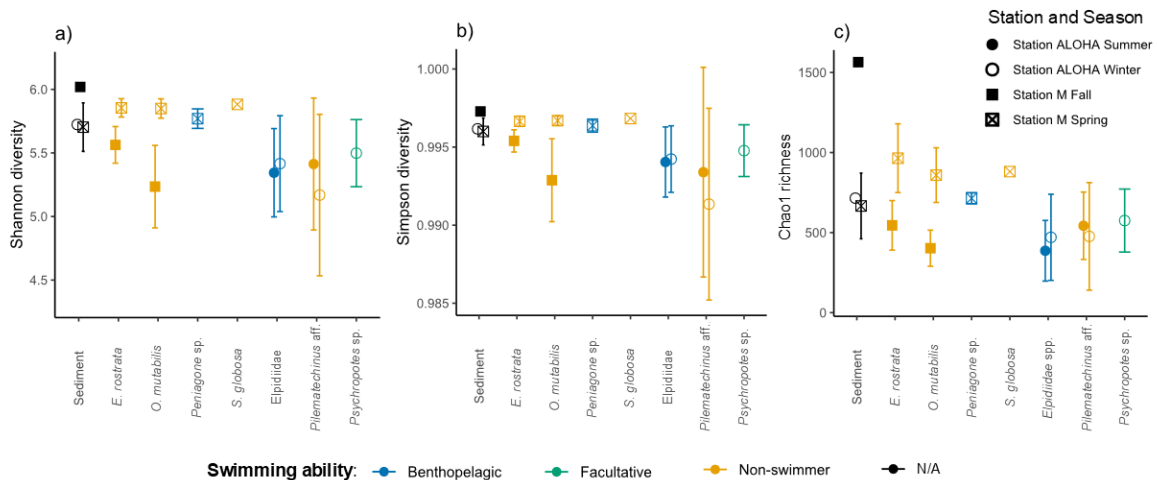


Figure 3.6. Microbial community alpha diversity in DF gut contents and sediments, quantified as a) Shannon diversity index, b) Simpson diversity index, and c) Chao1 estimated species

richness. Points are averages within a season and error bars represent standard deviations. Colors indicate the swimming ability of the deposit feeder species.

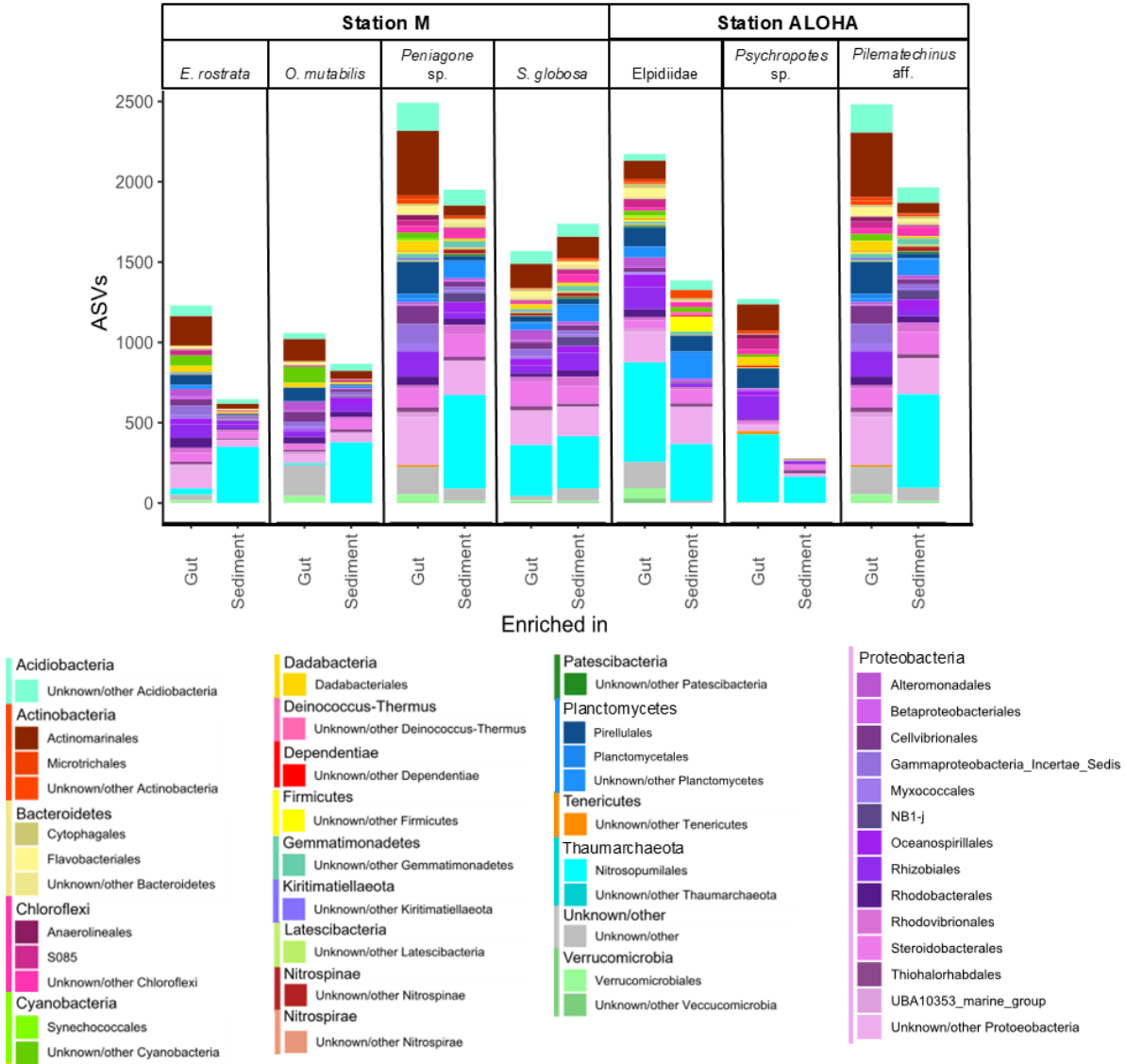


Figure 3.7. ASVs significantly enriched (DESeq2 differential abundance analysis, $P < 0.05$) in digestive tracts versus sediments, separated by DF taxon (Station M sediment $n = 4$, Station ALOHA sediment $n = 2$, *E. rostrata* $n = 10$, *O. mutabilis* $n = 11$, *Peniagone* sp. $n = 2$, *Elpidiidae* $n = 4$, *Psychropotes* spp. $n = 5$, *Pilematechinus* aff. $n = 18$).

3.5 Discussion

We found that deposit-feeding echinoderms on the abyssal plain are secondary consumers of sedimentary detritus. Our results are consistent at two sites of contrasting productivity and carbon export regimes [average carbon export flux 113.4 mg C⁻² d⁻¹ at Station M (Smith et al. 2018) and 27.9 mg C⁻² d⁻¹ and Station ALOHA (Karl et al. 2021)], which points to a remarkable generalization across the abyssal plain. However, the proportion of fresh versus recalcitrant POM they consume varies both between and within species. Abyssal DFs are known to exhibit niche partitioning based on morphological and behavioral adaptations including movement speed and tentacle shape (Iken et al. 2001; FitzGeorge-Balfour et al. 2010; Pierrat et al. 2022). It has been hypothesized, but until now not quantitatively shown, that swimming is another adaptation used by some deep-sea holothurians to access food pulses to the abyss (Chimienti et al. 2019; Gebruk and Kremenetskaia 2024). We found that species with documented swimming behavior consumed larger and fresher detrital particles than exclusively benthic species (Fig. 3.3), providing evidence that varying swimming ability is another strategy of niche partitioning on the abyssal plain. Interspecific differences in digestive tract microbiota may further reflect distinct dietary strategies on the abyssal plain.

3.5.1 Niche partitioning by particle type

Abyssal DFs consume a heterogeneous mixture of detrital types, here distinguished using different sampling methods of POM at 50 mab. Moored sediment traps at both sites captured material with low $\delta^{15}\text{N}_{\text{SAA}}$ values, similar to surface particles (Chapter 2 of this thesis), which is indicative of little microbial reworking and a prevalence of large, fast-sinking particles (Alldredge 1998; Guidi et al. 2008). We describe these trap-captured particles as a large, labile POM source. On the other hand, small (1-53 μm) particles filtered *in situ* at 50 mab had higher $\delta^{15}\text{N}_{\text{SAA}}$ values (Fig. 3.1a, b) and represented a more heavily reworked detrital source (Hannides et al. 2013; Wojtal et al. 2023; Chapter 2 of this thesis), here designated as small and recalcitrant particles. There is almost certainly overlap between these detrital sources, as sediment traps also capture some small particles (Buesseler 1991; Honjo et al. 2008; Buesseler et al. 2020). Other potentially important detrital endmembers such as salp carcasses (Smith et al. 2014) are missing from this analysis due to being under-sampled by both *in situ* filtration and sediment traps

(Buesseler 1991). However, the consistent differences in $\delta^{15}\text{N}_{\text{SAA}}$ values between the sediment trap material and small particles, despite seasonal variation, allowed the use of a mixing model to show niche partitioning among the DFs based on detrital food source. Both detrital types were important food sources for DFs at both sites, but the proportion of labile versus recalcitrant material differed by species and swimming ability (Fig. 3.3).

Of the DFs quantified here, benthopelagic *Peniagone* sp. were the most abundant at Station M while benthopelagic *E. eximia* and non-swimming *Pilematechinus* aff. were the most abundant at Station ALOHA during our collections in 2019 and 2020 (Table 2.1). However, abyssal DF community composition has changed significantly over time at the long-term monitored sites including the Porcupine Abyssal Plain (Billett et al. 2010) and Station M (Huffard et al. 2016; Kuhnz et al. 2020). There was an “elpidiid bloom” in 2012-2014 at Station M, where *Peniagone* sp. and *S. globosa* increased in density by up to an order of magnitude around the time of large pulses of phytodetritus and tunicate carcasses (Kuhnz et al. 2020), suggesting members of the family Elpidiidae have the ability to respond more intensely to food pulses than other DFs. Moreover, we found that *Peniagone* sp. and *E. eximia* consumed the highest proportion of large, labile material at their respective sites (Fig. 3.3). Hence, we suggest that the swimming behavior of the elpidiid *Peniagone* sp. and the pelagothuriid *E. eximia* may allow them to take better advantage of fresh phytodetritus pulses and dominate the megafaunal DF assemblages at both sites. On the other hand, $\delta^{15}\text{N}_{\text{SAA}}$ values of *Pilematechinus* aff. resemble more closely the small, recalcitrant particles, suggesting that this and other non-swimming and presumably other slow-moving abyssal echinoids such as *E. rostrata* (Vardaro et al. 2009) occupy a separate niche (Fig. 3.3). *Pilematechinus* aff. must therefore utilize other strategies to thrive on lower quality phytodetritus, which may include breakdown by gut microbiota.

We structure the following discussion by the three swimming categories (non-swimmers, facultative swimmers, and benthopelagic species) to examine their trophic ecology and the composition of their gut microbiomes. It is important to note that $\delta^{15}\text{N}$ values in tissue reflect the animal’s diet over months to years, while gut microbial composition is instead indicative of the diet when the animal was collected, so the relationship between the data types may be temporally inconsistent.

3.5.2 Trophic ecology and gut microbiomes of non-swimming deposit feeders

The non-swimming deposit feeders in this study include the echinod *E. rostrata* and the holothurians *O. mutabilis* and *S. globosa* at Station M, and the echinoid *Pilematechinus* aff. at Station ALOHA. Of these, the echinoids *E. rostrata* and *Pilematechinus* aff. depended mostly on small, recalcitrant particles (Fig. 3.3), suggesting a diminished ability to compete for nutritionally superior fresh pulses of phytodetritus. *E. rostrata* is slower-moving than the other DFs at Station M (Kaufmann and Smith 1997; Vardaro et al. 2009), but its relatively large size and long digestive tract may allow the digestion of more recalcitrant material, which is supported by the more degraded gut contents relative to other DFs (Romero-Romero et al. 2021). However, gut contents of *E. rostrata* collected during the high flux season (i.e. fall) contained 5.8 – 8.7 % cyanobacterial ASVs, indicative of the consumption of some fresh phytodetritus when it is abundant (Fig. 3.4). As an unknown species, very little is understood about the trophic ecology of *Pilematechinus* aff., although its large size, trophic position as a secondary consumer, and relatively high ΣV value of gut contents suggests similarities to *E. rostrata* (Fig. 3.1). We suggest that *Pilematechinus* aff. fill a similar niche at Station ALOHA to that of *E. rostrata* at Station M, with slower movement speeds requiring a gut microbiome capable of breaking down a more recalcitrant detrital diet.

The gut microbiomes of both *E. rostrata* and *Pilematechinus* aff. were enriched relative to sediments in ASVs belonging to the phyla Proteobacteria and Actinobacteria, common gut microbiome residents in marine invertebrates (De Corte et al. 2018) that may assist with the breakdown of their recalcitrant diet (Fig. 3.7). *E. rostrata* gut microbiota were overall dominated by Proteobacteria, more than most other DF species (Fig. 3.4). Proteobacteria are particularly abundant in both shallow and deep echinoderm digestive tracts (Amaro et al. 2009; Schwob et al. 2020; Rodríguez-Barreras et al. 2021; Gao et al. 2022). *Pilematechinus* aff., on the other hand, showed high variability in gut microbial community composition, with some gut samples dominated by the archaea Nitrosopumilales while in others they made up a minor proportion of reads (Fig. 3.4). Nitrosopumilales appear to be mainly derived from consumed sediments in both echinoids, rather than forming specific gut communities, because few ASVs in this order were unique to the gut contents (Fig. 3.7). Other microbial groups are more likely to contribute a distinct core microbiome within *Pilematechinus* aff. based on their increased abundance in gut contents relative to sediments. These include Actinomarinales, Pirellulales, and Dadabacteria, the

latter of which made up a larger proportion of *Pilematechinus* aff. gut reads than in other DF species (Fig. 3.4, 3.7). All of these phyla are abundant in abyssal sediments (Lindh et al. 2017; Shulse et al. 2017; Jroundi et al. 2020; Begmatov et al. 2021), and could be derived from the DFs' diets, although all have also been found in both shallow and deep holothurian gut contents (Amaro et al. 2009; Sha et al. 2016; Weigel 2020). Deep-sea Dadabacteria are heterotrophs able to break down low molecular weight organic matter and have streamlined genomes (Graham and Tully 2021), common among gut symbionts (Osman and Weinnig 2022). We suggest Dadabacteria may play a role in the gut microbiome of *Pilematechinus* aff. at Station ALOHA and contribute to their utilization of recalcitrant material.

The holothurians *O. mutabilis* and *S. globosa* are not known to exhibit swimming behavior, and their consumption of 29.9 ± 19.9 and 32.2 ± 11.4 % large particles, respectively, suggests a reduced capacity to select for fresh phytodetritus (Fig. 3.3a). This is in contrast to previous work showing high selectivity due to fast movement speeds, which are some of the highest among DFs at Station M (Kaufmann and Smith 1997; Amaro et al. 2019). However, in contrast to our isotope results, our gut microbiome results match the characterization of *O. mutabilis* as highly selective in its feeding, with gut contents reflective of fresh phytodetritus (FitzGeorge-Balfour et al. 2010), as we found that 33.8 – 28.2 % of the microbes in their gut contents during the fall were epipelagic Cyanobacteria, much more so than any other animal at either site (Fig. 3.4). In fact, these cyanobacterial gut content abundances are greater than those found in some shallow-water DFs (Rodríguez-Barreras et al. 2021). A high consumption of fresh cyanobacteria during the high flux period might also be expected for *S. globosa*; unfortunately, we only collected one gut content sample from this species during the lower flux Spring. Compound-specific isotope and fatty acid analyses at Station M and the Porcupine Abyssal Plain have previously suggested that *Oneirophanta* spp. are secondary consumers and primarily consume bacteria rather than phytodetritus (Drazen et al. 2008; Stratmann et al. 2023). When food is scarce, *O. mutabilis* appears to consume more recalcitrant, bacteria-derived material (Neto et al. 2006; FitzGeorge-Balfour et al. 2010), pointing to seasonal differences in POM utilization. In this sense, Romero-Romero et al. (2021) found that the $\delta^{13}\text{C}$ patterns of essential amino acids in *O. mutabilis* tissue changed seasonally, being more similar to those of their gut contents in a period of low food supply and more similar to the surrounding sediments in a more productive period. Like *E. rostrata*, the microbes that were enriched in the *O. mutabilis* gut

microbiome relative to the sediment are dominated by Proteobacteria and Actinobacteria, while the single *S. globosa* gut sample was enriched in Nitrosopumilales relative to the sediments (Fig. 3.7), suggesting archaea belonging to this order grow within the digestive tract in addition to being diet-derived.

3.5.3 Trophic ecology and gut microbiomes of facultatively swimming deposit feeders

At Station ALOHA, we considered *Benthodytes* spp. and *Psychropotes* spp. to be facultative swimmers, as they are observed occasionally taking off from the seafloor but spend the majority of their time on the benthos (Rogacheva et al. 2012). *Benthodytes* spp. had high $\delta^{15}\text{N}_{\text{SAA}}$ values indicative of approximately 70% utilization of small particles (Fig. 3.3b) and trophic position of 3.3 ± 0.1 (Fig. 3.1f). This suggests *Benthodytes* spp. utilize gut microbial products for nutrition, similar to the echinoids *E. rostrata* and *Pilematechinus* aff. *Benthodytes* sp. on the Porcupine Abyssal Plain also showed evidence of the consumption of heterotrophic bacteria, possibly hosted within their digestive tracts (Stratmann et al. 2023). Unfortunately, all *Benthodytes* spp. specimens were recovered with empty digestive tracts, preventing us from analyzing gut contents.

In contrast to *Benthodytes* spp., the low $\delta^{15}\text{N}_{\text{SAA}}$ values of *Psychropotes* spp. indicate that they consumed a greater proportion of large, fresh particles than many of the other Station ALOHA species (Fig. 3.3b). This is at odds with some previous findings that among abyssal holothurians *Psychropotes* spp. are less selective of fresh phytodetritus and consume more bacteria-derived material (FitzGeorge-Balfour et al. 2010; Amaro et al. 2019). However, these previous studies were conducted on the Porcupine Abyssal Plain and in the Western Pacific, both of which experience much higher particle flux than Station ALOHA (Frigstad et al. 2015; Amaro et al. 2019; Karl et al. 2021). Species-specific strategies for locating and consuming high-quality detritus may vary based on the flux regime. Unique among the animals in this study, one individual *Psychropotes* sp. had a higher trophic position in their gut contents than their tissue (Fig. 3.2b), which could be due to the consumption of high trophic level zooplankton carcasses, as suggested by Amaro et al. (2019). While gut contents represent a snapshot of the animal's diet, *Psychropotes* sp. tissue trophic positions, which integrate over a longer period of time, are similar to the other DFs, suggesting consumption of high trophic position material is not typical for that species.

Psychropotes spp. microbial communities were highly variable, sometimes dominated by and sometimes lacking *Nitrosopumilales* (Fig. 3.4). As with *Pilematechinus* aff., *Psychropotes* spp. gut microbiomes were distinguished from sediments in part by Dadabacteria (Fig. 3.7). One individual captured in the winter had a large proportion of Cyanobacteria in its guts (Fig. 3.4), suggesting an ability to select for fresh material even during this low flux season, possibly aided by a facultative swimming behavior allowing them to cover large distances (Gebruk and Kremenetskaia 2024).

3.5.4 Trophic ecology and gut microbiomes of benthopelagic deposit feeders

Benthopelagic holothurians, represented here by elpidiids at both sites, spend most of their time drifting in the water column and land on the benthos primarily to feed. This swimming behavior has been hypothesized to aid in locating fresh food pulses (Miller and Pawson 1990; Gebruk and Kremenetskaia 2024). At Station ALOHA, we grouped together three individuals belonging to the cryptic genera *Amperima* and *Peniagone* as *Elpidiidae* spp. We also collected one *E. eximia* individual at Station ALOHA, while *Peniagone* sp. were the only benthopelagic holothurians collected at Station M. The single *E. eximia* individual, based on $\delta^{15}\text{N}_{\text{SAA}}$ values, consumed approximately 60% large particles, more so than any other species at Station ALOHA (Fig. 3.3b). Selection for large particles, which are likely to be fresher and less recalcitrant based on lower $\delta^{15}\text{N}_{\text{SAA}}$ values and faster sinking times (Alldredge 1998), aligns with an ability to be highly selective by swimming, although Miller and Pawson (1990) hypothesized low selectivity of particles after landing on the seafloor. *E. eximia* had the highest trophic position of any DF in this study (4.1; Fig. 3.1f). The less degraded material that *E. eximia* apparently consume relative to other DFs could include zooplankton fecal pellets or carcasses, which sink much faster and arrive at the seafloor with minimal microbial reworking (Turner 2015; Doherty et al. 2021). The large, labile particles had higher trophic positions than other POM sources. Unfortunately, the specimen voided its gut contents during collection, so no data are available on the *E. eximia* gut microbiome.

Elpidiidae and *Peniagone* sp. had trophic positions consistent with secondary consumers, similar to the non-swimming and facultatively swimming species at both sites (Fig. 3.1). Along with *E. eximia*, they all consumed some of the highest proportions of fresh phytodetritus seen at both sites (Fig. 3.3). Elpidiidae on the Porcupine Abyssal Plain are selective feeders (FitzGeorge-

Balfour et al. 2010; Stratmann et al. 2023), which is supported by their increase in orders of magnitude in abundance following periods of higher flux (Wigham et al. 2003; Billett et al. 2010; Huffard et al. 2016). We found that Elpidiidae ΣV tissue values varied considerably, from 2.81 to 4.65, the highest value measured in any animal tissue in this study, suggesting that some individuals consume heavily reworked material (Fig. 3.1d). As with the isotopic data, we found high variability in gut microbial community composition among Elpidiidae (Fig. 3.5), although all three specimens had Cyanobacteria reads indicative of the consumption of fresh phytodetritus during both summer and winter (Fig. 3.4), possibly by swimming to increase chances of encountering fresh food sources. The four *Peniagone* sp. individuals in our study had high ΣV tissue values (2.97 ± 0.29 in the fall and 3.20 ± 0.31 in the spring), indicative of consumption of more heavily reworked material. No *Peniagone* sp. were recovered with intact gut contents during the fall, so our analysis of their gut microbiota is confined to the lower flux season (i.e. spring) during which Proteobacteria and Actinobacteria dominated the community composition, similar to other Station M species (Fig. 3.4).

3.5.5 Potential functions of gut microbiota in abyssal deposit feeders

Alpha diversity was overall lower in DF digestive tracts than in sediments (Fig. 3.6), suggesting that the gut environment among all species fostered a more selective and specialized community than that of the sediments. This could point to the development of a gut microbiome that is distinct from environmentally derived microbes, as indicated by the trophic step increase between sediment and gut contents at Station M (Fig. 3.2; Romero-Romero et al., 2021). With a differential abundance analysis, we were able to determine which ASVs were enriched in the gut contents relative to the sediments (Fig. 3.7). Some of these ASVs are likely derived from ingested material, such as the Cyanobacteria which we took to indicate utilization of fresh phytodetritus, similar to phytopigments as in FitzGeorge-Balfour et al. (2010). Abundant Cyanobacteria were found in the guts of the mobile species *O. mutabilis*, Elpidiidae spp., and *Psychropotes* spp., which in combination with low $\delta^{15}\text{N}_{\text{SAA}}$ tissue values supports the notion that their mobility allows for selectivity of fresher and larger detrital particles. Other ASVs enriched in gut contents relative to sediments may have increased in abundance within the guts due to a preference for the gut environment. However, we may have missed some of this core microbiome by not isolating DNA directly from gut walls (Schwob et al. 2020).

Ammonia oxidizing archaea (AOA) in the order Nitrosopumilales were abundant in most gut contents (Fig. 3.4), but they were mostly enriched in the sediments (Fig. 3.7). AOA are important nitrifiers in the upper water column, particularly in oligotrophic regions like Station ALOHA (Karner et al. 2001; Church et al. 2010), as well as in some abyssal sediments (Park et al. 2014; Hollingsworth et al. 2021). It is possible that Nitrosopumilales nitrification provides additional labile organic matter to the diets of abyssal DFs in the sediments before consumption or in their digestive tracts. In a similar way, some endosymbiotic Thaumarchaeota associate with sponges, fixing carbon and potentially providing additional nutrition to their hosts (Preston et al. 1996; Hallam et al. 2006; Haber et al. 2021). Nitrosopumilales were less abundant in the digestive tracts of animals that had consumed fresh phytodetritus (Fig. 3.4), possibly suggesting that during the seasons when mobile taxa are able to consume less recalcitrant material, they have less need to supplement their diet with AOA-derived organic material. However, the $\delta^{15}\text{N}$ values of AOA amino acids have not been measured, so we cannot determine whether the consumption of Nitrosopumilales biomass would contribute to the estimated trophic position of the DFs.

3.6 Conclusions

At both the eutrophic Station M and the oligotrophic Station ALOHA, abyssal DFs showed evidence of gut microbiomes distinct from the sediment. Gut microbiota and trophic isotopic indicators both revealed niche partitioning among the abyssal echinoderms, with fast-moving and swimming holothurians consuming a greater proportion of large, fresh phytodetritus. In contrast, the slower-moving, obligate benthic echinoids consume smaller and more recalcitrant detrital particles and showed evidence of additional microbial heterotrophy in their digestive tracts. Our findings support the hypothesis that swimming behavior in deep-sea holothurians enables the location and consumption of fresh food pulses. We also show that non-swimming DFs are more reliant on microbial reworking of ingested material, cultivating gut microbiomes dominated by Proteobacteria, Actinobacteria, and in some cases the ammonia-oxidizing Thaumarchaeota.

By combining isotopic trophic indicators with microbial community barcoding, we connect microbial and metazoan food webs on the abyssal plain. $\delta^{15}\text{N}$ AA-CSIA suggests that

microbial communities in sediments and digestive tracts act as trophic intermediates for DFs to the extent that the animals are secondary, rather than primary, consumers. This might appear to be a lengthening of the benthic food web, thus leading to less energy available for higher trophic levels that may consume the DFs. However, microbial communities likely break down detrital material that would be otherwise unavailable to metazoans (Mayor et al. 2014). Therefore, the addition of a gut microbiome trophic step to the abyssal food web may actually increase the detritus-based energy available to higher trophic levels on the food-limited abyssal plain, particularly energy from small particles that are not well represented in sediment traps.

CHAPTER 4. Changes in gut microbiota and increases in deposit feeder trophic position with depth from shallow reefs to the abyssal plain

Lee C. Miller, Sonia Romero-Romero, Brian N. Popp, Jeffrey C. Drazen

In prep

4.1 Abstract

Microbial communities influence deep-sea metazoans by producing, transforming, and altering the availability of the detritus that forms the base of their food webs. One area where microbes may directly affect the quality of detritus is in the digestive tracts of deposit feeders. We examined the trophic ecology and gut microbiomes of deposit-feeding echinoderms across a depth gradient ranging from shallow reefs to abyssal plains in the tropical North Pacific. We predicted that microbially reworked material, in particular from microbes residing in deposit feeder guts, would make up a larger proportion of their diets with increasing depth due to the declining quantity and quality of organic matter in detrital flux. Using compound-specific stable isotope analysis of individual amino acids, we found that deposit feeder trophic position increased by a full trophic step within the first 500 m of depth, indicating a shift from primary to secondary consumption of sediment detritus. The increase in trophic position correlated with a decrease in estimated particulate organic matter flux with depth, suggesting it is an adaptation to a decreased detrital food supply. Gut microbial community composition varied between detritovore fauna originating from different depth zones, although Proteobacteria and Planctomycetes were dominant throughout the depth range examined. Potential mutualistic gut bacteria, including Chloroflexi, Dadabacteria, and Dependientiae, increased in relative abundance with the depth of origin of hosts. Additionally, gut-associated ammonia-oxidizing archaea (family Nitrosopumilaceae) increased in relative abundance with host depth of origin, suggesting a possible role of archaea-derived organic material in the diets of deep-sea deposit feeders. $\delta^{13}\text{C}$ essential amino acid fingerprinting revealed that shallow water bacterial, fungal, and phytoplankton-based endmembers did not encompass the range of values of the deposit feeders below the euphotic zone. Archaea should be investigated as a potential additional endmember in deep-sea detrital food webs.

4.2 Introduction

Depth is a major driver of benthic community composition (Nepkin et al. 2014), diversity (Levin et al. 2001; Nepkin et al. 2014; Hoshino et al. 2020), abundance (Cornelius and Gooday 2004; Rex et al. 2006; Wei et al. 2010; Nepkin et al. 2014), biomass (Rex et al. 2006; Deming

and Carpenter 2008; Wei et al. 2010), and more. As depth increases, temperature decreases and pressure increases, influencing benthic communities (Levin et al. 2001). One of the biggest factors driving community changes, however, is the exponential decrease in food supply with depth that drives decreases in metazoan biomass and abundance (Wei et al. 2010). Benthic microbial and metazoan food webs intersect and influence one another in many ways, including through symbiotic relationships such as microbial communities in metazoan digestive tracts aiding in digestion. Gut communities aid in the breakdown of low-quality food such as phytodetritus in both shallow (Rodríguez-Barreras et al. 2021) and deep (Amaro et al. 2009; Peoples et al. 2024) detritivores. Given the depth-related changes in both microbial and metazoan communities due to decreases in food quantity and quality, it is likely that the nature and strength of gut symbioses may change across depth. However, to date there have been limited studies comparing the composition of animal gut microbiota and their functions across depth gradients.

Our understanding of the identity and function of gut microbiota in the deep sea is limited to certain taxa and environments, primary fish and chemosynthetic habitats (Osman and Weinnig 2022; Lu et al. 2023; Xiao et al. 2023). The few studies that have examined animal gut microbiomes across a depth range suggest that, as with many ecological patterns, depth is one of the primary drivers of microbiome community composition (Ohwada et al. 1980; Lu et al. 2023). This is due in part to the increasing dominance of piezophilic microbes (Ohwada et al. 1980; Li et al. 2024). However, the trophic position and feeding guild of the host animal is also an important influence on gut microbiome composition and function (Sullam et al. 2012). The gut microbiomes of detritivores, such as the deposit-feeding echinoderms that are the focus of the study, provide a unique environment with which to study the influence of decreasing food quality and quantity across depth on microbe-metazoan interactions in detritus-based food webs. In this study, we use 16S rRNA community barcoding to characterize the composition and diversity of microbial communities associated with deposit feeders across a nearly 5000 m depth range.

Carbon and nitrogen stable isotopic composition can be used to characterize trophic relationships between microbes and metazoans. Organic material, including tissue from animals at all trophic levels, shows logarithmic increases in $\delta^{15}\text{N}$ values with depth in both benthic and pelagic food webs (Altabet et al. 1999; Mintenbeck et al. 2007; Stasko et al. 2018; Chi et al. 2021). This increase is due to changing food supplies, with increasing heterotrophic reworking of

material as detritus sinks from the surface (Altabet et al. 1999). The effect is stronger in feeding guilds that feed on pelagic-derived material (e.g. suspension feeders) than benthivores (e.g. deposit feeders), but it is seen across taxa (Mintenbeck et al. 2007; Stasko et al. 2018; Guy-Haim et al. 2022). These increasing baseline $\delta^{15}\text{N}$ values make it difficult to isolate metazoan trophic dynamics, which also increase $\delta^{15}\text{N}$ values (Chikaraishi et al. 2009). Compound-specific stable isotope analysis of individual amino acids (AA-CSIA) is a technique which allows us to separately examine microbial and metazoan trophic dynamics, as well as identify the contribution of different sources of organic material to marine food webs. Amino acids are classified as trophic amino acids, which show consistent ^{15}N fractionation with metazoan trophic steps, and source amino acids, which fractionate primarily from microbial heterotrophic reworking (Chikaraishi et al. 2009; Ohkouchi et al. 2017). Comparing the $\delta^{15}\text{N}$ values of source and trophic amino acids allows for accurate estimates of animal trophic level without needing to know the $\delta^{15}\text{N}$ value of material at the base of the food web (Popp et al. 2007; Chikaraishi et al. 2009). Additionally, $\delta^{13}\text{C}$ values of essential amino acids, which cannot be synthesized by metazoans, create a “fingerprint” that can be used to estimate the contributions of different basal food sources such as bacteria, fungi, and algae to metazoan diets (Larsen et al. 2009, 2013; McMahon et al. 2016).

$\delta^{15}\text{N}$ and $\delta^{13}\text{C}$ AA-CSIA has revealed that deposit feeders (DFs) at two different abyssal plain sites in the North Pacific are secondary, rather than primary, consumers of detritus. A diverse group of holothurians and echinoids have estimated trophic positions of 3, while gut contents have a trophic position of 2 and sediments fall at trophic position 1. This suggests that microbial communities in gut contents are trophic intermediaries for the DFs (Romero-Romero et al. 2021, Chapter 3 of this thesis). This work has not been replicated on shallower DFs, leaving it uncertain as to whether this is a unique deep-sea adaptation to an extremely food-limited environment or instead a consistent feature of DFs across a range of depth habitats.

We set out to determine whether DFs show depth-related trends in trophic position, consumption of different detrital food sources, and gut microbiome composition and potential function, using depth as a proxy for food quantity and quality. To date, no single study has examined these factors across the full depth range covered here, from shallow reefs <5 m to the abyssal plain at ~4700 m deep. We hypothesized i) deposit feeder gut microbiota change with depth, ii) shallow deposit feeders are primary consumers of detritus but show an increase in

trophic position with depth as food quality decreases, and iii) bacteria constitute an increasing proportion of deposit feeder diet with depth.

4.3 Methods

4.3.1 Sample collection

We collected DFs and sediments from four sites in the central North Pacific between 2019 and 2023 (Fig. 4.1). We collected shallow reef holothurians in December 2023 from the Makai pier on the windward coast of O‘ahu, Hawai‘i (19.46°N, 157.67°W, “Makai pier”), which has a sandy bottom with scattered coral heads and rocky substrate. 5 holothurians (2 *Actinopygna obesa* and 3 *Holothuria atra*) were hand-collected at depths less than 5 m (Table 4.1). Fecal casts were collected next to the animals in falcon tubes, when they were observed. Four sediment cores were also collected near (<1 m away from) each animal, where possible. Holothurians were transferred to 1 L plastic bags filled with seawater, which were then placed on ice until animals could be dissected. Dissections occurred in a laboratory within 6 hours of collection. Fecal casts and sediment cores were also placed on ice and then frozen at -80°C until analysis. We collected samples from the slope off the Kona coast of the Big Island of Hawai‘i (19.45°N, 155.96°W, “Kona slope”) in December 2023 with the ROV *Lu‘ukai* aboard the R/V *Kilo Moana*, including three holothurians (1 Laetmogonidae, 2 *Mesothuria* sp.), two echinoids (*Eupatagus lymani*), and two sediment cores. Seamount and ridge samples were also collected within the Johnston Atoll EEZ (16.7°N, 170°W, “Johnston Atoll”) in June and July 2022 with the ROV *Hercules* aboard the E/V *Nautilus*, including ten holothurians (1 *Benthodytes* sp., 1 *Bohadscia paradoxis*, 3 Elpidiidae, 1 *Psychropotes* sp., 4 Synallactidae), four echinoids (1 Echinothuriidae, 1 *Phrissocystis multispina*, 2 *Tromikosoma hispidum*), and two sediment cores. Finally, abyssal samples were collected from Station ALOHA (22.75°N, 158°W, approx. 4700 m, “Station ALOHA”) in July 2019, January 2020, and July 2020 with the ROV *Lu‘ukai* aboard the R/V *Kilo Moana*, including 12 holothurians (3 *Benthodytes* spp., 1 *Enypniastes eximia*, 5 Elpidiidae, 3 *Psychropotes* spp.), nine echinoids (*Pilematechinus* aff.), and eight sediment cores (Table 4.1).

All animals were dissected using ethanol-sterilized tools to isolate gut contents and gut wall, and to take tissue samples for stable isotope analysis. Holothurians were opened with a longitudinal cut along the ventral side and echinoids were opened with a circular cut around the

dorsal side. Digestive tracts were carefully removed and opened to access gut contents. When gut contents were intact, they were removed from the foregut, midgut, and hindgut using a spatula. Foregut samples were taken near the mouth, hindgut samples near the anus, and midgut samples around the middle of the digestive tract. Sediment cores were sectioned to isolate the top 0-0.5 cm (Station ALOHA), top 0-1 cm (Kona slope, Johnston Atoll), or 0-5 cm (Makai pier). After processing, all samples were frozen at -80°C until processing.

4.3.2 POC flux

We estimated POC flux to the depth of each sample following the methods of Lutz et al. (2007). Satellite-derived Net Primary Production (NPP) was estimated using the global Standard Vertically Generalized Production Model (VGPM) from the Oregon State University's Ocean Productivity portal (www.science.oregonstate.edu/ocean.productivity/custom.php) at a resolution of 1/6th of a degree. The Seasonal Variation Index was also calculated as in Lutz et al. (2007), using an export zone depth of 100 m. We used a fixed euphotic zone depth of 100 m based on the latitude of our samples (Palevsky and Doney 2018). For the Makai Pier samples, which were collected above the export zone depth, we instead used average NPP value for that location.

4.3.3 Compound-specific stable isotope analysis

We analyzed the $\delta^{13}\text{C}$ and $\delta^{15}\text{N}$ values of individual amino acids in DF tissue, gut contents, and sediment following the methods of Hannides et al. (2013). Briefly, derivatized amino acids from freeze-dried samples were analyzed for $\delta^{15}\text{N}$ values on a Thermo Scientific Delta V Plus IRMS interfaced to a trace gas chromatograph (GC) fitted with a 60 m BPx5 capillary column through a GC-C III combustion furnace (980 °C), reduction furnace (680 °C) and liquid nitrogen cold trap. $\delta^{13}\text{C}$ values were measured using a Thermo-Fisher Scientific MAT 253 isotope ratio mass spectrometer interfaced with a Trace Ultra GC-III via ConFlo IV. Samples were co-injected with the internal reference amino acids norleucine and aminoadipic acid with known $\delta^{15}\text{N}$ or $\delta^{13}\text{C}$ values. In addition, every three sample injections we injected a full reference suite of amino acids with known $\delta^{15}\text{N}$ or $\delta^{13}\text{C}$ values for quality assurance. We normalized the $\delta^{15}\text{N}$ values of sample amino acids using a linear regression between reference suite and sample values. $\delta^{13}\text{C}$ values were corrected following the approach of Silfer et al. (1991). The uncertainty

for each amino acid $\delta^{15}\text{N}$ value was calculated as the standard deviation of three injections, where there was sufficient material available (see Fig. S1).

4.3.4 16S rRNA microbial community barcoding

Microbial communities in gut contents and sediments were characterized using 16S rRNA sequencing following the methods of Chapter 2 of this thesis. 16S rRNA sequences were processed and ASVs were generated using the DADA2 pipeline (Callahan et al. 2016), and alpha diversity was estimated using the phyloseq package (McMurdie and Holmes 2013) as described in Chapter 2 of this thesis.

4.3.5 Stable isotope data analysis

We calculated the trophic position of DF tissue, gut contents, and sediments using the $\delta^{15}\text{N}$ values of phenylalanine and glutamic acid following the methods of Chikaraishi et al. (2009): $\text{TP} = (\delta^{15}\text{N}_{\text{Glx}} - \delta^{15}\text{N}_{\text{Phe}} - \beta) / \text{TDF} + 1$. $\delta^{15}\text{N}_{\text{Glx}}$ and $\delta^{15}\text{N}_{\text{Phe}}$ are the $\delta^{15}\text{N}$ values of glutamic acid (Glx, including the contribution of glutamine) and phenylalanine (Phe) in the sample. β is the difference between $\delta^{15}\text{N}_{\text{Glx}}$ and $\delta^{15}\text{N}_{\text{Phe}}$ in primary producers ($3.4 \pm 1\%$), and TDF is the trophic discrimination factor ($7.6 \pm 1\%$), as defined in Chikaraishi et al. (2009). We calculated the uncertainty of our trophic position estimates as the propagated error of the $\delta^{15}\text{N}$ values of Glx and Phe, β and TDF (Ohkouchi et al. 2017).

We calculated the ΣV parameter, a proxy for heterotrophic resynthesis of amino acids, based on the methods of McCarthy et al. (2007): $\Sigma V = 1/n \Sigma \text{Abs}(\chi_i)$. In this equation, n is the total number of AAs used for the calculation and χ_i is the deviation of the $\delta^{15}\text{N}$ value of amino acid i from the mean $\delta^{15}\text{N}$ value of the n amino acids [$\delta^{15}\text{N}_i - (\Sigma \delta^{15}\text{N}_i / n)$]. ΣV was calculated based on the trophic amino acids alanine, valine, isoleucine, proline, aspartic acid, and glutamic acid.

4.3.6 Statistical analysis

Statistical analyses were done using the vegan package implemented in R (Oksanen et al. 2024). We used linear regressions to determine trends in trophic position, POC flux, and $\delta^{15}\text{N}_{\text{SAA}}$ values with depth, as well as to test the correlations between trophic position and POC flux. For

microbial community composition, we created a Principal Coordinate Analysis (PCoA) based on a Bray-Curtis dissimilarity matrix of ASV abundance. Additionally, we compared the Shannon diversity, Simpson diversity, and Chao1 richness of microbial communities between sample types with an analysis of variance (ANOVA).

To test the influence of depth, site, DF taxon, and sample type on microbial community composition, we used PERMANOVAs, with microbial abundance designated at the family level. For all analyses, $P < 0.05$ was considered significant.

Table 4.1. Animal and sediment collections at four sites.

Site	Species	n collected	Depth (m)	Latitude	Longitude	Month	Analyses
Makai pier	<i>Actinopygna obesa</i>	2	<5	21.32°N	157.67°W	December 2023	16S, AA-CSIA
	<i>Holothuria atra</i>	3					16S, AA-CSIA
	Fecal cast	3					16S
	Sediment	4					16S, AA-CSIA
Kona slope	<i>Eupatagus lymani</i>	2	302	19.46°N	155.94°W	December 2023	16S, AA-CSIA
	<i>Mesothuria</i> sp.	2	497-505	19.46°N	155.94°W		16S, AA-CSIA
	Laetmogonidae	1	899	19.45°N	155.96°W		16S, AA-CSIA
	Sediment	2	899-902	19.45°N	155.96°W		16S, AA-CSIA
Johnston Atoll	Elpidiidae	1	2903	18.71°N	171.32°W	July 2022	16S
	Elpidiidae	2	3263-3300	16.24°N	171.88°W	June 2022	16S, AA-CSIA
	<i>Bohadscia paradoxsis</i>	1	151	16.71°N	169.57°W	July 2022	16S, AA-CSIA
	Synallactidae	2	883-894	16.71°N	169.59°W	July 2022	16S, AA-CSIA
	Synallactidae	1	1206	16.70°N	169.62°W	July 2022	16S
	Echinothuriidae	1	1487	15.17°N	171.06°W	July 2022	16S, AA-CSIA
	<i>Tromikosoma hispidum</i>	1	1628	16.69°N	169.63°W	July 2022	16S
	<i>Tromikosoma hispidum</i>	1	1674	14.13°N	167.37°W	July 2022	16S, AA-CSIA
	Synallactidae	1	1904	18.67°N	180.94°W	July 2022	16S
	<i>Phrissocystis multispina</i>	1	1907	19.46°N	170.99°W	July 2022	16S
	<i>Psychropotes</i> sp.	1	2278	18.72°N	171.34°W	July 2022	16S, AA-CSIA
	<i>Benthodytes</i> sp.	1	2483	18.79°N	170.50°W	July 2022	16S
	Sediment	1	883	16.71°N	169.59°W	July 2022	16S, AA-CSIA
	Sediment	1	2289	18.72°N	171.34°W	July 2022	16S, AA-CSIA
Station ALOHA	<i>Benthodytes</i> spp.	2	~4700 m	22.75°N	158°W	July 2020	AA-CSIA
	<i>Enypniastes eximia</i>	1				July 2020	AA-CSIA
	Elpidiidae	1				January 2020	16S, AA-CSIA
	Elpidiidae	4				July 2020	16S
	<i>Pilematechinus</i> aff.	2				July 2019	AA-CSIA
	<i>Pilematechinus</i> aff.	1				January 2020	16S, AA-CSIA
	<i>Pilematechinus</i> aff.	6				July 2020	16S, AA-CSIA
	<i>Psychropotes</i> sp.	1				January 2020	16S
	<i>Psychropotes</i> spp.	2				July 2020	16S, AA-CSIA

Table 4.1. (Continued) Animal and sediment collections at four sites.

Sediment	2			July 2019	16S, AA-CSIA
Sediment	3			January 2020	16S, AA-CSIA
Sediment	3			July 2020	16S, AA-CSIA

4.4 Results

4.4.1 Trophic changes with depth

A number of trophic indicators changed with increasing habitat depth in the deposit feeders. The average $\delta^{15}\text{N}$ values of the source amino acids phenylalanine and lysine ($\delta^{15}\text{N}_{\text{SAA}}$) showed a logarithmic increase with depth for DF tissue (linear regression of log transformed data, $t = 3.03$, $P < 0.01$) but did not have a relationship with depth in gut contents (linear regression, $P > 0.05$) (Fig. 4.2a). We did not have enough data to determine whether there was a relationship between $\delta^{15}\text{N}_{\text{SAA}}$ and depth for sediments, as many of the sediment samples did not contain high enough quantities of amino acids for CSIA. We did not isolate enough amino acids from Station ALOHA sediment cores to calculate a trophic position, so we used POM sampled from the water column 50 meters above the bottom. This included material captured in moored sediment traps, as well as particles filtered in situ and size fractionated to 0.3-1 μm and 1-53 μm , previously reported in Chapter 2 of this thesis. The estimated trophic position of sediment and gut contents did not change with depth, remaining around 1 and 2, respectively (linear regression, $P > 0.05$). DF tissue trophic position, however, had a logarithmic increase with depth (Fig. 4.2b; linear regression, $t = 4.07$, $P < 0.001$) from about 2 to 3. Tissue trophic position had a negative linear relationship with POC flux (linear regression, $t = -3.34$, $P < 0.01$), which also decreased logarithmically with depth (linear regression, $t = -8.82$, $P < 0.0001$) (Fig. 4.2).

$\delta^{13}\text{C}$ EAA values were not influenced by depth, sample type, or DF species (Fig. 4.3, PERMANOVA, $P > 0.05$). We included five endmembers from Larsen et al. (2013) to our probabilistic PCA, including bacteria, fungi, macroalgae, microalgae, plants, and seagrass. The shallow and terrestrial endmembers (plants and seagrass) were included despite the deep-sea nature of most of our samples because of the possibility of terrestrial input in marine sediments close to major landmasses such as the Hawaiian Islands (Kandasamy and Nagender Nath 2016). We found that most of our samples did not cover the same PCA space as the endmembers, with the exception of tissue from *Bohadscia paradoxis* at 151 m and Synallactidae at 883 m, which overlapped with the bacteria and fungi endmembers (Fig. 4.3).

4.4.2 Gut microbiota changes with depth

Microbial community composition in both sediments and digestive tracts was influenced by depth (PERMANOVA, $F = 16.65$, $P < 0.001$; Fig. 4.4, 4.5). Community composition also differed between sediments and gut contents (PERMANOVA, $F = 2.66$, $P < 0.01$), as well as between the different digestive tract regions (foregut, midgut, hindgut; PERMANOVA, $F = 1.78$, $P < 0.01$). Shannon diversity, Simpson diversity, and Chao1 abundance did not change with depth (linear regression, $P > 0.05$). All three alpha diversity measures also did not differ between gut contents and sediment (t-test, $P > 0.05$). Shannon diversity differed by host species (ANOVA, $F = 2.28$, $P = 0.012$), as did Chao1 abundance (ANOVA, $F = 2.51$, $P = 0.0059$), but Simpson diversity did not (ANOVA, $P > 0.05$).

Among the 24 most abundant microbial families among all gut contents samples, 8 increased in proportional abundance with depth (Acidiobacteria, Actinobacteria other, Chloroflexi other, Dadabacteria, Dependitiae, Woeseiaceae, Hyphomicrobioaceae, and Nitrosopumilaceae; linear regression, $P < 0.05$), 8 decreased in proportional abundance with depth (Xenococcaceae, Cyanobacteria other, Firmicutes, Planctomycetes other, Pirellulaceae, Rhizobiaceae, Rhodobacteraceae, and DEV007; linear regression, $P < 0.05$), and 8 did not show a relationship with depth (Microtrichaceae, Bacteroidetes, Anaerolineaceae, Kiloniellaceae, Moritellaceae, Proteobacteria other, Tenericutes, and Microtrichaeae; linear regression, $P > 0.05$) (Fig. 4.6).

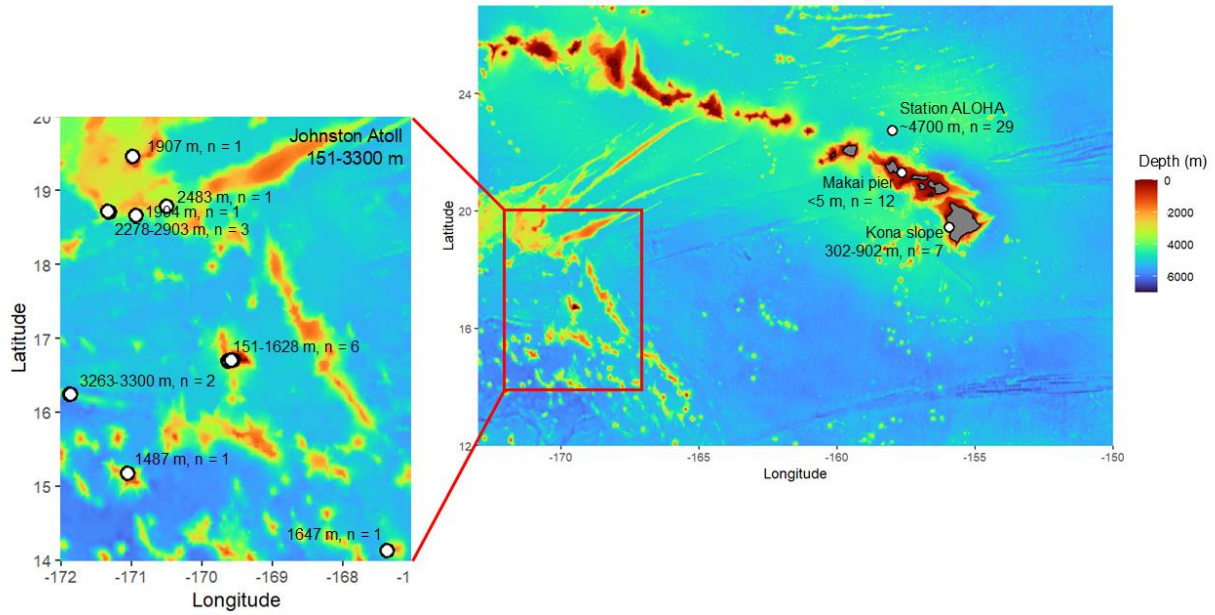


Figure 4.1. Sample locations, collection depths, and number of animals and sediment cores collected at each location. Inset shows Johnston Atoll sampling site, indicating individual sample locations within it.

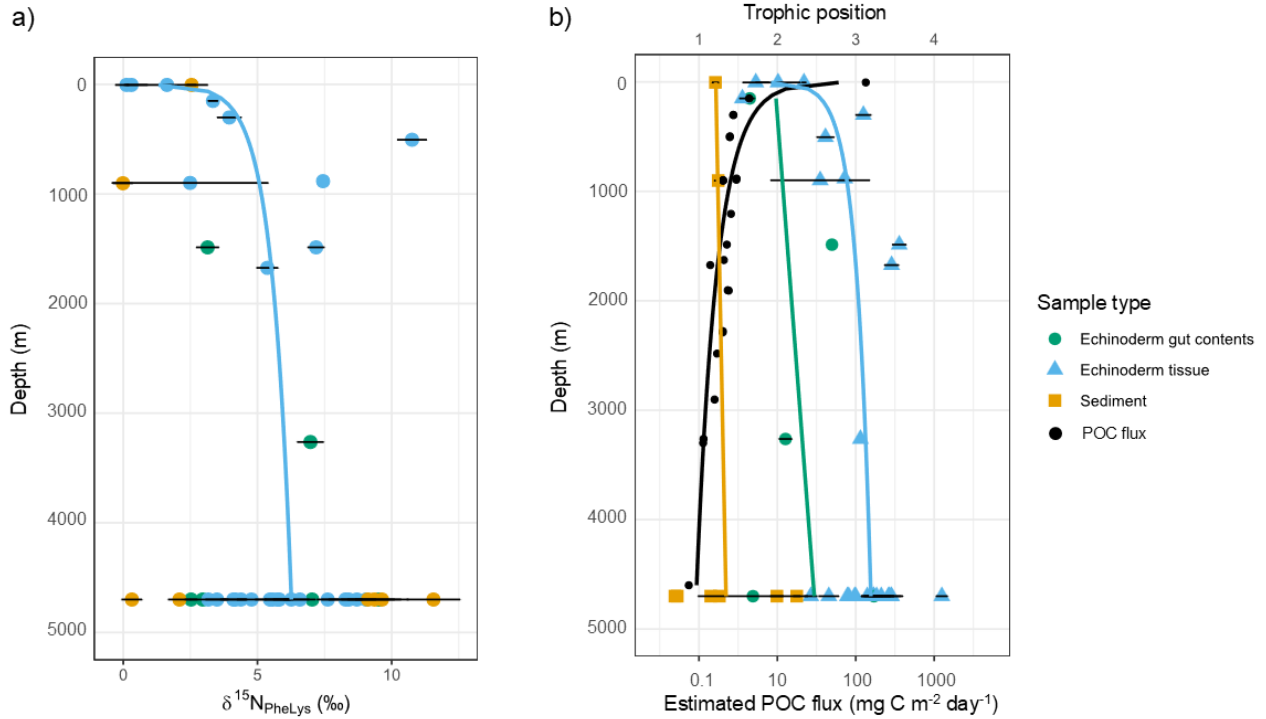
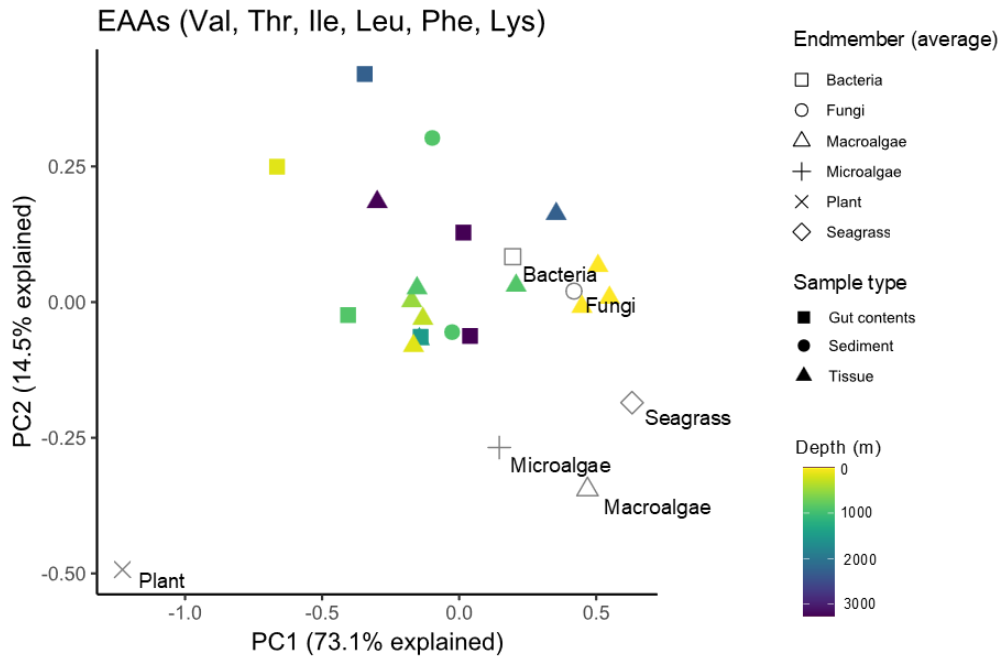
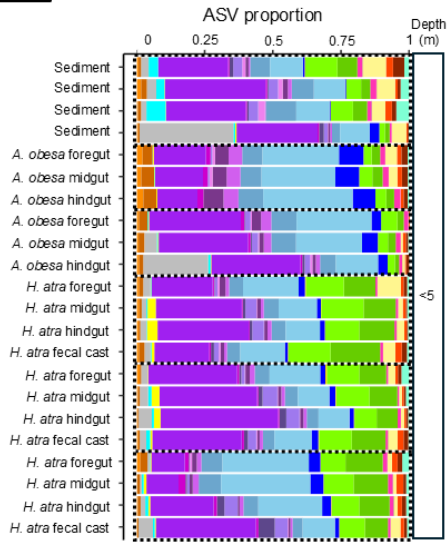


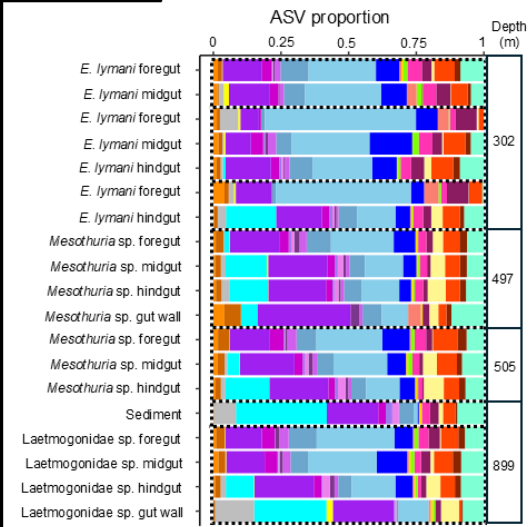
Figure 4.2. a) Average $\delta^{15}\text{N}$ value of the source amino acids phenylalanine and lysine and **b)** estimated trophic position of sediments (orange), gut contents (green), and tissue (blue) across depth. Error bars show **a)** standard deviation or **b)** propagated error. Lines show linear models for sediment ($y = 2664x + 5580$, $R^2 = 0.12$), gut contents ($y = 933.1x + 738.7$, $R^2 = 0.10$), and tissue ($\delta^{15}\text{NSAA} y = 1073\log(x) + 1657$, $R^2 = 0.27$; trophic position $y = 5740\log(x) - 2930$, $R^2 = 0.39$). Black points show estimated POC flux at the depth and location of each sample with logarithmic trend line ($y = 2240\log(x) - 1052$, $R^2 = 0.44$).



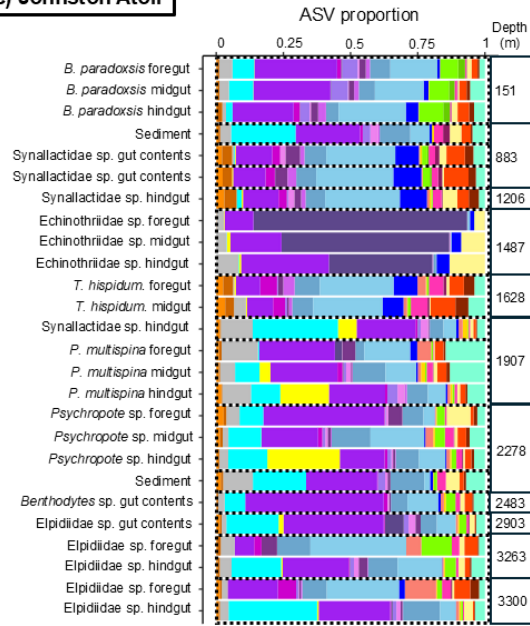
a) Makai pier



b) Kona slope



c) Johnston Atoll



d) Station ALOHA

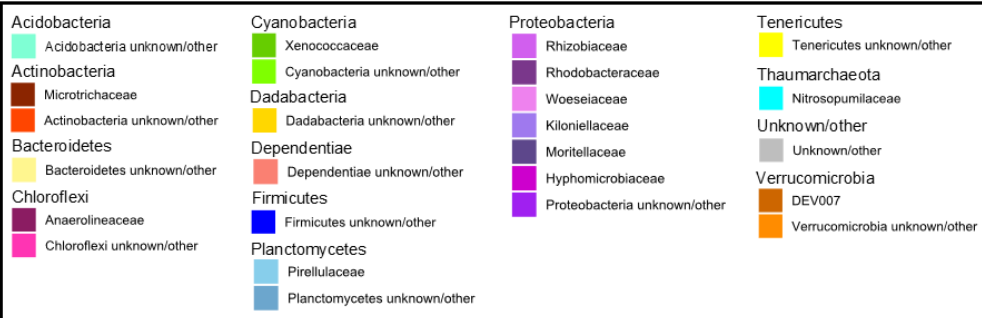
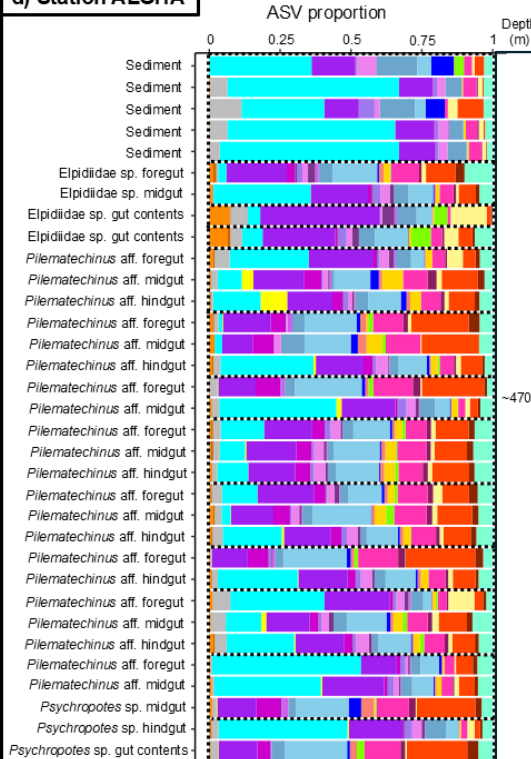


Figure 4.4. Proportion of ASVs within each sample from **a)** Makai pier, **b)** Kona slope, **c)** Johnston Atoll, and **d)** Station ALOHA, colored by family and phylum. When multiple samples were taken from a single individual, dotted black lines outline the individual. Samples are arranged by increasing depth within each site.

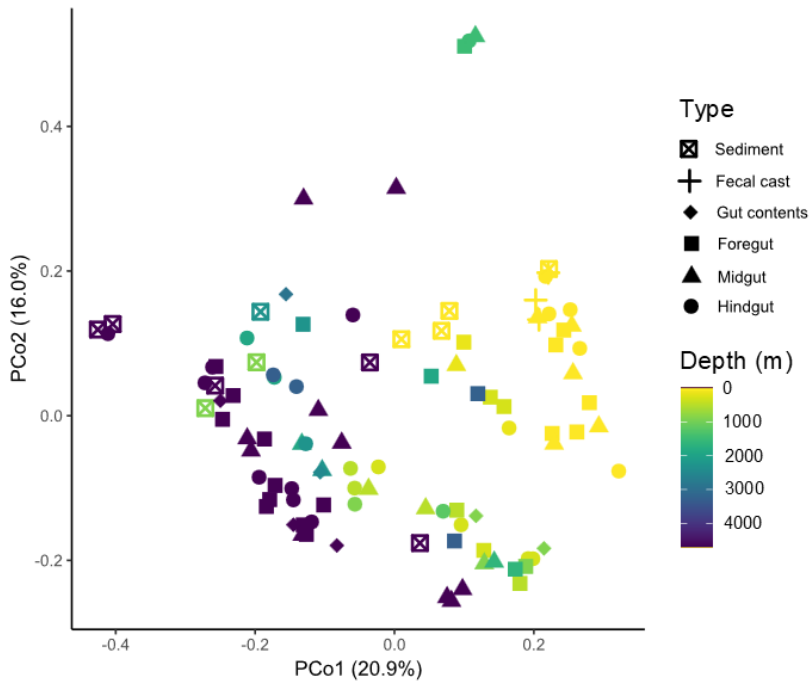


Figure 4.5. Principal coordinate analysis (PCoA) of microbial composition at the family level, colored by depth with shapes representing sample type.

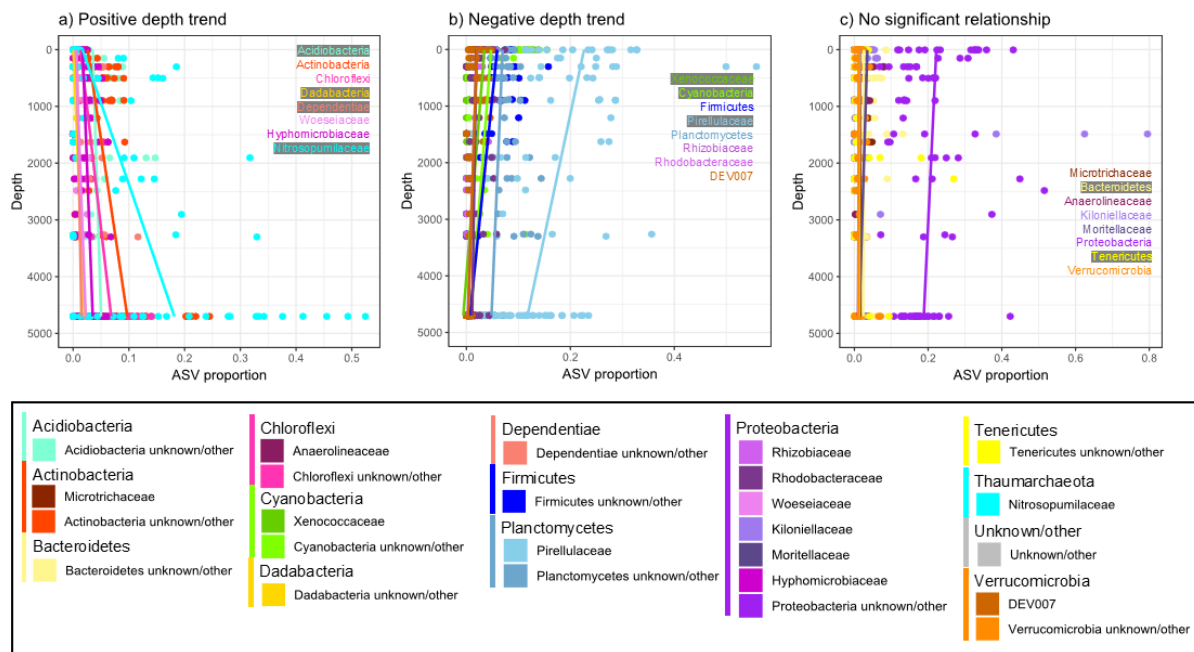


Figure 4.6. Depth trends for the most abundant microbial families and phyla among all gut, fecal cast, and sediment samples. **a)** Taxa that increased in proportional abundance with depth (linear regression, $P < 0.05$), **b)** taxa that decreased in proportional abundance with depth (linear regression, $P < 0.05$), and **c)** taxa that did not show trends in proportional abundance with depth (linear regression, $P > 0.05$). Points show individual samples while lines show linear regressions.

4.5 Discussion

4.5.1 Deposit feeder trophic position increases with depth

Depth was associated with changes in both trophic position and gut microbiome community composition for DFs from shallow reefs (<5 m) to abyssal plains (~4700 m). An increase in trophic position, from primary to secondary consumers, corresponded to the decrease in POC flux, occurring primarily within the upper 500 m (Fig. 4.2b). We calculated DF trophic position based on $\delta^{15}\text{N}$ values of phenylalanine and glutamic acid, which accounted for the increasing $\delta^{15}\text{N}_{\text{Phe}}$ with depth, meaning that this trophic increase was not simply a result of increasing baseline $\delta^{15}\text{N}$ values, which were highly variable across the depth range (Fig. 4.2a; Chikaraishi et al. 2009; Ohkouchi et al. 2017). In fact, the trophic position of sediments and gut

contents remained consistent across depth (Fig. 4.2b), suggesting that the DF tissue increase is reflective of changing ecological strategies rather than driven by the trophic position of ingested POM. It is important to note that samples of gut contents reflect the current diet while tissue samples integrate over longer periods of time; however we do not believe that the differing trends in the trophic position of these sample types were caused by the temporal mismatch. The trophic step increase from gut contents to tissue was seen across all three deep-sea sites and during all five sampling time periods, meaning that it is unlikely that it resulted from isolated flux events bringing unusually low trophic position material to the sediments.

At Station ALOHA we were unable to calculate trophic position from the sediments directly, so instead we looked at the trophic position of various types of POM captured at 50 meters above the bottom. Sediment detritus is likely made from a mixture of these sources, which ranged in trophic position from 0.69 to 2.24 (Fig. 4.2b; Chapter 2 of this thesis). The $\delta^{15}\text{N}$ source amino acid values of the DFs at Station ALOHA indicate that they consume multiple particle types (Chapter 3 of this thesis), suggesting that the average POM trophic position of 1.35 ± 0.65 is a reasonable estimate for the abyssal sediments. Together with the lack of change in gut content trophic position with depth, this lends confidence that the increase in DF trophic position is not primarily due to a change in baseline detritus trophic position. Instead, we suggest that the increase in trophic position may be attributed to increasing utilization of microbial gut communities as trophic intermediates. In particular, microbial communities within digestive tracts may contribute to DF detrital consumption in the deep sea, where food quantity and quality are poor.

4.5.2 Identity and potential function of gut-associated microbiota

In contrast to the change in trophic position, which primarily occurred within the first 500 m, DF gut microbiomes changed continuously with depth. The shallowest DF gut microbiomes, from <5 m and 151 m, were the most distinct from those of the other DFs, but the changes continued throughout the full depth range (Fig. 4.5). The gut communities of most DFs were dominated by Proteobacteria and Planctomycetes (Fig. 4.4), both of which are common gut symbiotes in other echinoderms (Gao et al. 2014; Hakim et al. 2016; Yamazaki et al. 2019; Rodríguez-Barreras et al. 2021). Within Proteobacteria, however, the most abundant families changed with depth, with an increasing proportion of Woesiaceae and Hyphomicrobiaceae and a

decreasing proportion of Rhizobiaceae and Rhodobacteraceae (Fig. 4.6). Woesiaceae are abundant in both shallow and deep marine sediments, where they are prominent heterotrophs as well as potential chemolithoautotrophs (Mußmann et al. 2017). Hyphomicrobiaceae and Rhizobiaceae, both members of the order Hyphomicrobiales, are often involved in nitrogen fixation, particularly in association with terrestrial plants (Li et al. 2023; diCenzo et al. 2024). Rhodobacteraceae are also known to have associations with marine animals including corals (Pujalte et al. 2014; Luo et al. 2021). All four families, as well as others in the phylum Proteobacteria, have a strong possibility of forming mutualistic relationships with the echinoderms in whose gut contents they were found.

We observed a decrease in the relative abundance of surface-living photoautotrophic Cyanobacteria with depth, particularly the family Xenococcaceae. This was likely a reflection of the decreasing quality of phytodetritus with depth, resulting in less labile material with cyanobacterial DNA. However, we did find Cyanobacteria reads in gut contents all the way down to the abyssal plain (Fig. 4.4), suggesting that the selective feeding of some DFs allows them to consume relatively fresh material (Chapter 3, this thesis). We might expect to find $\delta^{13}\text{C}_{\text{EAA}}$ fingerprints matching those of microalgae in the DFs with high proportions of Cyanobacteria, but all DFs matched more closely with the bacterial and fungal signals, suggesting that fresh phytodetritus is not the dominant source of energy for any of the echinoderms, even those from the reef (Fig. 4.3).

The microbial taxa that increased in relative abundance with depth included Acidobacteria, Actinobacteria, Chlorflexi, Dadabacteria, Dependientiae, and Nitrosopumilaceae. Acidobacteria, Actinobacteria, and Chloroflexi have been found to be enriched in the foregut but not hindgut contents of shallow holothurians relative to surrounding sediments, possibly due to selective feeding (Gao et al. 2014). Little is known about the phyla Dadabacteria and Dependientiae, but both show indications of host-dependent lifestyles through genome streamlining (Graham and Tully 2021; Weiss et al. 2023). Some members of Chloroflexi also form close symbioses with sponges (Bayer et al. 2018). While these taxa were found in DF gut tracts throughout the full depth range (Fig. 4.4), the increasing dominance of these potentially symbiotic phyla and families points to their possible role as endosymbiotic trophic intermediates for deep-sea DFs.

While we have focused on the putative mutualistic and commensal relationships between DFs and gut communities, pathogenic microbes likely also form part of the gut microbiota. Of note, one echinoid (Echinothuriidae) collected from 1487 m at Johnston Atoll had a gut community dominated by the family Moritellaceae, which made up a small proportion of ASVs in all other samples (Fig. 4.4). Moritellaceae includes well-known fish pathogens (Urakawa 2014), and the abundance of the genus *Moritella* increased in association with the progression of sea star wasting disease in shallow asteroids (McCracken et al. 2023), but Moritellaceae are not currently known to infect echinoids. Other techniques such as metagenomics and metatranscriptomics may be useful in elucidating the nature of gut symbioses, whether they be pathogenic, commensal, or mutualistic, in deep-sea animals.

4.5.3 Potential archaeal contributions to deposit feeder diets

One of the most prominent families, particularly in DFs and sediments below 500 m, was Nitrosopumilaceae, a primarily ammonia-oxidizing archaeal (AOA) family which contribute to nitrification in the deep water column and in sediments in the tropical Pacific (Beman et al. 2008; Hatzenpichler 2012; Hollingsworth et al. 2021). They have also been found as obligate symbiotes in both shallow coastal and deep-sea sponges (Preston et al. 1996; Haber et al. 2021). The high proportion of Nitrosopumilaceae reads in our deepest DF digestive tracts could be derived from diet, with the family also found in abyssal sediments (Fig. 4.4). Regardless of origin, diet versus resident gut microbes, the increasing AOA presence with depth indicates an increasing importance of archaea-derived nitrogen for DFs.

We expected to find an increase in the proportion of bacteria-derived material consumed by DFs with depth based on our hypothesis that the decreasing quality of phytodetritus would require deeper-living DFs to rely more on bacterial resynthesis. However, our use of $\delta^{13}\text{C}$ fingerprinting revealed that while our shallow reef DFs appeared to consume primarily bacteria- and fungi-derived material, most other DFs had $\delta^{13}\text{C}$ essential amino acid values that fell outside the range of the known endmembers outlined in Larsen et al. (2013) (Fig. 4.3). The $\delta^{13}\text{C}$ values of each essential amino acid were generally lower than any of the Larsen et al. (2013) endmembers except plant material, which had much lower values. While plant material may contribute to the diets of some of the shallower and near shore DFs, we do not think it explains the low values of animals collected from seamounts near Johnston Atoll, where very little plant

material would be expected due to a lack of significant landmass within hundreds of kilometers. This suggests deep-sea organic material incorporates additional endmember(s) not included in the shallow marine material generally used in $\delta^{13}\text{C}$ fingerprinting mixing models, something that has also been found in sinking particles using $\delta^{15}\text{N}$ analyses (Chapter 2 of this thesis).

Based on the increasing proportional abundance of ammonia-oxidizing Nitrosopumilaceae in both sediments and DF digestive tracts, we suggest that organic material generated from archaeal autotrophy should be considered as an additional potential endmember for deep-sea detritivores. Unfortunately, to our knowledge the $\delta^{13}\text{C}$ values of essential amino acids in AOA have not yet been quantified. However, Könneke et al. (2012) found that terrestrial Nitrosopumilaceae grown autotrophically in culture decrease bulk $\delta^{13}\text{C}$ values by as much as 19.8 ‰ relative to the inorganic carbon they consumed. Heterotrophic archaea have similar $\delta^{15}\text{N}$ values for most amino acids compared to bacteria (Yamaguchi et al. 2017), but the different amino acid pathways in autotrophic AOA versus heterotrophic bacteria (Wright and Lehtovirta-Morley 2023) could lead to different $\delta^{15}\text{N}$ and $\delta^{13}\text{C}$ fractionation.

We suggest that as depth increases, DFs at the base of benthic food webs may increasingly supplement their detrital food sources with archaea-derived organic material, possibly originating from their gut microbiota. However, additional isotopic analyses of archaea, ideally from the deep sea, will be necessary to investigate this hypothesis.

CHAPTER 5. Conclusions

Throughout my three data chapters, I combined compound-specific isotope analysis with 16S rRNA microbial community barcoding to understand how microbial communities affect detritus in the deep sea. Chapter 2 focuses on the microbial transformations that occur on particulate organic matter as it sinks from the euphotic zone to the abyssal seafloor. Chapters 3 and 4 look directly at microbial impacts on benthic animal food webs by examining the microbial communities associated with the digestive tracts of deposit-feeding echinoderms. I evaluate how these microbe-animal associations differ based on detrital food supply by comparing, in Chapter 3, abyssal deposit feeders (DFs) at a high flux site (Station M) versus a low flux site (Station ALOHA). In Chapter 4, I use a depth gradient as a proxy for food supply, characterizing the microbiomes of deposit feeders from a shallow reef down to the abyssal plain. With future work, I hope to continue these investigations with additional techniques that will allow me to more quantitatively understand the roles that gut microbiota play in deep-sea animal nutrition and food web structure.

5.1 Chapter 2: Transformations of particulate organic matter from the surface to the abyssal plain in the North Pacific as inferred from compound-specific stable isotope and microbial community analyses

One major finding from this chapter was how sampling method affects our understanding of particulate organic matter (POM) flux. Using the $\delta^{15}\text{N}$ values of the source amino acids (SAAs) phenylalanine and lysine, I found that the material captured in abyssal moored sediment traps resembles large, fast-sinking particles at both Station M and Station ALOHA (Fig. 2.2). This contrasted with particles filtered *in situ* from the water column at the same depths, which had higher $\delta^{15}\text{N}_{\text{SAA}}$ values indicative of more heterotrophic microbial reworking. The sediment trap material also had higher estimated trophic positions, suggesting metazoan-derived material such as zooplankton fecal pellets could be a source of the large particles captured in traps. This finding is important as sediment traps have typically been used to quantify and characterize the flux available to deep-sea organisms (Buesseler et al. 2007; Honjo et al. 2008). As I show in Chapter 3, the smaller and more microbially reworked particles captured with *in situ* filtration contribute substantially to the diets of deposit feeders at both sites. Therefore, if moored traps are

used as the primary method of collection for estimating POM flux, an important component of the flux is missed.

While the low $\delta^{15}\text{N}_{\text{SAA}}$ values and high trophic position of sediment trap material indicated a possible fecal pellet contribution, other isotopic analyses did not support that hypothesis. I recreated a mixing model based on phenylalanine-corrected $\delta^{15}\text{N}$ values of alanine and threonine, which Doherty et al. (2021) used to distinguish zooplankton fecal pellets from phytoplankton/phytodetritus and microbially degraded POM. At both sites, the sediment trap material had less than a 50% possible contribution of zooplankton-derived material, instead showing a greater proportion of microbially degraded material than the filtered particles. This finding, which was in contrast to that of the $\delta^{15}\text{N}_{\text{SAA}}$ values, was likely due to the $\delta^{15}\text{N}_{\text{Thr-Phe}}$ and $\delta^{15}\text{N}_{\text{Ala-Phe}}$ values of many of our samples, both particles and sediment traps, falling outside the range of values of the Doherty et al. (2021) endmembers (Fig. 2.3). I suggest that additional endmember characterization is needed to apply this analysis more confidently to deep-sea samples. In particular, microbial endmembers should include a variety of heterotrophic and autotrophic bacteria and archaea.

A more expected pattern that I observed was an increase in $\delta^{15}\text{N}_{\text{SAA}}$ values with depth, seen across all particle size fractions in both locations (Fig. 2.2). This is likely due to heterotrophic microbial activity (Hannides et al. 2013), which led to larger increases in the smaller size fractions as they take longer to sink, allowing for more time for microbial colonization and reworking (Alldredge 1998). The $\delta^{15}\text{N}_{\text{SAA}}$ value increase occurred primarily within the first 400 m of the water column for all size fractions (Fig. 2.2), marking the lower euphotic and upper mesopelagic as regions of significant microbial transformations of sinking detritus. Particles from this area of the water column at Station ALOHA contained high abundances of ammonia-oxidizing archaea belonging to the family Nitrosopumilaceae (Fig. 2.4). Across Station ALOHA particle samples, the relative abundance of Nitrosopumilaceae positively correlated with $\delta^{15}\text{N}_{\text{SAA}}$ values (Fig. 2.6). I suggest that this indicates high heterotrophic reworking produces waste products, such as ammonia, that support abundant ammonia-oxidizing archaea in the upper water column.

5.2 Chapter 3: Niche partitioning among abyssal deposit-feeding echinoderms is linked to mobility and gut microbiota

Building on Chapter 2, which examined microbial communities associated with sinking POM and their transformations of the detritus, in Chapter 3 I continued these analyses to the seafloor. In Romero-Romero et al. (2021) we used AA-CSIA to demonstrate that the abyssal DFs studied are secondary consumers of sedimentary detritus at Station M and postulated that gut microbiota act as trophic intermediates, breaking down low-quality phytodetritus ingested by DFs. I replicated these analyses at Station ALOHA, where the DFs studied were also found to be secondary consumers with trophic positions as high as 4 (Fig. 3.1). I also examined microbial community composition in the digestive tracts of animals at both sites and found lower diversity than in the sediments, indicating that DFs guts are a selective environment with microbial communities distinct from those associated with ingested sediment (Fig. 3.6). While the taxonomic composition of sediment and gut microbiota was similar, the many ASVs enriched in gut contents relative to sediment further supports the digestive tracts of DFs as unique microbial environments (Fig. 3.7).

Among the microbial taxa found in DF digestive tracts, Cyanobacteria were abundant in the Station M species *Echinocrepis rostrata* and *Oneirophanta mutabilis* during the high-flux fall season (Fig. 3.4). This finding supports the characterization of these species as selective feeders targeting fresh phytodetritus, particularly *O. mutabilis* which is fast-moving (Kaufmann and Smith 1997). However, fresh phytodetritus does not constitute the majority of either species' diet according to the results of a two-factor mixing model incorporating $\delta^{15}\text{N}_{\text{SAA}}$ values of the sediment trap material versus small, filtered particles from Chapter 2. *E. rostrata* and *O. mutabilis* primarily consumed a majority of small, recalcitrant material, in contrast to other species at both sites that consumed large, labile POM (Fig. 3.3).

The DFs that consumed the most sediment-trap captured material, which is likely fresher and therefore more nutritious (De La Rocha and Passow 2007), were holothurians capable of swimming. Swimming behavior is common among deep-sea holothurians, particularly in the family Elpidiidae, but its function in feeding via location or increased encounter of patches of fresh phytodetritus has previously only been speculated (Chimienti et al. 2019; Gebruk and Kremenetskaia 2024). I showed that benthopelagic and facultatively swimming holothurians at

both sites overall consumed fresher material with lower $\delta^{15}\text{N}_{\text{SAA}}$ values than fully benthic echinoids and holothurians (Fig. 3.3), pointing to swimming ability as an additional method of niche partitioning on the abyssal plain.

As they are less able to compete with swimming holothurians for fresh detritus following flux pulses, non-swimming echinoderms may therefore be more reliant on gut microbes to break down and increase the availability of the detritus they consume. Focusing on the gut communities of the echinoids *E. rostrata* at Station M and *Pilematechinus* aff. at Station ALOHA, I found they were enriched relative to sediments in a variety of microbial taxa, especially Proteobacteria and Actinobacteria (Fig. 3.7), known gut residents in shallow and deep echinoderms (Amaro et al. 2009; Schwob et al. 2020; Rodríguez-Barreras et al. 2021). Additionally, I found high relative abundances of Nitrosopumilaceae in sediments and most DF digestive tracts at both sites (Fig. 3.4). This shows that outside of their potential role in upper water column POM recycling, as described in Chapter 2, they may alter POM once it reaches sediments, potentially increasing its availability for abyssal DFs.

5.3 Chapter 4: Gut microbiota associated with increases in deposit feeder trophic position with depth from shallow reefs to the abyssal plain

In this chapter, I characterized the trophic positions and gut microbiota of DFs across a ~4700 m depth range, from a shallow reef to the abyssal plain, to examine the impact of food supply on trophic ecology in the deep sea. Comparing echinoids and holothurians from four sites around Hawai‘i (Table 4.1, Fig. 4.1), I found a logarithmic increase in trophic position following a shift from primary to secondary consumption (Fig. 4.2). This increase occurred within the first 500 m of depth, after which DF trophic position stayed around 3 despite interspecific variation. The increase in trophic position correlated negatively with estimated particulate organic carbon (POC) flux to each DF’s depth (Fig. 4.2), indicating it may be an adaptation to the decreasing food supply available to DFs below the euphotic zone.

Unlike trophic position, gut microbiome composition changed continuously throughout the depth range (Fig. 4.5). While Proteobacteria were dominant in all depths (Fig. 4.4), there was a shift with depth away from the relative abundance of certain groups including the phyla Cyanobacteria and Firmicutes and towards the abundance of other groups including the phyla

Actinobacteria, Chloroflexi, and Dada bacteria, and the family Nitrosopumilaceae (Fig. 4.6). The decrease in Cyanobacteria mirrors the declining POC flux, supporting my use of Cyanobacteria reads as a marker of consumption of fresh detritus in Chapter 3. Once again, Nitrosopumilaceae appear to be important members of the microbial community in deep-sea sediments and DF gut contents.

In addition to the ^{15}N analysis as performed in Chapters 2 and 3, I used $\delta^{13}\text{C}$ fingerprinting of essential amino acids (EAAs) to track changes in the contribution of different potential endmembers to DF diet with depth. Unexpectedly, most of my specimens fell outside the range of values of endmembers as characterized by Larsen et al. (2013): bacteria, fungi, seagrass, microalgae, macroalgae, and terrestrial plants (Fig. 4.3). While bacteria and fungi overlapped with the shallowest DFs in Principle Component Analysis (PCA) space (Fig. 4.3), many of the deep-sea individuals had EAA $\delta^{13}\text{C}$ values lower than any of the expected endmembers. As in Chapter 2, I suggest that additional endmember isotope analysis is needed to apply these analyses, which were developed in shallow water ecosystems, to the deep sea. Chemoautotrophic archaea, such as the Nitrosopumilaceae, that were increasingly abundant in DF gut microbiota with depth, may have distinct $\delta^{15}\text{N}_{\text{SAA}}$ and $\delta^{13}\text{C}_{\text{EAA}}$ values that could be used to quantify their contributions to deep-sea food webs.

5.4 Synthesis and future directions

When examining all three data chapters together, a few overarching conclusions emerge. First, the supply of POM to the deep sea is not homogenous. We can distinguish different particle sizes as captured with sediment traps versus in situ filtration, and their differing $\delta^{15}\text{N}_{\text{SAA}}$ values illuminate two distinct detrital food sources for benthic DFs: a large, fast-sinking fraction that is well-represented in sediment traps, and a small, slowly-sinking, and heavily reworked fraction that is missed by traps. Both detrital sources are consumed by abyssal DFs in both high- and low-flux sites, so characterizing flux using only sediment traps ignores a fraction of POM that is important to benthic food webs. Niche partitioning on the basis of mobility and particle selectivity allows some DFs to locate and consume seasonal pulses of fresh phytodetritus, while others are more reliant on the small and recalcitrant particles.

There were some similarities in the composition of microbial communities associated with all three detritus types (filtered particles, sediments, and DF gut contents). At the phylum level, Proteobacteria dominated most samples, although the lower taxonomic classifications within the phylum differed (Fig. 2.4, 3.4, 4.4). The other taxon that appeared most consistently was Nitrosopumilaceae, the ammonia-oxidizing archaea. Nitrosopumilaceae have previously been noted as nitrifiers in the upper water column (Ingalls et al. 2006; Church et al. 2010) and in abyssal sediments (Park et al. 2014; Hollingsworth et al. 2021) in the Pacific, so their presence in these samples is not unexpected. However, what was unexpected was the prominent role they appear to play in all three contexts. In the upper water column at Station ALOHA, their abundance was associated with a region of high heterotrophic reworking. On the other hand, Nitrosopumilaceae relative abundance increased in sediments and gut contents with depth despite the decreasing POC flux. Ammonia-oxidizing archaea are typically the dominant nitrifiers in oligotrophic waters and sediments, being able to utilize lower concentrations of ammonia than bacteria (Ward 2008; Martens-Habbena et al. 2009). Whether or not members of this family act as gut-specific symbionts, their dominance in the most food-limited deep-sea ecosystems suggests their transformations of organic material affect the detritus consumed by DFs that survive on low, poor-quality food.

My ability to quantify the role of archaea such as Nitrosopumilaceae in deep-sea food webs was limited due to a lack of information on their isotopic effects. No studies have quantified the $\delta^{13}\text{C}_{\text{EAA}}$ fractionation associated with archaeal chemoautotrophy, although (Könneke et al. 2012) showed that Nitrosopumilaceae deplete bulk ^{13}C by almost 20%. Based on their distinct amino acid synthesis pathways (Wright and Lehtovirta-Morley 2023), it is possible that ammonia-oxidizing and other chemoautotrophic archaea have distinct $\delta^{13}\text{C}$ EAA fingerprints from heterotrophic bacteria, which have previously been used as the sole microbial endmember (Larsen et al. 2013). It is also possible that deep-sea heterotrophic and chemoautotrophic bacteria, the vast majority of which have never been grown in cultures, have unique fingerprints as well. While deep-sea archaea are difficult to grow in culture, characterizing the amino acid $\delta^{13}\text{C}$ and $\delta^{15}\text{N}$ values of terrestrial Nitrosopumilaceae and other ammonia oxidizers will be an important step in determining whether they have unique isotopic signatures that could be used to trace their contributions to deep-sea food webs. My sediment trap, particle, and DF tissue samples that fell outside the $\delta^{15}\text{N}_{\text{SAA}}$ and $\delta^{13}\text{C}_{\text{EAA}}$ ranges of known endmembers indicate a need

for an expansion of endmembers in order to utilize AA-CSIA to its fullest extent in the deep sea. For example, if ammonia-oxidizing archaea have higher $\delta^{15}\text{N}_{\text{Ala}}$ values than heterotrophic bacteria, their presence could contribute to the deep sediment trap samples that I found did not match any of the endmembers used in Doherty et al. (2021) (Fig. 2.3a).

Another step to better understand microbe-DF interactions in the deep sea would be to capture DFs alive and perform controlled feeding experiments on them. Abyssal DFs collected with Remotely Operated Vehicles (ROVs), as they were in this study, are not generally retrieved alive, likely due to the extreme changes in temperature and pressure. However, shallower DFs collected from just below the euphotic zone and below 500m, where the greatest trophic changes were observed, may be more viable. I would like to collect deep-sea DFs and maintain them in aquaria as in Wilson et al. (2013). Once the animals are acclimated, their core microbiome could be determined by feeding them different types of sterilized detritus. Microbial taxa that are enriched following the consumption of sterilized, high-quality food could be identified as opportunistic microbiota taking advantage of fresh phytodetritus consumed by those species able to access it. Those enriched following the consumption of highly degraded detritus, on the other hand, could be taxa that help DFs survive on low-quality food they consume between pulses of fresh material. Furthermore, metagenomics and metatranscriptomics may reveal the specific metabolic pathways that certain microbial taxa use to break down recalcitrant material. For example, gut taxa identified as degrading chitin or cellulose, materials that animals cannot digest on their own, could be key microbiota enabling DFs to consume more nutrients from phytodetritus (Peoples et al. 2024).

Finally, I would like to extend these analyses to other deep-sea detrital food webs, namely those in the pelagic realm. Pelagic detritivores include zooplankton that repackage small, slowly-sinking particles into fast-sinking fecal pellets (Turner 2015). Giant larvaceans also collect particles on their mucus houses, which are discarded multiple times per day and sink quickly into the deep benthos (Davoll and Youngbluth 1990; Vargas et al. 2002). I would like to use metagenomics and metatranscriptomics, in combination with further 16S rRNA community barcoding, to characterize the identity and functions of microbial communities associated with larvacean and other zooplankton gut tracts, fecal pellets, and discarded houses. Differences in these communities may reveal how specific microbial taxa and communities aid in the zooplankton-mediated export of surface carbon and fuel the deep-sea benthos.

APPENDIX A

Table S1. ASVs with significant ($p < 0.05$) linear relationships with $\delta^{15}\text{N}$ values of source amino acids. Taxonomy shown was assigned using the Silva 138.1 prokaryotic SSU taxonomic training data (McLaren and Callahan 2021); “NA” indicates taxon unknown.

Phylum	Class	Order	Family	Genus	R ²	P
Euryarchaeota	Thermoplasmata	Marine Group II	NA	NA	0.649762	0.005
Euryarchaeota	Thermoplasmata	Marine Group III	NA	NA	0.490835	0.036
Nitrospinae	Nitrospina	Nitrospinales	Nitrospinaceae	LS-NOB	0.623400	0.005
Proteobacteria	Alphaproteobacteria	SAR11 clade	Clade II	NA	0.550543	0.007
Proteobacteria	Alphaproteobacteria	SAR11 clade	Clade II	NA	0.479082	0.019
Proteobacteria	Alphaproteobacteria	SAR11 clade	NA	NA	0.661245	0.004
Proteobacteria	Alphaproteobacteria	SAR11 clade	NA	NA	0.413056	0.047
Proteobacteria	Alphaproteobacteria	SAR11 clade	NA	NA	0.594870	0.006
Thaumarchaeota	Nitrososphaeria	Nitrosopumilales	Nitrosopumilaceae	NA	0.473214	0.019
Thaumarchaeota	Nitrososphaeria	Nitrosopumilales	Nitrosopumilaceae	NA	0.473330	0.021
Thaumarchaeota	Nitrososphaeria	Nitrosopumilales	Nitrosopumilaceae	NA	0.484479	0.019
Thaumarchaeota	Nitrososphaeria	Nitrosopumilales	Nitrosopumilaceae	NA	0.487312	0.018
Thaumarchaeota	Nitrososphaeria	Nitrosopumilales	Nitrosopumilaceae	NA	0.463552	0.025
Thaumarchaeota	Nitrososphaeria	Nitrosopumilales	Nitrosopumilaceae	NA	0.482778	0.019
Thaumarchaeota	Nitrososphaeria	Nitrosopumilales	Nitrosopumilaceae	NA	0.524742	0.014
Thaumarchaeota	Nitrososphaeria	Nitrosopumilales	Nitrosopumilaceae	NA	0.512159	0.016
Thaumarchaeota	Nitrososphaeria	Nitrosopumilales	Nitrosopumilaceae	NA	0.480043	0.020
Thaumarchaeota	Nitrososphaeria	Nitrosopumilales	Nitrosopumilaceae	NA	0.511774	0.015
Thaumarchaeota	Nitrososphaeria	Nitrosopumilales	Nitrosopumilaceae	NA	0.483227	0.020
Thaumarchaeota	Nitrososphaeria	Nitrosopumilales	Nitrosopumilaceae	NA	0.495907	0.018
Thaumarchaeota	Nitrososphaeria	Nitrosopumilales	Nitrosopumilaceae	NA	0.483025	0.019
Thaumarchaeota	Nitrososphaeria	Nitrosopumilales	Nitrosopumilaceae	NA	0.468326	0.024
Thaumarchaeota	Nitrososphaeria	Nitrosopumilales	Nitrosopumilaceae	NA	0.476938	0.020
Thaumarchaeota	Nitrososphaeria	Nitrosopumilales	Nitrosopumilaceae	NA	0.461502	0.024
Thaumarchaeota	Nitrososphaeria	Nitrosopumilales	Nitrosopumilaceae	NA	0.502540	0.015
Thaumarchaeota	Nitrososphaeria	Nitrosopumilales	Nitrosopumilaceae	NA	0.500988	0.017
Thaumarchaeota	Nitrososphaeria	Nitrosopumilales	Nitrosopumilaceae	NA	0.487219	0.019
Thaumarchaeota	Nitrososphaeria	Nitrosopumilales	Nitrosopumilaceae	NA	0.432853	0.039
Thaumarchaeota	Nitrososphaeria	Nitrosopumilales	Nitrosopumilaceae	NA	0.463348	0.024
Thaumarchaeota	Nitrososphaeria	Nitrosopumilales	Nitrosopumilaceae	NA	0.477300	0.019
Thaumarchaeota	Nitrososphaeria	Nitrosopumilales	Nitrosopumilaceae	NA	0.496419	0.016
Thaumarchaeota	Nitrososphaeria	Nitrosopumilales	Nitrosopumilaceae	NA	0.460802	0.025
Thaumarchaeota	Nitrososphaeria	Nitrosopumilales	Nitrosopumilaceae	NA	0.526137	0.015
Thaumarchaeota	Nitrososphaeria	Nitrosopumilales	Nitrosopumilaceae	NA	0.488683	0.019
Thaumarchaeota	Nitrososphaeria	Nitrosopumilales	Nitrosopumilaceae	NA	0.509615	0.015
Thaumarchaeota	Nitrososphaeria	Nitrosopumilales	Nitrosopumilaceae	NA	0.499644	0.016

Thaumarchaeota	Nitrososphaeria	Nitrosopumilales	Nitrosopumilaceae	NA	0.448044	0.029
Thaumarchaeota	Nitrososphaeria	Nitrosopumilales	Nitrosopumilaceae	NA	0.461012	0.027
Thaumarchaeota	Nitrososphaeria	Nitrosopumilales	Nitrosopumilaceae	NA	0.497367	0.018
Thaumarchaeota	Nitrososphaeria	Nitrosopumilales	Nitrosopumilaceae	NA	0.499275	0.016
Thaumarchaeota	Nitrososphaeria	Nitrosopumilales	Nitrosopumilaceae	NA	0.512689	0.015
Thaumarchaeota	Nitrososphaeria	Nitrosopumilales	Nitrosopumilaceae	NA	0.463039	0.030
Thaumarchaeota	Nitrososphaeria	Nitrosopumilales	Nitrosopumilaceae	NA	0.539029	0.010
Thaumarchaeota	Nitrososphaeria	Nitrosopumilales	Nitrosopumilaceae	NA	0.513770	0.015
Thaumarchaeota	Nitrososphaeria	Nitrosopumilales	Nitrosopumilaceae	NA	0.589621	0.005
Thaumarchaeota	Nitrososphaeria	Nitrosopumilales	Nitrosopumilaceae	NA	0.490932	0.019
Thaumarchaeota	Nitrososphaeria	Nitrosopumilales	Nitrosopumilaceae	NA	0.523183	0.013
Thaumarchaeota	Nitrososphaeria	Nitrosopumilales	Nitrosopumilaceae	NA	0.505305	0.017
Thaumarchaeota	Nitrososphaeria	Nitrosopumilales	Nitrosopumilaceae	NA	0.475114	0.019
Thaumarchaeota	Nitrososphaeria	Nitrosopumilales	Nitrosopumilaceae	NA	0.624182	0.005
Thaumarchaeota	Nitrososphaeria	Nitrosopumilales	Nitrosopumilaceae	NA	0.515351	0.015
Thaumarchaeota	Nitrososphaeria	Nitrosopumilales	Nitrosopumilaceae	NA	0.644124	0.004
Thaumarchaeota	Nitrososphaeria	Nitrosopumilales	Nitrosopumilaceae	NA	0.493779	0.016
Thaumarchaeota	Nitrososphaeria	Nitrosopumilales	Nitrosopumilaceae	NA	0.549777	0.010
Thaumarchaeota	Nitrososphaeria	Nitrosopumilales	Nitrosopumilaceae	NA	0.394628	0.045
Thaumarchaeota	Nitrososphaeria	Nitrosopumilales	Nitrosopumilaceae	NA	0.486290	0.019
Thaumarchaeota	Nitrososphaeria	Nitrosopumilales	Nitrosopumilaceae	NA	0.476611	0.021
Verrucomicrobia	Verrucomicrobiae	Arctic97B-4 Marine Group	NA	NA	0.438842	0.033

APPENDIX B

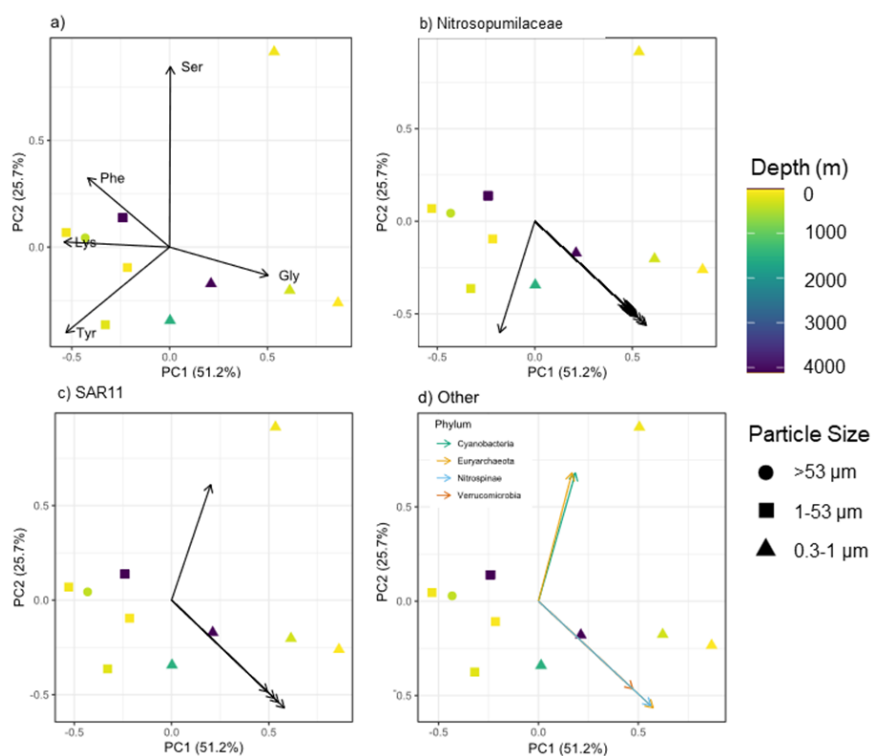


Figure S1. Probabilistic PCA of particles incorporating the $\delta^{15}\text{N}_{\text{SAA}}$ values, with vectors indicating **a)** individual source amino acids or **b-d)** abundance of ASVs significantly ($p < 0.05$) correlated with the isotope-based Principle Components. Plots are split up to show vectors belonging to significant ASVs assigned to **b)** the Nitrosopumilaceae family ($n = 49$), **c)** the SAR11 clade ($n = 5$), and **d)** other taxa ($n = 6$), with colors indicating Phylum. Points are colored by depth and shapes indicate particle size.

REFERENCES

- Abramson, L., C. Lee, Z. Liu, S. G. Wakeham, and J. Szlosek. 2010. Exchange between suspended and sinking particles in the northwest Mediterranean as inferred from the organic composition of *in situ* pump and sediment trap samples. *Limnol. Oceanogr.* 55: 725–739. doi:10.4319/lo.2010.55.2.0725
- Allredge, A. 1998. The carbon, nitrogen and mass content of marine snow as a function of aggregate size. *Deep Sea Res. Part I* 45: 529–541. doi:10.1016/S0967-0637(97)00048-4
- Allredge, A. L. 2000. Interstitial dissolved organic carbon (DOC) concentrations within sinking marine aggregates and their potential contribution to carbon flux. *Limnol. Oceanogr.* 45: 1245–1253. doi:10.4319/lo.2000.45.6.1245
- Altabet, M. A., W. G. Deuser, S. Honjo, and C. Stienen. 1991. Seasonal and depth-related changes in the source of sinking particles in the North Atlantic. *Nature* 354: 136–139. doi:10.1038/354136a0
- Amaro, T., R. Danovaro, Y. Matsui, E. Rastelli, G. A. Wolff, and H. Nomaki. 2019. Possible links between holothurian lipid compositions and differences in organic matter (OM) supply at the western Pacific abyssal plains. *Deep Sea Res. Part I* 152: 103085. doi:10.1016/j.dsr.2019.103085
- Amaro, T., G. M. Luna, R. Danovaro, D. S. M. Billett, and M. R. Cunha. 2012. High prokaryotic biodiversity associated with gut contents of the holothurian *Molpadia musculus* from the Nazaré Canyon (NE Atlantic). *Deep Sea Res. Part I* 63: 82–90. doi:10.1016/j.dsr.2012.01.007
- Amaro, T., H. Witte, G. J. Herndl, M. R. Cunha, and D. S. M. Billett. 2009. Deep-sea bacterial communities in sediments and guts of deposit-feeding holothurians in Portuguese canyons (NE Atlantic). *Deep Sea Res. Part I* 56: 1834–1843. doi:10.1016/j.dsr.2009.05.014
- Aronson, H. S., A. J. Zellmer, and S. K. Goffredi. 2016. The Specific and Exclusive Microbiome of the Deep-Sea Bone-Eating Snail, *Rubyspira osteovora*. *FEMS Microbiol. Ecol.* fiw250. doi:10.1093/femsec/fiw250
- Azam, F. 1998. Microbial Control of Oceanic Carbon Flux: The Plot Thickens. *Science* 280:

- 694–696. doi:10.1126/science.280.5364.694
- Bartlett, D. H. 1999. Microbial adaptations to the psychrosphere/piezosphere. *J Mol. Microbiol. Biotechnol.* 1: 93–100.
- Bayer, K., M. T. Jahn, B. M. Slaby, L. Moitinho-Silva, and U. Hentschel. 2018. Marine Sponges as Chloroflexi Hot Spots: Genomic Insights and High-Resolution Visualization of an Abundant and Diverse Symbiotic Clade K.G. Lloyd [ed.]. *mSystems* 3: 10.1128/msystems.00150-18. doi:10.1128/msystems.00150-18
- Beaulieu, S. 2002. Accumulation and Fate of Phytodetritus on the Sea Floor, p. 171–232. *In* R. Atkinson and M. Barnes [eds.], *Oceanogr. Mar. Biol.* Volume 40. CRC Press.
- Begmatov, S. and others. 2021. Microbial Communities Involved in Methane, Sulfur, and Nitrogen Cycling in the Sediments of the Barents Sea. *Microorganisms* 9: 2362. doi:10.3390/microorganisms9112362
- Beman, J. M., B. N. Popp, and S. E. Alford. 2012. Quantification of ammonia oxidation rates and ammonia-oxidizing archaea and bacteria at high resolution in the Gulf of California and eastern tropical North Pacific Ocean. *Limnol. Oceanogr.* 57: 711–726. doi:10.4319/lo.2012.57.3.0711
- Beman, J. M., B. N. Popp, and C. A. Francis. 2008. Molecular and biogeochemical evidence for ammonia oxidation by marine Crenarchaeota in the Gulf of California. *ISME J* 2: 429–441. doi:10.1038/ismej.2007.118
- Benson, A. K. and others. 2010. Individuality in gut microbiota composition is a complex polygenic trait shaped by multiple environmental and host genetic factors. *Proc. Natl. Acad. Sci. U.S.A.* 107: 18933–18938. doi:10.1073/pnas.1007028107
- Billett, D. S. M., B. J. Bett, W. D. K. Reid, B. Boorman, and I. G. Priede. 2010. Long-term change in the abyssal NE Atlantic: The ‘Amperima Event’ revisited. *Deep Sea Res. Part II* 57: 1406–1417. doi:10.1016/j.dsr2.2009.02.001
- Bishop, J. K. B., P. J. Lam, and T. J. Wood. 2012. Getting good particles: Accurate sampling of particles by large volume in-situ filtration. *Limnol. Oceanogr. Methods* 10: 681–710. doi:10.4319/lom.2012.10.681
- Boeuf, D., B. R. Edwards, J. M. Eppley, and others. 2019. Biological composition and microbial dynamics of sinking particulate organic matter at abyssal depths in the oligotrophic open ocean. *Proc. Natl. Acad. Sci. U.S.A.* 116: 11824–11832. doi:10.1073/pnas.1903080116

- Bochdansky, A. B., M. A. Clouse, and G. J. Herndl. 2017. Eukaryotic microbes, principally fungi and labyrinthulomycetes, dominate biomass on bathypelagic marine snow. *ISME J* 11: 362–373. doi:10.1038/ismej.2016.113
- Boucher, D. H., S. James, and K. H. Keeler. 1982. The Ecology of Mutualism. *Annu. Rev. Ecol. Syst.* 13: 315–347. doi:10.1146/annurev.es.13.110182.001531
- Bryant, J. A., F. O. Aylward, J. M. Eppley, D. M. Karl, M. J. Church, and E. F. DeLong. 2016. Wind and sunlight shape microbial diversity in surface waters of the North Pacific Subtropical Gyre. *ISME J* 10: 1308–1322. doi:10.1038/ismej.2015.221
- Buesseler, K. O. 1991. Do upper-ocean sediment traps provide an accurate record of particle flux? *Nature* 353: 420–423. doi:10.1038/353420a0
- Buesseler, K. O., D. K. Steinberg, A. F. Michaels, R. J. Johnson, J. E. Andrews, J. R. Valdes, and J. F. Price. 2000. A comparison of the quantity and composition of material caught in a neutrally buoyant versus surface-tethered sediment trap. *Deep Sea Res. Part I* 47: 277–294. doi:10.1016/S0967-0637(99)00056-4
- Buesseler, K. O. and others. 2006. An assessment of particulate organic carbon to thorium-234 ratios in the ocean and their impact on the application of ^{234}Th as a POC flux proxy. *Mar. Chem.* 100: 213–233. doi:10.1016/j.marchem.2005.10.013
- Buesseler, K. O. and others. 2007. Revisiting Carbon Flux Through the Ocean’s Twilight Zone. *Science* 316: 567–570. doi:10.1126/science.1137959
- Buesseler, K. O., D. K. Steinberg, A. F. Michaels, R. J. Johnson, J. E. Andrews, J. R. Valdes, and J. F. Price. 2000. A comparison of the quantity and composition of material caught in a neutrally buoyant versus surface-tethered sediment trap. *Deep Sea Res. Part I* 47: 277–294. doi:10.1016/S0967-0637(99)00056-4
- Callahan, B. J., P. J. McMurdie, M. J. Rosen, A. W. Han, A. J. A. Johnson, and S. P. Holmes. 2016. DADA2: High-resolution sample inference from Illumina amplicon data. *Nat. Methods* 13: 581–583. doi:10.1038/nmeth.3869
- Casciotti, K. L., T. W. Trull, D. M. Glover, and D. Davies. 2008. Constraints on nitrogen cycling at the subtropical North Pacific Station ALOHA from isotopic measurements of nitrate and particulate nitrogen. *Deep Sea Res. Part II* 55: 1661–1672. doi:10.1016/j.dsr2.2008.04.017
- Chaston, J., and H. Goodrich-Blair. 2010. Common trends in mutualism revealed by model

- associations between invertebrates and bacteria. *FEMS Microbiol Rev* 34: 41–58.
doi:10.1111/j.1574-6976.2009.00193.x
- Chikaraishi, Y. and others. 2009. Determination of aquatic food-web structure based on compound-specific nitrogen isotopic composition of amino acids: Trophic level estimation by amino acid $\delta^{15}\text{N}$. *Limnol. Oceanogr. Methods* 7: 740–750.
doi:10.4319/lom.2009.7.740
- Chikaraishi, Y., Y. Kashiyama, N. Ogawa, H. Kitazato, and N. Ohkouchi. 2007. Metabolic control of nitrogen isotope composition of amino acids in macroalgae and gastropods: implications for aquatic food web studies. *Mar. Ecol. Prog. Ser.* 342: 85–90.
doi:10.3354/meps342085
- Chimienti, G., R. Aguilar, A. V. Gebruk, and F. Mastrototaro. 2019. Distribution and swimming ability of the deep-sea holothuroid *Penipidia ludwigi* (Holothuroidea: Elasipodida: Elpidiidae). *Mar. Biodiv.* 49: 2369–2380. doi:10.1007/s12526-019-00973-9
- Chi, X. and others. 2021. Tackling the jelly web: Trophic ecology of gelatinous zooplankton in oceanic food webs of the eastern tropical Atlantic assessed by stable isotope analysis. *Limnol Oceanogr* 66: 289–305. doi:10.1002/lno.11605
- Church, M. J., B. Wai, D. M. Karl, and E. F. DeLong. 2010. Abundances of crenarchaeal *amoA* genes and transcripts in the Pacific Ocean. *Environ. Microbiol.* 12: 679–688.
doi:10.1111/j.1462-2920.2009.02108.x
- Comstock, J. and others. 2024. Marine particle size-fractionation indicates organic matter is processed by differing microbial communities on depth-specific particles. *ISME Communications* 4: ycae090. doi:10.1093/ismeco/ycae090
- Corinaldesi, C. 2015. New perspectives in benthic deep-sea microbial ecology. *Front. Mar. Sci.* 2. doi:10.3389/fmars.2015.00017
- Cornelius, N., and A. J. Gooday. 2004. ‘Live’ (stained) deep-sea benthic foraminiferans in the western Weddell Sea: trends in abundance, diversity and taxonomic composition along a depth transect. *Deep Sea Res. Part II* 51: 1571–1602. doi:10.1016/j.dsr2.2004.06.024
- Datta, M. S., E. Sliwerska, J. Gore, M. F. Polz, and O. X. Cordero. 2016. Microbial interactions lead to rapid micro-scale successions on model marine particles. *Nat. Commun/* 7: 11965. doi:10.1038/ncomms11965
- Dauwe, B., J. J. Middelburg, P. M. J. Herman, and C. H. R. Heip. 1999. Linking diagenetic

- alteration of amino acids and bulk organic matter reactivity. *Limnol. Oceanogr.* 44: 1809–1814. doi:10.4319/lo.1999.44.7.1809
- Davoll, P. J., and M. J. Youngbluth. 1990. Heterotrophic activity on appendicularian (Tunicata: Appendicularia) houses in mesopelagic regions and their potential contribution to particle flux. *Deep Sea Res. Part I* 37: 285–294. doi:10.1016/0198-0149(90)90128-I
- De Corte, D. and others. 2018. Metagenomic insights into zooplankton-associated bacterial communities. *Environ. Microbiol.* 20: 492–505. doi:10.1111/1462-2920.13944
- Décima, M., and M. Landry. 2020. Resilience of plankton trophic structure to an eddy-stimulated diatom bloom in the North Pacific Subtropical Gyre. *Mar. Ecol. Prog. Ser.* 643: 33–48. doi:10.3354/meps13333
- DeLong, E. F., C. M. Preston, T. Mincer, and others. 2006. Community genomics among stratified microbial assemblages in the ocean’s interior. *Science* 311: 496–503. doi:10.1126/science.1120250
- Deming, J. W., P. S. Tabor, and R. R. Colwell. 1981. Barophilic growth of bacteria from intestinal tracts of deep-sea invertebrates. *Microb. Ecol.* 7: 85–94. doi:10.1007/BF02010480
- Deming, J. W., and S. D. Carpenter. 2008. Factors influencing benthic bacterial abundance, biomass, and activity on the northern continental margin and deep basin of the Gulf of Mexico. *Deep Sea Res. Part II* 55: 2597–2606. doi:10.1016/j.dsr2.2008.07.009
- De La Rocha, C. L., and U. Passow. 2007. Factors influencing the sinking of POC and the efficiency of the biological carbon pump. *Deep Sea Res. Part II* 54: 639–658. doi:10.1016/j.dsr2.2007.01.004
- diCenzo, G. C., Y. Yang, J. P. W. Young, and N. Kuzmanović. 2024. Refining the taxonomy of the order Hyphomicrobiales (Rhizobiales) based on whole genome comparisons of over 130 type strains. *Int. J. Syst. Evol. Microbiol.* 74. doi:10.1099/ijsem.0.006328
- Dick, G. J. 2019. The microbiomes of deep-sea hydrothermal vents: distributed globally, shaped locally. *Nat. Rev. Microbiol.* 17: 271–283. doi:10.1038/s41579-019-0160-2
- Doherty, S. C., A. E. Maas, D. K. Steinberg, B. N. Popp, and H. G. Close. 2021. Distinguishing zooplankton fecal pellets as a component of the biological pump using compound-specific isotope analysis of amino acids. *Limnol. Oceanogr.* 66: 2827–2841. doi:10.1002/lno.11793

- Dore, J. E., and D. M. Karl. 1996. Nitrification in the euphotic zone as a source for nitrite, nitrate, and nitrous oxide at Station ALOHA. *Limnol. Oceanogr.* 41: 1619–1628. doi:10.4319/lo.1996.41.8.1619
- Dore, J. E., B. N. Popp, D. M. Karl, and F. J. Sansone. 1998. A large source of atmospheric nitrous oxide from subtropical North Pacific surface waters. *Nature* 396: 63–66. doi:10.1038/23921.
- Drazen, J. C., C. F. Phleger, M. A. Guest, and P. D. Nichols. 2008. Lipid, sterols and fatty acid composition of abyssal holothurians and ophiuroids from the North-East Pacific Ocean: Food web implications. *Comp. Biochem. Physiol., Part B:Biochem. Mol. Biol.* 151: 79–87. doi:10.1016/j.cbpb.2008.05.013
- Dubilier, N., C. Bergin, and C. Lott. 2008. Symbiotic diversity in marine animals: the art of harnessing chemosynthesis. *Nat. Rev. Microbiol.* 6: 725–740. doi:10.1038/nrmicro1992
- Durden, J. M., B. J. Bett, C. L. Huffard, C. Pebody, H. A. Ruhl, and K. L. Smith. 2020. Response of deep-sea deposit-feeders to detrital inputs: A comparison of two abyssal time-series sites. *Deep Sea Res. Part II* 173: 104677. doi:10.1016/j.dsr2.2019.104677
- Duret, M. T., R. S. Lampitt, and P. Lam. 2019. Prokaryotic niche partitioning between suspended and sinking marine particles. *Environ. Microbiol. Rep.* 11: 386–400. doi:10.1111/1758-2229.12692
- Durkin, C. A., K. O. Buesseler, I. Cetinić, M. L. Estapa, R. P. Kelly, and M. Omand. 2021. A Visual Tour of Carbon Export by Sinking Particles. *Global Biogeochem. Cycles* 35: e2021GB006985. doi:10.1029/2021GB006985
- FitzGeorge-Balfour, T., D. S. M. Billett, G. A. Wolff, A. Thompson, and P. A. Tyler. 2010. Phytopigments as biomarkers of selectivity in abyssal holothurians; interspecific differences in response to a changing food supply. *Deep Sea Res. Part II* 57: 1418–1428. doi:10.1016/j.dsr2.2010.01.013
- Frigstad, H., S. A. Henson, S. E. Hartman, A. M. Omar, E. Jeansson, H. Cole, C. Pebody, and R. S. Lampitt. 2015. Links between surface productivity and deep ocean particle flux at the Porcupine Abyssal Plain sustained observatory. *Biogeosciences* 12: 5885–5897. doi:10.5194/bg-12-5885-2015
- Gao, F., Y. Zhang, P. Wu, M. Chen, L. He, Q. Xu, and A. Wang. 2022. Bacterial community

- composition in gut content and ambient sediment of two tropical wild sea cucumbers (*Holothuria atra* and *H. leucospilota*). *J. Ocean. Limnol.* 40: 360–372.
doi:10.1007/s00343-021-1001-5
- Gebruk, A., and A. Kremenetskaia. 2024. Swimming sea cucumbers, p. 351–359. *In The World of Sea Cucumbers*. Elsevier.
- Gibson, R. N., M. Barnes, and R. J. A. Atkinson, eds. 2002. A riot of species in an environmental calm: the paradox of the species-rich deep-sea floor, p. 319–320. *In Oceanography and Marine Biology, An Annual Review, Volume 40*. CRC Press.
- Ginger, M. L. and others. 2001. Organic matter assimilation and selective feeding by holothurians in the deep sea: some observations and comments. *Prog. Oceanogr.* 50: 407–421. doi:10.1016/S0079-6611(01)00063-5
- Gloeckler, K., C. A. Choy, C. C. S. Hannides, H. G. Close, E. Goetze, B. N. Popp, and J. C. Drazen. 2018. Stable isotope analysis of micronekton around Hawaii reveals suspended particles are an important nutritional source in the lower mesopelagic and upper bathypelagic zones: Suspended particles as a mesopelagic food source. *Limnol. Oceanogr.* 63: 1168–1180. doi:10.1002/lno.10762
- Gooday, A. J., and J. A. Hughes. 2002. Foraminifera associated with phytodetritus deposits at a bathyal site in the northern Rockall Trough (NE Atlantic): seasonal contrasts and a comparison of stained and dead assemblages. *Mar. Micropaleontol.* 46: 83–110.
doi:10.1016/S0377-8398(02)00050-6
- Grabowski, E., R. M. Letelier, E. A. Laws, and D. M. Karl. 2019. Coupling carbon and energy fluxes in the North Pacific Subtropical Gyre. *Nat. Commun.* 10: 1895.
doi:10.1038/s41467-019-09772-z
- Graham, E. D., and B. J. Tully. 2021. Marine Dada bacteria exhibit genome streamlining and phototrophy-driven niche partitioning. *The ISME Journal* 15: 1248–1256.
doi:10.1038/s41396-020-00834-5
- Grossart, H.-P., T. Kiørboe, K. Tang, and H. Ploug. 2003. Bacterial Colonization of Particles: Growth and Interactions. *Appl Environ Microbiol* 69: 3500–3509.
doi:10.1128/AEM.69.6.3500-3509.2003
- Guidi, L., G. A. Jackson, L. Stemmann, J. C. Miquel, M. Picheral, and G. Gorsky. 2008.

- Relationship between particle size distribution and flux in the mesopelagic zone. *Deep Sea Res. Part I* 55: 1364–1374. doi:10.1016/j.dsr.2008.05.014
- Guy-Haim, T., N. Stern, and G. Sisma-Ventura. 2022. Trophic Ecology of Deep-Sea Megafauna in the Ultra-Oligotrophic Southeastern Mediterranean Sea. *Front. Mar. Sci.* 9: 857179. doi:10.3389/fmars.2022.857179
- Haber, M., I. Burgsdorf, K. M. Handley, M. Rubin-Blum, and L. Steindler. 2021. Genomic Insights Into the Lifestyles of Thaumarchaeota Inside Sponges. *Front. Microbiol.* 11: 622824. doi:10.3389/fmicb.2020.622824
- Hakim, J. A., H. Koo, R. Kumar, E. J. Lefkowitz, C. D. Morrow, M. L. Powell, S. A. Watts, and A. K. Bej. 2016. The gut microbiome of the sea urchin, *Lytechinus variegatus*, from its natural habitat demonstrates selective attributes of microbial taxa and predictive metabolic profiles J. Marchesi [ed.]. *FEMS Microbiology Ecology* 92: fiw146. doi:10.1093/femsec/fiw146
- Hallam, S. J., T. J. Mincer, C. Schleper, C. M. Preston, K. Roberts, P. M. Richardson, and E. F. DeLong. 2006. Pathways of Carbon Assimilation and Ammonia Oxidation Suggested by Environmental Genomic Analyses of Marine Crenarchaeota S. Sievert [ed.]. *PLoS Biol* 4: e95. doi:10.1371/journal.pbio.0040095
- Hannides, C. C. S., B. N. Popp, C. A. Choy, and J. C. Drazen. 2013. Midwater zooplankton and suspended particle dynamics in the North Pacific Subtropical Gyre: A stable isotope perspective. *Limnol. Oceanogr.* 58: 1931–1946. doi:10.4319/lo.2013.58.6.1931
- Hannides, C. C. S., B. N. Popp, M. R. Landry, and B. S. Graham. 2009. Quantification of zooplankton trophic position in the North Pacific Subtropical Gyre using stable nitrogen isotopes. *Limnol. Oceanogr.* 54: 50–61. doi:10.4319/lo.2009.54.1.0050
- Hannides, C. C. S. and others. 2020. Seasonal dynamics of midwater zooplankton and relation to particle cycling in the North Pacific Subtropical Gyre. *Progr. Oceanogr.* 182: 102266. doi:10.1016/j.pocean.2020.102266
- Hatzenpichler, R. 2012. Diversity, Physiology, and Niche Differentiation of Ammonia-Oxidizing Archaea. *Appl Environ Microbiol* 78: 7501–7510. doi:10.1128/AEM.01960-12
- He, L.-S., P.-W. Zhang, J.-M. Huang, F.-C. Zhu, A. Danchin, and Y. Wang. 2018. The Enigmatic Genome of an Obligate Ancient Spiroplasma Symbiont in a Hadal Holothurian H.L. Drake [ed.]. *Appl. Environ. Microbiol.* 84: e01965-17. doi:10.1128/AEM.01965-17

- Henson, S. A., R. Sanders, and E. Madsen. 2012. Global patterns in efficiency of particulate organic carbon export and transfer to the deep ocean. *Global Biogeochem. Cycles* 26: 2011GB004099. doi:10.1029/2011GB004099
- Herndl, G. J., and T. Reinthaler. 2013. Microbial control of the dark end of the biological pump. *Nature Geosci.* 6: 718–724. doi:10.1038/ngeo1921
- Hessler, R. R., and P. A. Jumars. 1974. Abyssal community analysis from replicate box cores in the central North Pacific. *Deep-Sea Res. Oceanogr. Abstr.* 21: 185–209. doi:10.1016/0011-7471(74)90058-8
- Hoffmann, K., C. Hassenrück, V. Salman-Carvalho, M. Holtappels, and C. Bienhold. 2017. Response of Bacterial Communities to Different Detritus Compositions in Arctic Deep-Sea Sediments. *Front. Microbiol.* 8. doi:10.3389/fmicb.2017.00266
- Hofmann, E. E., J. M. Klinck, and G.-A. Paffenhöfer. 1981. Concentrations and vertical fluxes of zooplankton fecal pellets on a continental shelf. *Mar. Biol.* 61: 327–335. doi:10.1007/BF00401572
- Hollingsworth, A. L., D. O. B. Jones, and C. R. Young. 2021. Spatial Variability of Abyssal Nitrifying Microbes in the North-Eastern Clarion-Clipperton Zone. *Front. Mar. Sci.* 8: 663420. doi:10.3389/fmars.2021.663420
- Honjo, S., S. J. Manganini, R. A. Krishfield, and R. Francois. 2008. Particulate organic carbon fluxes to the ocean interior and factors controlling the biological pump: A synthesis of global sediment trap programs since 1983. *Prog. Oceanogr.* 76: 217–285. doi:10.1016/j.pocean.2007.11.003
- Hoshino, T. and others. 2020. Global diversity of microbial communities in marine sediment. *Proc. Natl. Acad. Sci. U.S.A.* 117: 27587–27597. doi:10.1073/pnas.1919139117
- Huang, J. and others. 2022. *Trypoxylus dichotomus* Gut Bacteria Provides an Effective System for Bamboo Lignocellulose Degradation J. Claesen [ed.]. *Microbiol. Spectr.* 10: e02147-22. doi:10.1128/spectrum.02147-22
- Huang, Q., R. C. Sham, Y. Deng, Y. Mao, C. Wang, T. Zhang, and K. M. Y. Leung. 2020. Diversity of gut microbiomes in marine fishes is shaped by host-related factors. *Mol. Ecol.* 29: 5019–5034. doi:10.1111/mec.15699
- Huffard, C. L., L. A. Kuhnz, L. Lemon, A. D. Sherman, and K. L. Smith. 2016. Demographic

- indicators of change in a deposit-feeding abyssal holothurian community (Station M, 4000 m). *Deep Sea Res. Part I* 109: 27–39. doi:10.1016/j.dsr.2016.01.002
- Iken, K., T. Brey, U. Wand, J. Voigt, and P. Junghans. 2001. Food web structure of the benthic community at the Porcupine Abyssal Plain (NE Atlantic): a stable isotope analysis. *Prog. Oceanogr.* 50: 383–405. doi:10.1016/S0079-6611(01)00062-3
- Ingalls, A. E., S. R. Shah, R. L. Hansman, L. I. Aluwihare, G. M. Santos, E. R. M. Druffel, and A. Pearson. 2006. Quantifying archaeal community autotrophy in the mesopelagic ocean using natural radiocarbon. *Proc. Natl. Acad. Sci. U.S.A.* 103: 6442–6447. doi:10.1073/pnas.0510157103
- Jameson, B. D., S. A. Murdock, Q. Ji, C. J. Stevens, D. S. Grundle, and S. Kim Juniper. 2023. Network analysis of 16S rRNA sequences suggests microbial keystone taxa contribute to marine N₂O cycling. *Commun. Biol.* 6: 212. doi:10.1038/s42003-023-04597-5
- Johnson, N. A., J. W. Campbell, T. S. Moore, M. A. Rex, R. J. Etter, C. R. McClain, and M. D. Dowell. 2007. The relationship between the standing stock of deep-sea macrobenthos and surface production in the western North Atlantic. *Deep Sea Res. Part I* 54: 1350–1360. doi:10.1016/j.dsr.2007.04.011
- Jroundi, F., F. Martinez-Ruiz, M. L. Merroun, and M. T. Gonzalez-Muñoz. 2020. Exploring bacterial community composition in Mediterranean deep-sea sediments and their role in heavy metal accumulation. *Sci. Total Environ.* 712: 135660. doi:10.1016/j.scitotenv.2019.135660
- Jumars, P. A., L. M. Mayer, J. W. Deming, J. A. Baross, and R. A. Wheatcroft. 1990. Deep-sea deposit-feeding strategies suggested by environmental and feeding constraints. *Phil. Trans. R. Soc. Lond. A* 331: 85–101. doi:10.1098/rsta.1990.0058
- Kahru, M., R. Goericke, T. B. Kelly, and M. R. Stukel. 2020. Satellite estimation of carbon export by sinking particles in the California Current calibrated with sediment trap data. *Deep Sea Res. Part II* 173: 104639. doi:10.1016/j.dsr2.2019.104639
- Kandasamy, S., and B. Nagender Nath. 2016. Perspectives on the Terrestrial Organic Matter Transport and Burial along the Land-Deep Sea Continuum: Caveats in Our Understanding of Biogeochemical Processes and Future Needs. *Front. Mar. Sci.* 3. doi:10.3389/fmars.2016.00259
- Karl, D. M., and M. J. Church. 2017. Ecosystem structure and dynamics in the North Pacific

- Subtropical Gyre: New views of an old ocean. *Ecosystems* 20: 433–457.
doi:10.1007/s10021-017-0117-0
- Karl, D. M., M. J. Church, J. E. Dore, R. M. Letelier, and C. Mahaffey. 2012. Predictable and efficient carbon sequestration in the North Pacific Ocean supported by symbiotic nitrogen fixation. *Proc. Natl. Acad. Sci. U.S.A.* 109: 1842–1849. doi:10.1073/pnas.1120312109
- Karl, D. M., R. M. Letelier, R. R. Bidigare, K. M. Björkman, M. J. Church, J. E. Dore, and A. E. White. 2021. Seasonal-to-decadal scale variability in primary production and particulate matter export at Station ALOHA. *Prog. Oceanogr.* 195: 102563.
doi:10.1016/j.pocean.2021.102563
- Karl, D. M., and R. Lukas. 1996. The Hawaii Ocean Time-series (HOT) program: Background, rationale and field implementation. *Deep Sea Res. Part II* 43: 129–156.
doi:10.1016/0967-0645(96)00005-7
- Karl, D. M., G. A. Knauer, J. H. Martin, and B. B. Ward. 1984. Bacterial chemolithotrophy in the ocean is associated with sinking particles. *Nature* 309: 54–56. doi:10.1038/309054a0
- Karner, M. B., E. F. DeLong, and D. M. Karl. 2001. Archaeal dominance in the mesopelagic zone of the Pacific Ocean. *Nature* 409: 507–510. doi: 10.1038/35054051
- Kaufmann, R. S., and K. L. Smith. 1997. Activity patterns of mobile epibenthic megafauna at an abyssal site in the eastern North Pacific: results from a 17-month time-lapse photographic study. *Deep Sea Res. Part I* 44: 559–579. doi:10.1016/S0967-0637(97)00005-8
- Kharlamenko, V. I., A. S. Maiorova, and E. V. Ermolenko. 2018. Fatty acid composition as an indicator of the trophic position of abyssal megabenthic deposit feeders in the Kuril Basin of the Sea of Okhotsk. *Deep Sea Res. Part II* 154: 374–382.
doi:10.1016/j.dsr2.2018.03.005
- Könneke, M., J. S. Lipp, and K.-U. Hinrichs. 2012. Carbon isotope fractionation by the marine ammonia-oxidizing archaeon *Nitrosopumilus maritimus*. *Org. Geochem.* 48: 21–24.
doi:10.1016/j.orggeochem.2012.04.007
- Kuhnz, L. A., H. A. Ruhl, C. L. Huffard, and K. L. Smith. 2020. Benthic megafauna assemblage change over three decades in the abyss: Variations from species to functional groups. *Deep Sea Res. Part II* 173: 104761. doi:10.1016/j.dsr2.2020.104761
- Larsen, T., D. L. Taylor, M. B. Leigh, and D. M. O'Brien. 2009. Stable isotope fingerprinting: a

- novel method for identifying plant, fungal, or bacterial origins of amino acids. *Ecology* 90: 3526–3535. doi:10.1890/08-1695.1
- Larsen, T., M. Ventura, N. Andersen, D. M. O'Brien, U. Piatkowski, and M. D. McCarthy. 2013. Tracing Carbon Sources through Aquatic and Terrestrial Food Webs Using Amino Acid Stable Isotope Fingerprinting C. Savage [ed.]. *PLoS ONE* 8: e73441. doi:10.1371/journal.pone.0073441
- Lauerman, L. M. L., J. M. Smoak, T. J. Shaw, W. S. Moore, and K. L. Smith. 1997. ²³⁴Th and ²¹⁰Pb evidence for rapid ingestion of settling particles by mobile epibenthic megafauna in the abyssal NE Pacific. *Limnol. Oceanogr.* 42: 589–595. doi:10.4319/lo.1997.42.3.0589
- Lindh, M. V., B. M. Maillot, C. N. Shulse, A. J. Gooday, D. J. Amon, C. R. Smith, and M. J. Church. 2017. From the Surface to the Deep-Sea: Bacterial Distributions across Polymetallic Nodule Fields in the Clarion-Clipperton Zone of the Pacific Ocean. *Front. Microbiol.* 8: 1696. doi:10.3389/fmicb.2017.01696
- Lebrato, M., P. D. J. Mendes, D. K. Steinberg, J. E. Cartes, B. M. Jones, L. M. Birsa, R. Benavides, and A. Oschlies. 2013. Jelly biomass sinking speed reveals a fast carbon export mechanism. *Limnol. Oceanogr.* 58: 1113–1122. doi:10.4319/lo.2013.58.3.1113
- Levin, L. A. and others. 2001. Environmental Influences on Regional Deep-Sea Species Diversity. *Annu. Rev. Ecol. Syst.* 32: 51–93. doi:10.1146/annurev.ecolsys.32.081501.114002
- Li, S., S. Wang, C. Pan, Y. Luo, S. Liang, S. Long, X. Yang, and B. Wang. 2023. Differences in Physiological Performance and Gut Microbiota between Deep-Sea and Coastal Aquaculture of *Thachinotus Ovatus*: A Metagenomic Approach. *Animals* 13: 3365. doi:10.3390/ani13213365
- Li, F., A. Burger, J. M. Eppley, K. E. Poff, D. M. Karl, and E. F. DeLong. 2023. Planktonic microbial signatures of sinking particle export in the open ocean's interior. *Nat. Commun.* 14: 7177. doi:10.1038/s41467-023-42909-9
- Li, Y. and others. 2023. Chemolithotrophic Biological Nitrogen Fixation Fueled by Antimonite Oxidation May Be Widespread in Sb-Contaminated Habitats. *Environ. Sci. Technol.* 57: 231–243. doi:10.1021/acs.est.2c06424
- Li, Y. and others. 2024. Depth shapes microbiome assembly and network stability in the Mariana

- Trench E.F.Y. Hom [ed.]. *Microbiol Spectr* 12: e02110-23. doi:10.1128/spectrum.02110-23
- Lu, J., K. Wong, C. Yu, and A. Zhou. 2023. Ocean spatial geography drives the midgut microbial composition of marine fish. *UJEMI* 28.
- Luo, D. and others. 2021. Population differentiation of Rhodobacteraceae along with coral compartments. *The ISME Journal* 15: 3286–3302. doi:10.1038/s41396-021-01009-6
- Lutz, M. J., K. Caldeira, R. B. Dunbar, and M. J. Behrenfeld. 2007. Seasonal rhythms of net primary production and particulate organic carbon flux to depth describe the efficiency of biological pump in the global ocean. *J. Geophys. Res.* 112: C10011. doi:10.1029/2006JC003706
- Ma, Z., P. Mara, L. Su, L. Wang, H. Li, R. Zhang, V. P. Edgcomb, and J. Li. 2024. Particle size shapes prokaryotic communities and vertical connectivity in the water columns of the slope and central basin of the South China Sea. *Global Planet. Change* 239: 104497. doi:10.1016/j.gloplacha.2024.104497
- Marsay, C. M., R. J. Sanders, S. A. Henson, K. Pabortsava, E. P. Achterberg, and R. S. Lampitt. 2015. Attenuation of sinking particulate organic carbon flux through the mesopelagic ocean. *Proc. Natl. Acad. Sci. U.S.A.* 112: 1089–1094. doi:10.1073/pnas.1415311112
- Martens-Habbena, W., P. M. Berube, H. Urakawa, J. R. De La Torre, and D. A. Stahl. 2009. Ammonia oxidation kinetics determine niche separation of nitrifying Archaea and Bacteria. *Nature* 461: 976–979. doi:10.1038/nature08465
- Martín-Cuadrado, A.-B., P. López-García, J.-C. Alba, D. Moreira, L. Monticelli, A. Strittmatter, G. Gottschalk, and F. Rodríguez-Valera. 2007. Metagenomics of the Deep Mediterranean, a Warm Bathypelagic Habitat N. Ahmed [ed.]. *PLoS ONE* 2: e914. doi:10.1371/journal.pone.0000914
- Mayor, D. J., R. Sanders, S. L. C. Giering, and T. R. Anderson. 2014. Microbial gardening in the ocean's twilight zone: Detritivorous metazoans benefit from fragmenting, rather than ingesting, sinking detritus. *BioEssays* 36: 1132–1137. doi:10.1002/bies.201400100
- McCarthy, M. D., R. Benner, C. Lee, and M. L. Fogel. 2007. Amino acid nitrogen isotopic fractionation patterns as indicators of heterotrophy in plankton, particulate, and dissolved organic matter. *Geochim. Cosmochim. Acta* 71: 4727–4744. doi:10.1016/j.gca.2007.06.061

- McCarthy, M. D., J. Lehman, and R. Kudela. 2013. Compound-specific amino acid $\delta^{15}\text{N}$ patterns in marine algae: Tracer potential for cyanobacterial vs. eukaryotic organic nitrogen sources in the ocean. *Geochim. Cosmochim. Acta* 103: 104–120.
doi:10.1016/j.gca.2012.10.037
- McClelland, J. W., and J. P. Montoya. 2002. Trophic Relationships and the Nitrogen Isotopic Composition of Amino Acids in Plankton. *Ecology* 83: 2173–2180. doi:10.2307/3072049
- McCracken, A. R., B. M. Christensen, D. Munteanu, B. K. M. Case, M. Lloyd, K. P. Herbert, and M. H. Pespeni. 2023. Microbial dysbiosis precedes signs of sea star wasting disease in wild populations of *Pycnopodia helianthoides*. *Front. Mar. Sci.* 10: 1130912.
doi:10.3389/fmars.2023.1130912
- McLaren, M. R., and B. J. Callahan. 2021. Silva 138.1 prokaryotic SSU taxonomic training data formatted for DADA2. doi:10.5281/ZENODO.4587955
- McMahon, K. W., S. R. Thorrold, T. S. Elsdon, and M. D. McCarthy. 2015. Trophic discrimination of nitrogen stable isotopes in amino acids varies with diet quality in a marine fish. *Limnol. Oceanogr.* 60: 1076–1087. doi:10.1002/lno.10081
- McMahon, K. W., S. R. Thorrold, L. A. Houghton, and M. L. Berumen. 2016. Tracing carbon flow through coral reef food webs using a compound-specific stable isotope approach. *Oecologia* 180: 809–821. doi:10.1007/s00442-015-3475-3
- McMurdie, P. J., and S. Holmes. 2013. phyloseq: An R Package for Reproducible Interactive Analysis and Graphics of Microbiome Census Data M. Watson [ed.]. *PLoS ONE* 8: e61217. doi:10.1371/journal.pone.0061217
- de Melo Virissimo, F., A. P. Martin, and S. A. Henson. 2022. Influence of Seasonal Variability in Flux Attenuation on Global Organic Carbon Fluxes and Nutrient Distributions. *Global Biogeochem. Cycles* 36. doi:10.1029/2021GB007101
- Mende, D. R., D. Boeuf, and E. F. DeLong. 2019. Persistent core populations shape the microbiome throughout the water column in the North Pacific Subtropical Gyre. *Front. Microbiol.* 10: 2273. doi:10.3389/fmicb.2019.02273
- Mende, D. R., J. A. Bryant, F. O. Aylward, J. M. Eppley, T. Nielsen, D. M. Karl, and E. F. DeLong. 2017. Environmental drivers of a microbial genomic transition zone in the ocean's interior. *Nat. Microbiol.* 2: 1367–1373. doi:10.1038/s41564-017-0008-3
- Mestre, M., C. Ruiz-González, R. Logares, C. M. Duarte, J. M. Gasol, and M. M. Sala. 2018.

- Sinking particles promote vertical connectivity in the ocean microbiome. *Proc. Natl. Acad. Sci. U.S.A.* 115. doi:10.1073/pnas.1802470115
- Miller, J. E., and D. L. Pawson. 1990. Swimming sea cucumbers (Echinodermata: Holothuroidea): a survey, with analysis of swimming behavior in four bathyal species. *Smithson. Contrib. Mar. Sci.* 1–18. doi:10.5479/si.01960768.35.1
- Miller, R. J., C. R. Smith, D. J. Demaster, and W. L. Fornes. 2000. Feeding selectivity and rapid particle processing by deep-sea megafaunal deposit feeders: A ^{234}Th tracer approach. *J. Mar. Res.* 58: 653–673. doi:10.1357/002224000321511061
- Mincer, T. J., M. J. Church, L. T. Taylor, C. Preston, D. M. Karl, and E. F. DeLong. 2007. Quantitative distribution of presumptive archaeal and bacterial nitrifiers in Monterey Bay and the North Pacific Subtropical Gyre. *Environ. Microbiol.* 9: 1162–1175. doi:10.1111/j.1462-2920.2007.01239.x
- Mintenbeck, K., U. Jacob, R. Knust, W. E. Arntz, and T. Brey. 2007. Depth-dependence in stable isotope ratio $\delta^{15}\text{N}$ of benthic POM consumers: The role of particle dynamics and organism trophic guild. *Deep Sea Res. Part I* 54: 1015–1023. doi:10.1016/j.dsr.2007.03.005
- Mußmann, M., P. Pjevac, K. Krüger, and S. Dykstra. 2017. Genomic repertoire of the Woeseiaceae /JTB255, cosmopolitan and abundant core members of microbial communities in marine sediments. *The ISME Journal* 11: 1276–1281. doi:10.1038/ismej.2016.185
- Nephtin, J., S. K. Juniper, and P. Archambault. 2014. Diversity, Abundance and Community Structure of Benthic Macro- and Megafauna on the Beaufort Shelf and Slope K. Swadling [ed.]. *PLoS ONE* 9: e101556. doi:10.1371/journal.pone.0101556
- Neto, R. R., G. A. Wolff, D. S. M. Billett, K. L. Mackenzie, and A. Thompson. 2006. The influence of changing food supply on the lipid biochemistry of deep-sea holothurians. *Deep Sea Res. Part I* 53: 516–527. doi:10.1016/j.dsr.2005.12.001
- Nomaki, H. and others. 2021. In situ experimental evidences for responses of abyssal benthic biota to shifts in phytodetritus compositions linked to global climate change. *Global Change Biol.* 27: 6139–6155. doi:10.1111/gcb.15882
- Ohkouchi, N. and others. 2017. Advances in the application of amino acid nitrogen isotopic

- analysis in ecological and biogeochemical studies. *Org. Geochem.* 113: 150–174.
doi:10.1016/j.orggeochem.2017.07.009
- Ohta, S. 1985. Photographic observations of the swimming behavior of the deep-sea pelagothuriid holothurian *Enypniastes* (Elasipoda, Holothurioidea). *J. Oceanogr. Soc. Jpn.* 41: 121–133. doi:10.1007/BF02109182
- Ohwada, K., P. S. Tabor, and R. R. Colwell. 1980. Species Composition and Barotolerance of Gut Microflora of Deep-Sea Benthic Macrofauna Collected at Various Depths in the Atlantic Ocean. *Appl. Environ. Microbiol.* 40: 746–755. doi:10.1128/aem.40.4.746-755.1980
- Oksanen, J. and others. 2024. *vegan: Community Ecology Package.*
- Osman, E. O., and A. M. Weinnig. 2022. Microbiomes and Obligate Symbiosis of Deep-Sea Animals. *Annu. Rev. Anim. Biosci.* 10: 151–176. doi:10.1146/annurev-animal-081621-112021
- Palevsky, H. I., and S. C. Doney. 2018. How Choice of Depth Horizon Influences the Estimated Spatial Patterns and Global Magnitude of Ocean Carbon Export Flux. *Geophys. Res. Lett.* 45: 4171–4179. doi:10.1029/2017GL076498
- Park, S.-J. and others. 2014. Genomes of Two New Ammonia-Oxidizing Archaea Enriched from Deep Marine Sediments C. Brochier-Armanet [ed.]. *PLoS ONE* 9: e96449.
doi:10.1371/journal.pone.0096449
- Pelve, E. A., K. M. Fontanez, and E. F. DeLong. 2017. Bacterial Succession on Sinking Particles in the Ocean's Interior. *Front. Microbiol.* 8: 2269. doi:10.3389/fmicb.2017.02269
- Peoples, L. M. and others. 2024. A deep-sea isopod that consumes *Sargassum* sinking from the ocean's surface. *Proc. R. Soc. B.* 291: 20240823. doi:10.1098/rspb.2024.0823
- Pierrat, J., A. Bédier, I. Eeckhaut, H. Magalon, and P. Frouin. 2022. Sophistication in a seemingly simple creature: a review of wild holothurian nutrition in marine ecosystems. *Biol. Rev.* 97: 273–298. doi:10.1111/brv.12799
- Pike, S. M., K. O. Buesseler, J. Andrews, and N. Savoye. 2005. Quantification of ²³⁴Th recovery in small volume sea water samples by inductively coupled plasma-mass spectrometry. *J Radioanal. Nucl. Chem.* 263: 355–360. doi:10.1007/s10967-005-0062-9
- Poff, K. E., A. O. Leu, J. M. Eppley, D. M. Karl, and E. F. DeLong. 2021. Microbial dynamics of

- elevated carbon flux in the open ocean's abyss. *Proc. Natl. Acad. Sci. U.S.A.* 118: e2018269118. doi:10.1073/pnas.2018269118
- Popp, B. N., B. S. Graham, R. J. Olson, C. C. S. Hannides, M. J. Lott, G. A. López-Ibarra, F. Galván-Magaña, and B. Fry. 2007. Insight into the Trophic Ecology of Yellowfin Tuna, *Thunnus albacares*, from Compound-Specific Nitrogen Isotope Analysis of Proteinaceous Amino Acids, p. 173–190. *In* *Terrestrial Ecology*. Elsevier.
- Preston, C. M., K. Y. Wu, T. F. Molinski, and E. F. DeLong. 1996. A psychrophilic crenarchaeon inhabits a marine sponge: *Cenarchaeum symbiosum* gen. nov., sp. nov. *Proc. Natl. Acad. Sci. U.S.A.* 93: 6241–6246. doi:10.1073/pnas.93.13.6241
- Pujalte, M. J., T. Lucena, M. A. Ruvira, D. R. Arahal, and M. C. Macián. 2014. The Family Rhodobacteraceae, p. 439–512. *In* E. Rosenberg, E.F. DeLong, S. Lory, E. Stackebrandt, and F. Thompson [eds.], *The Prokaryotes*. Springer Berlin Heidelberg.
- Reintjes, G., H. E. Tegetmeyer, M. Bürgisser, and others. 2019. On-site analysis of bacterial communities of the ultraoligotrophic South Pacific Gyre H. Nojiri [ed.]. *Appl. Environ. Microbiol.* 85: e00184-19. doi:10.1128/AEM.00184-19
- Rex, M. and others. 2006. Global bathymetric patterns of standing stock and body size in the deep-sea benthos. *Mar. Ecol. Prog. Ser.* 317: 1–8. doi:10.3354/meps317001
- Rodríguez-Barreras, R., A. Dominicci-Maura, E. L. Tosado-Rodríguez, and F. Godoy-Vitorino. 2023. The Epibiotic Microbiota of Wild Caribbean Sea Urchin Spines Is Species Specific. *Microorganisms* 11: 391. doi:10.3390/microorganisms11020391
- Rodríguez-Barreras, R., E. L. Tosado-Rodríguez, and F. Godoy-Vitorino. 2021. Trophic niches reflect compositional differences in microbiota among Caribbean sea urchins. *PeerJ* 9: e12084. doi:10.7717/peerj.12084
- Rogacheva, A., A. Gebruk, and C. H. S. Alt. 2012. Swimming deep-sea holothurians (Echinodermata: Holothuroidea) on the northern Mid-Atlantic Ridge. *Zoosymposia* 7: 213–224. doi:10.11646/zoosymposia.7.1.19
- Rice, A. L., D. S. M. Billett, J. Fry, A. W. G. John, R. S. Lampitt, R. F. C. Mantoura, and R. J. Morris. 1986. Seasonal deposition of phytodetritus to the deep-sea floor. *Proc. R. Soc. Edinburgh, Sect. B: Biol. Sci.* 88: 265–279. doi:10.1017/S0269727000004590
- Richardson, T. L., and G. A. Jackson. 2007. Small Phytoplankton and Carbon Export from the Surface Ocean. *Science* 315: 838–840. doi:10.1126/science.1133471

- Rieck, A., D. P. R. Herlemann, K. Jürgens, and H.-P. Grossart. 2015. Particle-Associated Differ from Free-Living Bacteria in Surface Waters of the Baltic Sea. *Front. Microbiol.* 6. doi:10.3389/fmicb.2015.01297
- Roberts, D., D. S. M. Billett, G. McCartney, and G. E. Hayes. 1991. Procaryotes on the tentacles of deep-sea holothurians: A novel form of dietary supplementation. *Limnol. Oceanogr.* 36: 1447–1451. doi:10.4319/lo.1991.36.7.1447
- Roberts, D., A. V. Gebruk, V. Levin, and B. A. D. Manship. 2000. Feeding and digestive strategies in deposit-feeding holothurians. *Oceanogr. Mar. Biol.* 38: 257–310.
- Rodkina, S. A., S. I. Kiyashko, and V. V. Mordukhovich. 2023. Diet of deep-sea holothurians in the Volcanologists Massif, Bering sea, as inferred from stable isotope and fatty acid analyses. *Deep Sea Res. Part II* 208: 105266. doi:10.1016/j.dsr2.2023.105266
- Rolff, C. 2000. Seasonal variation in $\delta^{13}\text{C}$ and $\delta^{15}\text{N}$ of size-fractionated plankton at a coastal station in the northern Baltic proper. *Mar. Ecol. Prog. Ser.* 203: 47–65.
- Romero-Romero, S., C. A. Ka'apu-Lyons, B. P. Umhau, C. R. Benitez-Nelson, C. C. S. Hannides, H. G. Close, J. C. Drazen, and B. N. Popp. 2020. Deep zooplankton rely on small particles when particle fluxes are low. *Limnol Oceanogr* 5: 410–416. doi:10.1002/lol2.10163
- Romero-Romero, S., E. C. Miller, J. A. Black, B. N. Popp, and J. C. Drazen. 2021. Abyssal deposit feeders are secondary consumers of detritus and rely on nutrition derived from microbial communities in their guts. *Sci. Rep.* 11: 12594. doi:10.1038/s41598-021-91927-4
- Ruhl, H. A. 2007. Abundance and size distribution dynamics of abyssal epibenthic megafauna in the Northeast Pacific. *Ecology* 88: 1250–1262. doi:10.1890/06-0890
- Ruhl, H. A., and K. L. Smith. 2004. Shifts in Deep-Sea Community Structure Linked to Climate and Food Supply. *Science* 305: 513–515. doi:10.1126/science.1099759
- Saba, G. K. and others. 2021. Toward a better understanding of fish-based contribution to ocean carbon flux. *Limnol. Oceanogr.* 66: 1639–1664. doi:10.1002/lno.11709
- Saino, T., and A. Hattori. 1980. ^{15}N natural abundance in oceanic suspended particulate matter. *Nature* 283: 752–754. doi:10.1038/283752a0
- Salazar, G., F. M. Cornejo-Castillo, V. Benítez-Barrios, E. Fraile-Nuez, X. A. Álvarez-Salgado,

- C. M. Duarte, J. M. Gasol, and S. G. Acinas. 2016. Global diversity and biogeography of deep-sea pelagic prokaryotes. *ISME J* 10: 596–608. doi:10.1038/ismej.2015.137
- Schwob, G., L. Cabrol, E. Poulin, and J. Orlando. 2020. Characterization of the Gut Microbiota of the Antarctic Heart Urchin (Spatangoida) *Abatus agassizii*. *Front. Microbiol.* 11: 308. doi:10.3389/fmicb.2020.00308
- Sha, Y., M. Liu, B. Wang, K. Jiang, G. Sun, and L. Wang. 2016. Gut bacterial diversity of farmed sea cucumbers *Apostichopus japonicus* with different growth rates. *Microbiology* 85: 109–115. doi:10.1134/S0026261716010112
- Shulse, C. N., B. Maillot, C. R. Smith, and M. J. Church. 2017. Polymetallic nodules, sediments, and deep waters in the equatorial North Pacific exhibit highly diverse and distinct bacterial, archaeal, and microeukaryotic communities. *MicrobiologyOpen* 6: e00428. doi:10.1002/mbo3.428
- Silfer, J. A., M. H. Engel, S. A. Macko, and E. J. Jumeau. 1991. Stable carbon isotope analysis of amino acid enantiomers by conventional isotope ratio mass spectrometry and combined gas chromatography/isotope ratio mass spectrometry. *Anal. Chem.* 63: 370–374. doi:10.1021/ac00004a014
- Smith, C. R., W. Berelson, D. J. Demaster, F. C. Dobbs, D. Hammond, D. J. Hoover, R. H. Pope, and M. Stephens. 1997. Latitudinal variations in benthic processes in the abyssal equatorial Pacific: control by biogenic particle flux. *Deep Sea Res. Part II* 44: 2295–2317. doi:10.1016/S0967-0645(97)00022-2
- Smith, Jr, K. L., and E. R. M. Druffel. 1998. Long time-series monitoring of an abyssal site in the NE Pacific. *Deep Sea Res. Part II* 45: 573–586. doi:10.1016/S0967-0645(97)00094-5
- Smith, K. L., R. J. Baldwin, D. M. Karl, and A. Boetius. 2002a. Benthic community responses to pulses in pelagic food supply: North Pacific Subtropical Gyre. *Deep Sea Res. Part I* 49: 971–990. doi:10.1016/S0967-0637(02)00006-7
- Smith, S. L., S. M. Henrichs, and T. Rho. 2002b. Stable C and N isotopic composition of sinking particles and zooplankton over the southeastern Bering Sea shelf. *Deep Sea Res. Part II* 49: 6031–6050. doi:10.1016/S0967-0645(02)00332-6
- Smith, C., F. Deleo, A. Bernardino, A. Sweetman, and P. Arbizu. 2008a. Abyssal food limitation, ecosystem structure and climate change. *Trends Ecol. Evol.* 23: 518–528. doi:10.1016/j.tree.2008.05.002

- Smith, K. L., H. A. Ruhl, R. S. Kaufmann, and M. Kahru. 2008b. Tracing abyssal food supply back to upper-ocean processes over a 17-year time series in the northeast Pacific. *Limnol. Oceanogr.* 53: 2655–2667. doi:10.4319/lo.2008.53.6.2655
- Smith, K. L., H. A. Ruhl, M. Kahru, C. L. Huffard, and A. D. Sherman. 2013. Deep ocean communities impacted by changing climate over 24 y in the abyssal northeast Pacific Ocean. *Proc. Natl. Acad. Sci. U.S.A.* 110: 19838–19841. doi:10.1073/pnas.1315447110
- Smith, K. L., Jr. and others. 2014. Large salp bloom export from the upper ocean and benthic community response in the abyssal northeast Pacific: Day to week resolution. *Limnol. Oceanogr.* 59: 745–757. doi:10.4319/lo.2014.59.3.0745
- Smith, K. L., H. A. Ruhl, C. L. Huffard, M. Messié, and M. Kahru. 2018. Episodic organic carbon fluxes from surface ocean to abyssal depths during long-term monitoring in NE Pacific. *Proc. Natl. Acad. Sci. U.S.A.* 115: 12235–12240. doi:10.1073/pnas.1814559115
- Stagaman, K., A. R. Burns, K. Guillemain, and B. J. M. Bohannan. 2017. The role of adaptive immunity as an ecological filter on the gut microbiota in zebrafish. *The ISME Journal* 11: 1630–1639. doi:10.1038/ismej.2017.28
- Stasko, A. D., B. A. Bluhm, J. D. Reist, H. Swanson, and M. Power. 2018. Relationships between depth and $\delta^{15}\text{N}$ of Arctic benthos vary among regions and trophic functional groups. *Deep Sea Res. Part I* 135: 56–64. doi:10.1016/j.dsr.2018.03.010
- Steffan, S. A., Y. Chikaraishi, C. R. Currie, H. Horn, H. R. Gaines-Day, J. N. Pauli, J. E. Zalapa, and N. Ohkouchi. 2015. Microbes are trophic analogs of animals. *Proc. Natl. Acad. Sci. U.S.A.* 112: 15119–15124. doi:10.1073/pnas.1508782112
- Steinberg, D. K., and M. R. Landry. 2017. Zooplankton and the Ocean Carbon Cycle. *Annu. Rev. Mar. Sci.* 9: 413–444. doi:10.1146/annurev-marine-010814-015924
- Stephens, B. M. and others. 2024. Direct observations of microbial community succession on sinking marine particles. *The ISME Journal* 18: wrad010. doi:10.1093/ismejo/wrad010
- Stock, B. C., A. L. Jackson, E. J. Ward, A. C. Parnell, D. L. Phillips, and B. X. Semmens. 2018. Analyzing mixing systems using a new generation of Bayesian tracer mixing models. *PeerJ* 6: e5096. doi:10.7717/peerj.5096
- Stratmann, T., P. Van Breugel, A. K. Sweetman, and D. Van Oevelen. 2023. Deconvolving

- feeding niches and strategies of abyssal holothurians from their stable isotope, amino acid, and fatty acid composition. *Mar. Biodivers.* 53: 80. doi:10.1007/s12526-023-01389-2
- Sullam, K. E., S. D. Essinger, C. A. Lozupone, M. P. O'Connor, G. L. Rosen, R. Knight, S. S. Kilham, and J. A. Russell. 2012. Environmental and ecological factors that shape the gut bacterial communities of fish: a meta-analysis. *Mol. Ecol.* 21: 3363–3378. doi:10.1111/j.1365-294X.2012.05552.x
- Suzuki, S., R. Kaneko, T. Kodama, F. Hashihama, S. Suwa, I. Tanita, K. Furuya, and K. Hamasaki. 2017. Comparison of community structures between particle-associated and free-living prokaryotes in tropical and subtropical Pacific Ocean surface waters. *J. Oceanogr.* 73: 383–395. doi:10.1007/s10872-016-0410-0
- Swan, B. K. and others. 2011. Potential for Chemolithoautotrophy Among Ubiquitous Bacteria Lineages in the Dark Ocean. *Science* 333: 1296–1300. doi:10.1126/science.1203690
- Sweetman, A., and U. Witte. 2008. Response of an abyssal macrofaunal community to a phytodetrital pulse. *Mar. Ecol. Prog. Ser.* 355: 73–84. doi:10.3354/meps07240
- Thiel, H., G. Schriever, K. Lochte, A. J. Gooday, C. Hemleben, R. F. G. Manidura, and C. M. Turley. 1989. Phytodetritus on the Deep-Sea Floor in a Central Oceanic Region of the Northeast Atlantic. *Biol. Oceanogr.* 6: 203-239.
- Turner, J. T. 2015. Zooplankton fecal pellets, marine snow, phytodetritus and the ocean's biological pump. *Progr. Oceanogr.* 130: 205–248. doi:10.1016/j.pocean.2014.08.005
- Urakawa, H. 2014. The Family Moritellaceae, p. 477–489. In E. Rosenberg, E.F. DeLong, S. Lory, E. Stackebrandt, and F. Thompson [eds.], *The Prokaryotes*. Springer Berlin Heidelberg.
- Umhau, B. P., C. R. Benitez-Nelson, H. G. Close, C. C. S. Hannides, L. Motta, B. N. Popp, J. D. Blum, and J. C. Drazen. 2019. Seasonal and spatial changes in carbon and nitrogen fluxes estimated using ^{234}Th : ^{238}U disequilibria in the North Pacific tropical and subtropical gyre. *Mar. Chem.* 217: 103705. doi:10.1016/j.marchem.2019.103705
- Uthicke, S., B. Schaffelke, and M. Byrne. 2009. A boom–bust phylum? Ecological and evolutionary consequences of density variations in echinoderms. *Ecol. Monogr.* 79: 3–24. doi:10.1890/07-2136.1
- Vardaro, M. F., H. A. Ruhl, and K. Jr. L. Smith. 2009. Climate variation, carbon flux, and

- bioturbation in the abyssal North Pacific. *Limnol. Oceanogr.* 54: 2081–2088.
doi:10.4319/lo.2009.54.6.2081
- Vargas, C. and others. 2002. Importance of copepods versus appendicularians in vertical carbon fluxes in a Swedish fjord. *Mar. Ecol. Prog. Ser.* 241: 125–138. doi:10.3354/meps241125
- Wakeham, S. G., C. Lee, J. W. Farrington, and R. B. Gagosian. 1984. Biogeochemistry of particulate organic matter in the oceans: results from sediment trap experiments. *Deep Sea Res Part I* 31: 509–528. doi:10.1016/0198-0149(84)90099-2
- Ward, B. B. 2008. Nitrification in Marine Systems, p. 199–261. *In* Nitrogen in the Marine Environment. Elsevier.
- Wei, C.-L. and others. 2010. Global Patterns and Predictions of Seafloor Biomass Using Random Forests T.N. Romanuk [ed.]. *PLoS ONE* 5: e15323. doi:10.1371/journal.pone.0015323
- Weigel, B. L. 2020. Sea Cucumber Intestinal Regeneration Reveals Deterministic Assembly of the Gut Microbiome H.L. Drake [ed.]. *Appl. Environ. Microbiol.* 86: e00489-20. doi:10.1128/AEM.00489-20
- Weiss, A. S. and others. 2023. Nutritional and host environments determine community ecology and keystone species in a synthetic gut bacterial community. *Nat. Commun.* 14: 4780. doi:10.1038/s41467-023-40372-0
- Wigham, B. D., I. R. Hudson, D. S. M. Billett, and G. A. Wolff. 2003. Is long-term change in the abyssal Northeast Atlantic driven by qualitative changes in export flux? Evidence from selective feeding in deep-sea holothurians. *Prog. Oceanogr.* 59: 409–441. doi:10.1016/j.pocean.2003.11.003
- Wilson, S., J. Yeh, K. E. Korsmeyer, and J. C. Drazen. 2013. Metabolism of shallow and deep sea benthic crustaceans and echinoderms in Hawaii. *Mar. Biol.* 160: 2363–2373. doi:10.1007/s00227-013-2230-8
- Witbaard, R., G. C. A. Duineveld, A. Kok, J. van der Weele, and E. M. Berghuis. 2001. The response of *Oneirophanta mutabilis* (Holothuroidea) to the seasonal deposition of phytopigments at the Porcupine Abyssal Plain in the Northeast Atlantic. *Prog. Oceanogr.* 50: 423–441. doi:10.1016/S0079-6611(01)00064-7
- Wojtal, P. K., S. C. Doherty, C. H. Shea, and others. 2023. Deconvolving mechanisms of particle flux attenuation using nitrogen isotope analyses of amino acids. *Limnol. Oceanogr.* 68: 1965–1981. doi:10.1002/lno.12398

- Wright, C. L., and L. E. Lehtovirta-Morley. 2023. Nitrification and beyond: metabolic versatility of ammonia oxidising archaea. *The ISME Journal* 17: 1358–1368. doi:10.1038/s41396-023-01467-0
- Xiao, Y. and others. 2023. Changes in community structures and functions of the gut microbiomes of deep-sea cold seep mussels during in situ transplantation experiment. *Anim. Microbiome* 5: 17. doi:10.1186/s42523-023-00238-8
- Yamaguchi, Y. T., Y. Chikaraishi, Y. Takano, N. O. Ogawa, H. Imachi, Y. Yokoyama, and N. Ohkouchi. 2017. Fractionation of nitrogen isotopes during amino acid metabolism in heterotrophic and chemolithoautotrophic microbes across Eukarya, Bacteria, and Archaea: Effects of nitrogen sources and metabolic pathways. *Org. Geochem.* 111: 101–112. doi:10.1016/j.orggeochem.2017.04.004
- Yamaguchi, Y. T., Y. Chikaraishi, Y. Takano, N. O. Ogawa, H. Imachi, Y. Yokoyama, and N. Ohkouchi. 2017. Fractionation of nitrogen isotopes during amino acid metabolism in heterotrophic and chemolithoautotrophic microbes across Eukarya, Bacteria, and Archaea: Effects of nitrogen sources and metabolic pathways. *Org. Geochem.* 111: 101–112. doi:10.1016/j.orggeochem.2017.04.004
- Yamaguchi, Y. T., and M. D. McCarthy. 2018. Sources and transformation of dissolved and particulate organic nitrogen in the North Pacific Subtropical Gyre indicated by compound-specific $\delta^{15}\text{N}$ analysis of amino acids. *Geochim. Cosmochim. Acta* 220: 329–347. doi:10.1016/j.gca.2017.07.036
- Yamazaki, Y., Y. Sakai, S. Mino, W. Suda, M. Hattori, P. M. Meirelles, F. Thompson, and T. Sawabe. 2019. Repeated selective enrichment process of sediment microbiota occurred in sea cucumber guts. *Environ. Microbiol. Rep.* 1758-2229.12791. doi:10.1111/1758-2229.1279
- Yang, G., Z. Xu, X. Tian, S. Dong, and M. Peng. 2015. Intestinal microbiota and immune related genes in sea cucumber (*Apostichopus japonicus*) response to dietary β -glucan supplementation. *Biochem. Biophys. Res. Commun.* 458: 98–103. doi:10.1016/j.bbrc.2015.01.074
- Yayanos, A. A. 1995. Microbiology to 10,500 meters in the deep sea. *Annu. Rev. Microbiol.* 49: 777–805. doi:10.1146/annurev.mi.49.100195.004021
- Zanden, M. J. V., and J. B. Rasmussen. 2001. Variation in $\delta^{15}\text{N}$ and $\delta^{13}\text{C}$ trophic fractionation:

Implications for aquatic food web studies. *Limnol. Oceanogr.* 46: 2061–2066.
doi:10.4319/lo.2001.46.8.2061

Zhao, Z., F. Baltar, and G. J. Herndl. 2020. Linking extracellular enzymes to phylogeny indicates a predominantly particle-associated lifestyle of deep-sea prokaryotes. *Sci. Adv.* 6: eaaz4354. doi:10.1126/sciadv.aaz4354

Zhao, R., S. L. Jørgensen, and A. R. Babbín. 2023. A new abundant nitrite-oxidizing phylum in oligotrophic marine sediments. *Communications Biology* 7: 449.